BIOGEOCHEMICAL CYCLING OF TOXIC METALS IN LAKE COEUR D'ALENE SEDIMENTS

By

JAMES GILL MOBERLY

A thesis submitted in partial fulfillment
of the requirements for the degree of

Master of Science in Chemical Engineering

Washington State University
School of Chemical Engineering and Bioengineering

August 2006

To the Faculty of Washington State University:

The members of the Committee appointed to examine this thesis of JAMES GILL MOBERLY find it satisfactory and recommend that it be accepted.

_____

Chair

_____

_____

ACKNOWLEDGMENT

I would like to thank Rajesh Sani for being a mentor, advisor, and friend to me at the beginning of my graduate career, Brent Peyton for giving me a chance to start on this project and giving me invaluable suggestions along the way, and Richard Zollars for agreeing to join my committee and for his excellent instruction in courses I have taken. I would like to thank our collaborators, Timothy Ginn, Nic Spyker, and Thomas Borch for their contributions and helpful advice along the way. I would like to thank the Director, Office of Science, Office of Basic Energy Sciences, of the U.S. Department of Energy under Contract No. DE-AC02-05CH11231 for support of the Advanced Light Source User Facility where Thomas analyzed our x-ray samples. I would also like to thank the Department of Chemical Engineering at Washington State University (now School of Chemical Engineering and Bioengineering) including Diana Thornton, Jo Ann McCabe and Senja Estes for helping me bring order to chaos and helping to support me both financially and otherwise. I would like to thank the National Science Foundation (Award # EAR-0420374) for their financial support as none of this would have been possible without their support. I would also like to thank all those who have helped out, big and small, during my tenure here, Gary Held at the Engineering Machine Shop, Rich Conrey, Diane Johnson Cornelius, and Charles Knaack at the Geo Analytical Lab at WSU for geochemical analysis and putting up with my numerous questions, my lab-mates Chris Taylor, Sutapa Barua, John Aston, Rehana Parveen, Sevinc Sengor, and especially Ranjeet Tokala who was my sounding board for many ideas, giving me suggestions when I was stuck, and sampling when I couldn't. Any acknowledgement would not be complete without giving thanks to my family, my mother for raising me and raising my

children when I am at school and my father for the same reasons and for lending me his wife to do these things. And a very special thanks to my wife for her continued support and love and willingness to let me continue my goals with full support.

BIOGEOCHEMICAL CYCLING OF TOXIC METALS IN LAKE COEUR D'ALENE SEDIMENTS

Abstract

By James Gill Moberly, M.S.
Washington State University
August 2006

Chair: Rajesh K. Sani

Historic mining in the Coeur d'Alene area of Idaho has contaminated sediments, soils, and waters with heavy metals including, but not limited to, lead, copper, and zinc. Metal contamination continues to be introduced into Lake Coeur d'Alene and its tributaries by a variety of factors including seasonal changes, flooding, acid mine drainage, and air borne dust and this poses a significant health hazard to humans and biota. Bacteria residing in Lake Coeur d'Alene are capable of detoxifying metals using largely unknown processes. However, heavy metals exert toxic effects on the indigenous bacteria and these toxic effects highly depend on metal speciation, chemical properties, and geochemical factors. Therefore to develop an effective understanding of the metal toxicity in this environment and its effects on indigenous microorganisms, metal concentration, speciation, associated mineral phase, microbial toxicity, and microbial biogeochemical contributions to metal cycling must be studied.

This work is broken up into five chapters. The first deals with the historic contamination, toxic metal transport, and microbial interactions with toxic metals,

focused mainly on lead, copper, and zinc. Chapter two launches a more in depth look at the geochemistry of the Coeur d'Alene River Delta, both aqueous and sediment, using synchrotron based X-ray analyses to characterize the sediments. Chapter two also proposes some theoretical interactions between these identified mineral phases and microbes. The third chapter focuses on bacterial enrichments, isolation, and identification from the sediments using a novel flow reactor and batch culturing. The fourth chapter examines the toxic effects of zinc on *Arthrobacter* sp., an isolate from the novel reactor. This chapter includes a dual-Monod kinetic model to represent zinc inhibition of this organism. The model represents the experimental data very well at low metal concentrations and deviates at higher metal concentrations and this could be due to lag-components not included in the model or a variety of other reasons. Chapter five discusses some future work in biogeochemical metal cycling as it pertains to Coeur d'Alene.

TABLE OF CONTENTS

LIST OF TABLES

LIST OF FIGURES

Dedication

This thesis is dedicated to my wonderful wife

who continues to put up with me even

when I end up living at the lab

for weeks at a time.

CHAPTER ONE

Introduction

Coeur d'Alene (CdA) Lake, a natural lake in Northern Idaho between the Selkirk and CdA Mountains, was formed by glacial meltwaters which overflowed from Lake Missoula approximately 14,000 ago [1-3]. Lake CdA is joined on the southern portion of the lake by the St. Joe and CdA River [1-5]. These two rivers contribute approximately 94% of the influent flow into Lake CdA [3]. The CdA River is composed of two main rivers; the South Fork of the CdA River and its tributaries flows through the CdA Mining District and the North Fork which joins the South Fork before continuing through an area of lateral lakes and deltas and into Lake CdA [1-4]. The South Fork of the CdA River is of particular interest as it and its tributaries are the primary drainage source for the CdA Mining District [1, 3]. The mineralogy of the CdA Mining District is composed primarily of quartzite and siderite [$FeCO_3$] veins containing stratified deposits of galena [PbS], sphalerite [ZnS], and tetrahedrite [$Cu_{12}Sb_4S_{13}$] [6]. Pyrite [FeS_2], chalcopyrite [$CuFeS_2$], and pyrrhotite [Fe_xS x=0.8,1] are also locally abundant [6].

Though in the recent past only two mines out of over 90 mines were in operation, the CdA Mining district has been a world class producer of lead, zinc and antimony [1, 3, 4, 7]. Over 3 million tons of zinc, 34 thousand tons of silver, and 7 million tons of lead have been mined from the CdA Mining district, stretching from Coeur d'Alene, Idaho to Superior, Montana [6].

Toxic Metal Contaminant Transport

Prior to 1915 ore separation techniques, using grinding and gravity separation, produced large amounts of coarse metal-enriched tailings [4]. Between 1915 and 1925

separation techniques improved to reduce the metal content in these mine wastes, producing a finer grain tailing [4]. The majority of these metal-enriched tailings were directly discharged into the South Fork of the CdA River until in 1968 tailing ponds were introduced to trap and settle these mining wastes [1-4]. Over time, the majority of these fluvial tailings have been pushed downstream into the lower Coeur d'Alene River delta adjacent to Harrison, Idaho and Lake CdA sediments [3, 8, 9]. Presently, approximately 72 million tons of these metal-enriched tailings reside in the CdA River and its tributaries [4].

Metal concentrations vary greatly between interstitial sediment waters (porewater) and free flowing river water [4]. Seasonal changes can also effect the concentration of metallic species in aqueous phases as the cycling of organic matter and precipitation loading resulting in dilution and sorption, (Table 1) [4, 10, 11]. The geochemistry of aqueous phase metals is complex and depends not only on concentration but thermodynamic and kinetic factors, metal-organic complexation, and biogeochemical contributions, such as biologically mediated iron cycling; much is still needed to develop a comprehensive understanding of this system [4, 7, 10].

Metal contamination continues to proliferate in the region as sulfide containing mining-exposed minerals, chiefly pyrite, combined with oxygen-rich conditions, sulfur oxidizing bacteria, and water to produce sulfuric acid [12]. These low pH conditions (typically 2.6-3.8) leach metals, primarily lead, cadmium, and zinc from the local geology [12]. This low pH metal-contaminated water, called acid-mine drainage (AMD), is carried into rivers and lakes where the acid is diluted and pH neutralized causing precipitation of the dissolved metals into river and lake sediments [10, 12-14].

Table 1: Literature Comparison: Composition of Coeur d'Alene River and Pore Water

Species	Units	Reference # [7] Coeur d'Alene River	Reference # [4] Coeur d'Alene River	Reference # [4] Cataldo Porewater
Temperature	^{o}C	22.1	-	-
pH		7.36	7.21	6.58
Alkalinity	mg $CaCO_3$/L	1.4	0.54	4.76
Total Organic Carbon	mg/L	-	0.7	43
Fluoride	mg/L	0.1	-	-
Chloride	mg/L	3.0	18.081	8.154
Nitrate-N	mg/L	0.9	-	-
Sulfate	mg/L	24	19.213	374.648
Arsenic	mg/L	<0.001	<0.001	0.262
Barium	mg/L	0.067	0.029	0.030
Cadmium	mg/L	0.009	0.002	0.002
Calcium	mg/L	21.0	10.020	56.109
Chromium	mg/L	<0.001	-	0.012
Cobalt	mg/L	<0.001	<0.001	0.088
Copper	mg/L	0.002	-	0.002
Iron	mg/L	0.200	0.011	54.172
Lead	mg/L	0.012	0.001	0.003
Magnesium	mg/L	6.30	3.646	68.054
Manganese	mg/L	<0.001	0.110	10.988
Nickel	mg/L	<0.001	<0.001	0.016
Potassium	mg/L	1.290	21.113	1.994
Zinc	mg/L	1.070	0.458	8.416

-=Not Reported

An average of 1,500 gallons per minute of AMD is continuously discharged from privately owned underground workings in the CdA area [12]. This AMD is currently being treated at a United States environmental protection agency-supported treatment facility, illustrating the long term nature of the contamination in the CdA area [12]. Additionally soluble iron, aluminum, and manganese hydroxides sorb many of the toxic metals, mobilizing them from the sediments into river and lake waters, making them both

easily transportable and bioavailable [10, 13-18]. These hydroxide compounds once reduced by either abiotic or biotic means reintroduce the sorbed metals into the environment [8, 15, 17]. Nutrient loading and flooding both contribute to the release of toxic metals, specifically lead, zinc, and manganese; additionally shifts in pH are capable of releasing carbonate bound metals [15, 19]. Significant metal release may also occur as sediments shift from anoxic to oxic conditions during anthropogenic activities, seasonal turnover, or drought conditions where water levels decrease substantially [19]. It is estimated that 70 billion tons of contaminated sediments reside in Lake CdA downstream from the CdA Mining District, illustrating both the mobility and extent of contamination [20].

Biogeochemical Aspects

The toxicity and mobility of heavy metals depends greatly on speciation, concentration, and associated mineral phase as well as other geochemical factors. Sediments typically contain approximately 10-15% iron [17, 21, 22]. Zinc and lead also make up a significant fraction of the total heavy metal load, (Table 2) [2, 3, 21]. Metal species vary with sediment depth and grain size [1-3, 21-23].

Table 2: Literature Comparison of Metal Concentration in Lake Coeur d'Alene Sediment Cores

	Reference # [21]		Reference # [3]	
Species	Mean mg/kg sediment	Maximum mg/kg sediment	Mean mg/kg sediment	Maximum mg/kg sediment
Pb	3,820	21,413	3,200	27,500
Cu	-	-	91	650
Zn	2,995	11,169	2,400	14,000
Mn	5,953	9,208	4,500	69,000
Fe	82,486	123,200	67,000	137,000
As	201	568	103	845

- not reported

Concentrations of redox-active elements such as iron and arsenic increase toward the sediment-water interface, while concentrations of less redox-active elements such as lead and zinc increase with sediment depth [1, 2, 21]. The sequentially extracted operationally defined mineral phase also changes with depth; a greater fraction of zinc (hydr)oxide minerals are present near the sediment-water interface while carbonate and sulfidic zinc minerals are present in greater abundance with depth, primarily governed by the redox state of zinc [24].

Iron minerals including magnetite, pyrrhotite, troilite, goethite, hematite, and more commonly metastable ferrihydrite are found across the CdA area [17, 25]. Patterns in the distribution of both arsenic and iron suggest post-depositional mobilization of these elements [17, 21]. Microbes are capable of reducing these elements and these post-depositional changes may be due to microbial biogeochemical cycling [16, 18, 22]. Other elements such as zinc and cadmium may undergo mobilization with changes in pH, redox-potential, and binding to organic matter, mediated by microbial populations [14].

It is theorized that iron and sulfate reducing bacteria significantly contribute to metal cycling in this system though the main mechanisms are not well understood [1, 3, 9, 17, 18, 26]. It is probable that iron reducing organisms may free sorbed metals by reduction of iron and manganese hydroxides [8, 17]. Sulfate reducing organisms may arrest mobile metals by precipitating metals through production and reaction of biogenic hydrogen sulfide with the metal [27]. These microbial mediated metal interactions illustrate the important role that microorganisms play in the biogeochemical cycling of toxic metals in CdA sediments.

Bacterial Diversity in Contaminated Sediments

The bacteria in the CdA area are capable of growth in this contaminated environment though at significantly lower numbers and less microbial diversity than from similar pristine areas [26]. Typical microbial abundance numbers in CdA sediments range between 10^5 and 10^8 cells/g wet sediment, a shift of between 10 and 100 times lower than metal free controls [9, 22]. *Geobacter* species are a diverse group of disimilatory metal reducing bacteria which are present in Lake CdA regardless of sediment-metal content [9, 17]. Lead resistant forms of *Pseudomonas, Bacillus, Cotynebacterium*, and *Enterobacter* have been identified [26]. Several novel genera and species of bacteria have been isolated from these contaminated sediments, highlighting that even with high levels of toxic metals bacteria are able to adapt to these harsh environments [18, 28].

Metal Resistance Schemes

Many heavy metals, such as zinc, copper, molybdenum, and nickel are used as binding sites in key enzymes and proteins, but are only needed at very low concentrations [29]. Zinc is not able to undergo redox changes under physiological conditions and thus makes it ideal for redox sensitive functions, such as binding polypeptide chains and acting as a Lewis base to activate water [30]. It is involved in a variety of DNA-binding proteins and other enzymes [29, 30]. Zinc superoxide dismutase helps protect the cell from radicals by converting them into less reactive constituents [30].

For a metal to become toxic to the cell it must be taken up by the cell in sufficient quantity to interfere with cellular processes. Metal toxicity can decrease cell size, effect growth rates, inactivate and precipitate proteins, disrupt the cell membrane causing

leakage of mobile metabolites such as potassium and calcium, and cause premature cell death [26, 31]. Cells have developed more specific uptake systems (typically ATP driven) for certain key metals while other metal species enter the cell through "open-gate" pathways designed for multiple metabolite species, (Table 3) [30].

Table 3: Protein families important for heavy-metal transport.

Protein Family	Direction of Transport	Energy	Metal Ions	Composition
ABC	Uptake	ATP	Mn^{2+}, Zn^{2+}, Ni^{2+}, Fe^{2+}	membrane-integral parts + 2 ATPase parts = ABC core + periplasmic binding protein
	Efflux	ATP	-	ATP ± ABC core + membrane fusion protein and outer membrane factor
P-type	Both	ATP	Mg^{2+}, Mn^{2+}, Ca^{2+}, K^{+}, Cu^{2+}, Zn^{2+}, Cd^{2+}, Pb^{2+}, Ag^{+}	1 membrane-bound protein as core
A-type	Efflux	ATP	As^{3+}	1 membrane-integral protein + a dimeric ATPase subunit
RND	Efflux	Proton gradient	Co^{2+}, Zn^{2+}, Cd^{2+}, Ni^{2+}, Cu^{2+}?, Ag^{+}?	1 CPM proton/cation antiporter + membrane fusion protein (dimer?) + outer membrane factor: CBA transport systems
HoxN	Uptake	Chemiosmotic	Co^{2+}, Ni^{2+}	Membrane-Integral protein
CHR	Antiport?	Chemiosmotic	CrO_4^{2-}	Membrane-integral protein (ChrA)
MIT	Uptake	Chemiosmotic	Most cations	Membrane-integral protein (CorA)
CDF	Efflux	Chemiosmotic	Zn^{2+}, Cd^{2+}, Co^{2+}, Fe^{2+}?	Membrane-integral protein (CzcD, ZRC1p, ZnT1)

Adapted from Reference # [30]. CPM, cytoplasmic membrane; ABC, ATP-binding cassette; RND, resistance, nodulation, cell division; CHR, chromate transport; MIT, metal inorganic transport; CDF, cation-diffusion facilitators.

Often these slower more specific pathways require the expenditure of energy in the form of adenine tri-phosphate (ATP) or proton gradients and are induced by starvation and special metabolic needs [30]. Because metals differ very little in size and charge from other essential metabolites, such as calcium and magnesium, the cell must increase substrate specificity to desired metabolic products which often is time consuming and energetically unfavorable [30]. Thus the "fast" uptake systems are the main path for which heavy metals enter the cell and cause a toxic response [30].

Zinc cannot undergo redox changes under physiological conditions and its toxicity mainly stems from its ability to complex with cellular machinery [30]. It is theorized that interactions between heavy metals and sulfur or phosphate groups in proteins or enzymes are the main mechanism of metal-complex toxicity as metals are often strongly bound to sulfur and phosphate and may cause abnormal or lack of function in these proteins and enzymes [31, 32].

It has been shown that the majority of environmental resistances are bestowed by genes encoded on plasmid bound DNA [29, 30, 33-35]. Metal resistance genes are also present on genomic DNA and these genes work in concert with their plasmid counterparts to protect the cell [30, 34]. These plasmid encoded genes can be transferred between bacteria via horizontal and lateral gene transfer [36].

Bacteria rely on metal exclusion for preventing heavy metals from reaching toxic concentrations in the cell or by altering the metal into a less toxic form. Three main mechanisms protect the cell from metal contaminated environments: metal efflux, biotransformation, and metal binding [27, 30, 33-35, 37-40].

Two mechanisms rely on exclusion of metals: metal efflux and binding. Of all metal resistance mechanisms, efflux is the most energetically favorable [30]. Under aerobic conditions 16 ATP are required to produce one metal sulfide where only one ATP is required to pump the offending metal outside the cell; other metal chelating proteins are even more expensive to produce [30]. Efflux does not detoxify the environment for other more sensitive species of bacteria [30, 35]. Efflux is accomplished by a variety of transporters (Table 3) [30].

Metal binding prevents the metal access into the cell via extra cellular polysaccharides (EPS) or proteins at the cell membrane which bind to the metal [30, 37, 39, 41]. These can be inducible, in the case of metal binding proteins, but are often produced regardless of metal concentration, as in EPS [30, 39, 41]. EPS is often produced by bacteria to trap and concentrate trace metabolites but in this case protects the cell by preventing heavy metal entry into the cell [39].

Biotransformation, as defined herein, includes mechanisms such as biological metal reduction, precipitation, and alkylation or methylation. The reduction of mercury to its elemental form is one of the most widely studied examples for biotransformation of heavy metals [37]. Often reduction is coupled with oxidation of a carbon source and generates metabolic energy. Dissimilatory metal reducing bacteria have been reported in the CdA area which can reduce arsenic, selenium, iron and manganese as the sole electron acceptors [18], however this produces more toxic compounds, as in the case of arsenic, than the parent products and there is likely other detoxification mechanisms at work. Bacteria have been found which use As(III) as the electron donor in aerobic growth, producing the less soluble form, As(V) [37]. Alkylation or methylation are more energy intensive processes that produce less soluble less toxic products or can produce more soluble products which can more easily be discharged from the cell [40]. It is unlikely that bacteria use direct reduction to reduce the toxicity of zinc as zinc is not able to undergo reduction under physiological conditions, though attaching a functional group or metal-protein complex to make this metal less toxic is a possibility.

Precipitation of metals is often a side product of metabolism and does not necessarily confer metal resistance to microorganisms [37]. Precipitation is

accomplished by production of sulfides, phosphates, or carbonates either by an induced pathway or a product of regular cellular processes [37]. It has been shown that sulfide production can be an inducible pathway under metal stress but is also a natural product of sulfate reducing bacteria [30, 37]. Phosphate is not generally released in great quantities in the cell due to its limiting nature in natural systems [37]. However, *Acinetobacter johnsonii* can precipitate metals anaerobically as it consumes aerobically produced ATP to adenine di-phosphate (ADP) freeing one inorganic phosphate [37]. Metal carbonate formation is the product of carbon dioxide from metabolically active cells combined with efflux mechanisms which concentrates metals at the cell membrane [37]. Carbon dioxide, a byproduct of respiration, abiotically forms carbonate ions which react with soluble metals to produce metal precipitates.

The precipitation of these metals may persist in the environment as biogenic minerals. Some examples of minerals which may be formed by biogenic metal precipitation are iron sulfides [FeS_x], hopeite [$Zn_3(PO_4)_2 \bullet nH_2O$], vivianite [$Fe_3(PO_4)_2 \bullet nH_2O$], earlshannonite [$MnFe_2(PO_4)_2(OH)_2 \bullet 4H_2O$], siderite [$FeCO_3$], smithsonite [$ZnCO_3$], and cerussite [$PbCO_3$]. It is also likely that bacteria produce amorphous mineral types which are unlikely to be identified by more traditional techniques such as x-ray diffraction.

Metal resistance mechanisms can be used solitarily but more often multiple resistance schemes are used simultaneously [30]. Though metal resistant bacteria have been identified from the Lake CdA area, little literature has been published concerning their contributions to biogeochemical processes. Small changes, even simply lowering metal concentrations by sorption onto EPS, or changing the local pH may alter the abiotic

factors which would precipitate metal species. These detoxification mechanisms may be key to understanding the biogeochemical metal cycling, as both inducible and indirect metabolic metal precipitation and bio-mineral formation contribute to biogeochemical processes.

Metal contamination continues to be introduced into Lake CdA and its tributaries by a number of both point sources and diffuse contributors and this poses a significant health hazard to humans and biota [1-5, 7, 10, 12-14, 42]. Heavy metals exert toxic effects on the indigenous bacteria and these toxic effects highly depend on metal speciation, chemical properties, and geochemical factors [26]. Therefore to develop an effective understanding of this environment and its effects on microorganisms, metal concentration, speciation, associated mineral phase, microbial metal toxicity, and microbial biogeochemical contributions to metal cycling must be studied.

CHAPTER TWO

GEOCHEMISTRY OF THE COEUR D'ALENE RIVER DELTA

Abstract

Not only does metal concentration but also mineral phase plays an important role in the toxicity or lack of such to biota and microorganisms as well as the remobilization of these toxic metals. Thus characterizing the physical and chemical properties of CdA waters and sediments will give an additional indicator of the potential for toxicity and remobilization. Aqueous geochemistry of CdA waters compares well with literature values and shows elevated levels of lead, zinc, and other heavy metals. Sectioned analyses of sediment cores reveals that the majority of sediment particles are below 75 microns and that these small particles contribute over 60% of the mass in the top 2 inches of sediment posing a significant remobilization problem if disturbed. Additionally, lead and zinc-bearing mineral phases indicated using synchrotron based X-ray diffraction analyses were dundasite, coronadite, stolzite, mattheddleite, and bindheimite and zinc minerals were smithsonite. These analyses help to better characterize the geochemistry of this contaminated environment and aid in developing further biogeochemical interaction models.

Introduction

In order to more accurately describe the biogeochemical metal cycling in CdA, metal concentration in both the aqueous and sediments phases must be described as well as the associated mineral phase. The presence of mineral phases in batch cultures greatly influences the metal inhibition kinetics and toxicity to microorganisms and can lead to remobilization or immobilization of toxic metals, such as uranium, depending on mineral species and substrate conditions [43, 44]. Thus both aqueous and sediment geochemical analyses must be performed to address the interactions between toxic metal and biota.

Materials and Methods

Sample Collection

Sample cores were taken from the upper delta region 1.8 miles north east of Harrison, Idaho on East Blue Lake Road [N(47°28'43.8") W(116°43'59.6")], (Figure 1). Samples were collected using 2" schedule 20 polyvinylchloride (PVC) piping with matching acrylonitrile, butadiene, and styrene (ABS) copolymer plastic caps. Sample cores were 15±3cm in length. The PVC sampler was hand driven into undisturbed sediments, capped on exposed end, extracted from sediments, and further caped underwater. Sealed samples were placed on ice in plastic bags and transported directly to Washington State University (WSU) where they were frozen at -25°C. Free stream river water was also collected in 1L acid washed Nalgene® containers, capped underwater to prevent head space contamination, and stored on ice. Upon arrival at WSU, water samples were placed at 4°C until analysis.

Water Analyses

Dissolved oxygen was measured on site with a portable dissolved oxygen meter (Extech Instruments Model 407510) at 6.7°C. Free stream temperature was measured using an alcohol thermometer at 5.5°C. For pore water extraction, frozen cores were thawed in an anaerobic chamber (Forma Scientific Inc. Model 1025), placed in acid washed Nalgene® bottles, sealed, and centrifuged at 7000 rpm for 20 minutes. Supernatant was removed once Nalgene® bottles were returned to anaerobic chamber. Samples were sent to Analytical Sciences Laboratory at the University of Idaho for analysis (EPA methods 200.7, 200.8, 300.0, 310.7, and 415.1).

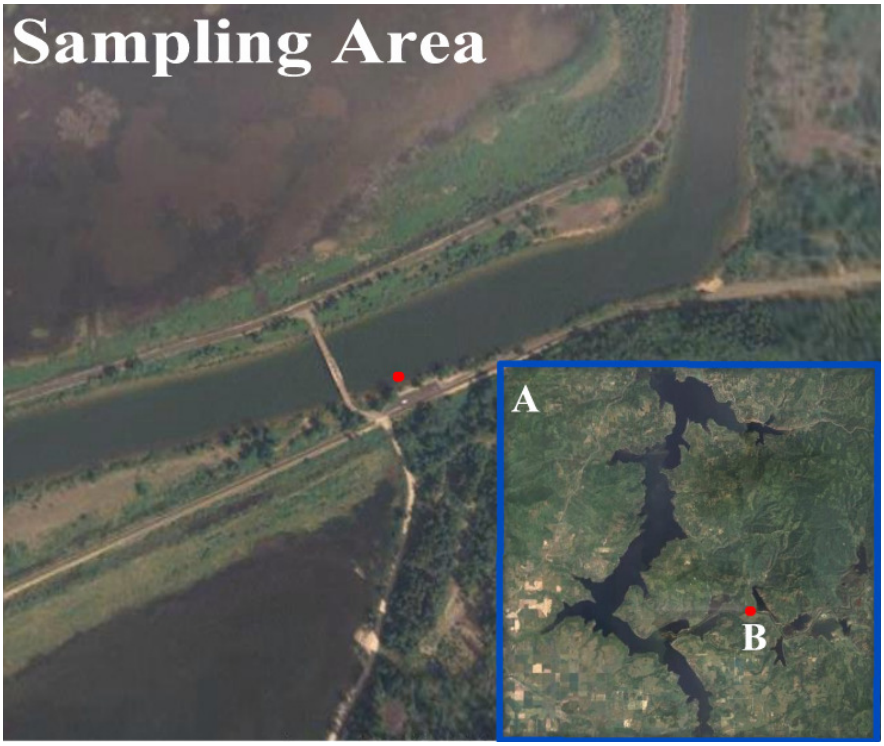

Figure 1: Coeur d'Alene Sampling Area A. Overhead of Coeur d'Alene Lake B. Sampling area

Sediment Analyses

Frozen cores were cut into 2" sections and grouped into top, middle, and bottom sections and dried at 80^{o}C. Sectioned sediments were sent to Geo Analytical Laboratories at WSU for elemental analysis using X-ray florescence spectroscopy (XRF). The samples were finely ground using a tungsten carbide bowl and weighed with the addition of a lithium tetraborate flux (2:1 flux:sediment). Sediments were then heated to 1000^{o}C in a muffle furnace to drive off volatile compounds and fused with the flux. After heating, the vitrified sample was reweighed to determine the loss of volatile compounds during the melting process. Analysis was carried out on an automated ThermoARL Advant'XP+ sequential X-ray fluorescence spectrometer. Standard

reference materials were obtained from the National Institute of Standards and Technology and pure quartz controls were run to determine grinding bowl contamination which was subtracted to give the final sediment elemental composition.

A portion of sediment was air dried in the anaerobic chamber, sealed under anaerobic conditions, and sent to Thomas Borch for micro X-ray diffraction (μXRD) and florescence (μXRF) spectroscopic analysis at the Advanced Light Source User Facility at Stanford Synchrotron Radiation Laboratories. Samples were prepared as in Ginder-Vogel et al. [45]. Kapton® tape enclosed the sediment samples to prevent oxidation. The samples were analyzed on beamline 10.3.2 using a water-cooled Si(111) monochromator, two Si mirrors in Kirkpatrick-Baez geometry, and a Bruker X-ray CCD camera at 14,000 keV corresponding to a wavelength of 0.8856Å. Images were processed using Fit2D, corrected to remove background Kapton® tape, and interpreted using JADE® (Materials Data Inc version 6.5) software.

Bulk sediment samples were derived from two complete cores that were dried at 80°C and then homogenized. Grain size distribution of each segment was obtained using dry separation of US sieve sizes 16, 30, 60, 100, 140, and 200. Each sieve tray was washed and weighed prior to separation. Sieves were stacked, and then loaded into a shaker where they were shaken and solids separated. Sieves were removed and weighted to determine grain size fractions in each.

Bulk sediment analysis using a Coulter SA 3100 Brunauer Emmett Teller (BET) instrument was performed for surface area analysis and pore size distribution. A sample size of approximately two grams of bulk sediment was used for BET analysis. Samples for BET analysis were loaded into glass sample bulbs and weighed. Sample bulbs were

then loaded into the instrument, outgassed for 60 minutes at 120^{o}C, capped and reweighed to determine loss of volatile components and water. Sample bulbs were immersed in a dewar flask of liquid nitrogen and BET analysis was performed at a relative pressure range of 0.05 to 0.2. Both adsorption and desorbtion isotherms were characterized and pore size and volume were determined. Three sample analysis runs were performed with corresponding correlation coefficients greater of than 99.9%.

Concentrations of acid soluble iron(II) were measured after digestion of 0.143±0.01 g dry sediment with 750 µL of 6N HCl for 15 minutes. The digest was centrifuged at 7000Xg for 5 minutes and 100 µL of the supernatant was added to 9.9 mL of 2.5 N HCl. One hundred µL of this acid-diluted sample was added to 5 mL of ferrozine reagent as outlined in Cummings et al. [9] (1 g 3-(2-pyridyl)-5,6-bis(4-phenylsulfonic acid)-1,2,4-triazine per liter of 50 mM HEPES buffer; pH 6.5). Absorbance measurements were read at 562 nm after 1 minute and readings were compared with acidified standard solutions of ferrous sulfate. Verification of the leach was repeated after 24 hours.

Results and Discussion

Aqueous Geochemistry

The aqueous geochemistry in this study compares relatively well with reported literature, (Table 4) [4, 7]. In general, it appears that most species concentrations increase from river to porewater, probably due to diffusion of the concentration species within the solid phase to the porewater and from the porewater to free stream waters. Trends in this study opposite of other studies with potassium and chloride species follow this logic. Soluble iron concentrations appear to be greater in the river water than in the

porewater however this value approaches the method detection limit and may be an artifact or may be due to abiotic seasonal factors and further long term and seasonal studies may be warranted to observe these variations [4]. Notable magnitude differences in alkalinity, organic carbon, sulfate, soluble iron and manganese may be due to seasonal fluxuations which can change pH, redox potential, and nutrient content in the CdA River. Seasonal changes in temperature can alter the dominant members of the microbial community and this may also effect the biogeochemical metal cycling [46]. These changes highlight the complex and dynamic nature of these contaminated sediments.

Table 4: Composition of Coeur d'Alene River and Porewater: April 2005

		Coeur d'Alene			Ref #[8]	Ref #[8]
species	units	River water	Pore water	MDL†	CdA River	Cataldo Porewater
Temperature	°C	5.5	-		-	-
pH		7.2	6.4		7.21	6.58
	equivalent					
Alkalinity	mg $CaCO_3$/L	19	57	3	0.54	4.76
Total Organic Carbon	mg/L	1.6	170	0.5	0.7	43
Fluoride	mg/L	*	1.7	0.15	-	-
Chloride	mg/L	0.690	2.800	0.200	18.081	8.154
Nitrite-N	mg/L	ND¤	0.810	0.050	-	-
Nitrate-N	mg/L	ND¤	6.800	0.050	-	-
Sulfate	mg/L	5.600	59.000	0.200	19.213	374.648
Arsenic	mg/L	*	0.009	< 0.001	< 0.001	0.262
Barium	mg/L	0.018	0.160	0.010	0.029	0.030
Cadmium	mg/L	< 0.001	0.018	< 0.001	0.002	0.002
Calcium	mg/L	5.500	25.000	0.050	10.020	56.109
Chromium	mg/L	*	0.009	0.001	-	0.012
Cobalt	mg/L	*	0.023	< 0.001	< 0.001	0.088
Copper	mg/L	< 0.001	0.003	< 0.001	-	0.002
Iron	mg/L	0.030	*	0.020	0.011	54.172
Lead	mg/L	0.003	0.130	< 0.001	0.001	0.003
Magnesium	mg/L	2.100	7.300	0.020	3.646	68.054
Manganese	mg/L	0.032	27.000	0.005	0.110	10.988
Nickel	mg/L	< 0.001	0.013	< 0.001	< 0.001	0.016
Potassium	mg/L	*	5.200	0.500	21.113	1.994
Vanadium	mg/L	*	0.002	< 0.001	-	-
Zinc	mg/L	0.160	2.700	0.003	0.458	8.416

* Below method detection limit
- Not reported
† Method detection limit
¤Not detected

Sediment Geochemistry

Analysis of bulk sediment shows that greater than 50% of pore sizes are larger than 80 nanometers, however approximately 12% of sediment pores are less than 6 nanometers in size, (Table 5). These pore sizes are capable of sequestering organic matter and metal (hydr)oxides which could also trap toxic metals. Mayer et al. reported that although organic matter does sorb to small mesopores and clay mineral surfaces, the smallest pore sizes do not contain the largest portion of organic matter and thus the majority of organic matter is not removed from microbial attack [47]. Therefore pore sequestration in this system is not a feasible means of long-term sequestration of toxic metals.

Table 5: Pore Size Distribution

Pore Size Range (nm)	Pore Volume mL/g	%
under 6	0.00095	12.08%
6-8	0.00044	5.63%
8-10	0.00037	4.64%
10-12	0.00036	4.61%
12-16	0.00047	6.01%
16-20	0.00049	6.22%
20-80	0.00255	32.47%
over 80	0.00223	28.33%
	Total	99.99%

Sectioned analysis of bulk sediments using dry grain size fractioning reveals that the majority, by mass, of sediment particles are in the smallest fraction, below 75 microns, and this phenomenon is most pronounced in the upper 2 inches of sediment, (Figure 2). Horowitz et al. reported that the majority of metal contamination is within the smallest fractions (<63 μm) [1]. As the majority of these metal-laden grains are within the top 2 inches, this poses a significant remobilization problem should these sediments be disturbed by flooding or anthropogenic activities, such as dredging. These

particle size analyses may further support post-depositional mobilization as the smallest particles should migrate deeper into the sediments rather than the reverse and may also be microbial mediated.

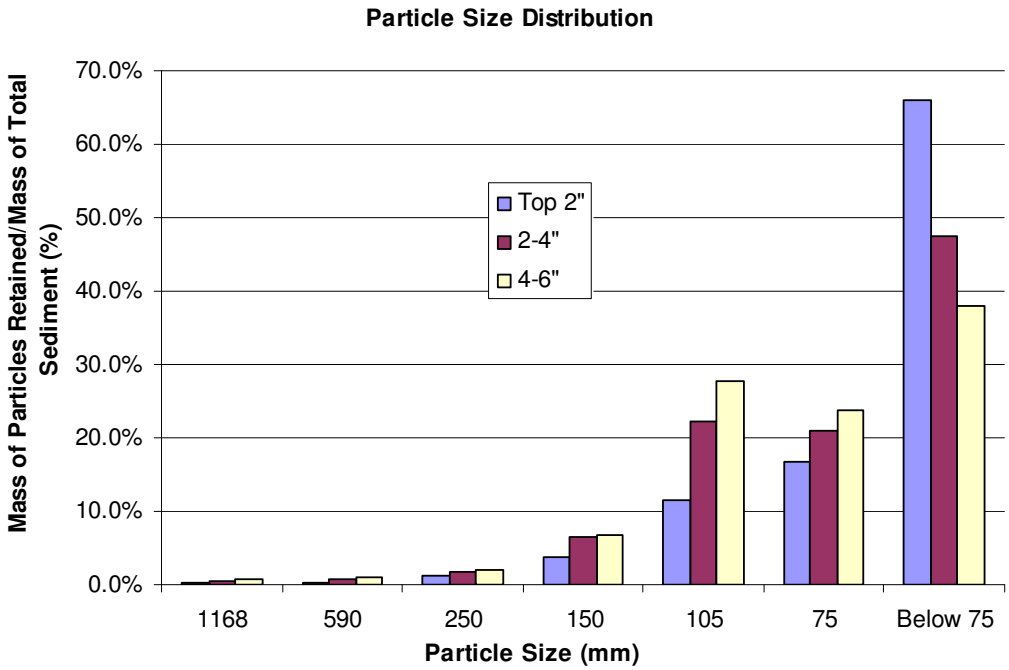

Figure 2: Particle Size Distribution of sectioned bulk sediment using dry sieve technique

Total metal content in this study compares well with reported literature. This site is enriched with high levels of zinc and lead both of which are toxic to biota, (Table 6). Feris et al. found that although seasonal organic nutrients changes had some effect on community structure, the most significant contributor to community change was heavy metal content [11, 48]. Feris et al. did not take into account heavy metal speciation and focused solely on total metal content; this may play an important role in community response in environments where heavy metal speciation plays a greater role in toxicity. While total elemental analysis is important to determine the extent of contamination,

mineral phase and speciation are key to determining the toxicity and bioavailability of heavy metal species.

Table 6:
X-ray Fluorescence Spectroscopic Analysis of Major and Trace Elements in CdA Sediment

Primary Sediment Constituents (% Mass)		Trace Elements (% Mass)	
SiO_2	68.7	CuO	0.014
TiO_2	0.42	ZnO	0.747
Al_2O_3	7.03	PbO	0.467
Fe_2O_3	15.3	Rb_2O	0.008
MnO	1.58	SrO	0.003
MgO	0.93	ZrO_2	0.035
CaO	0.41	Y_2O_3	0.005
Na_2O	0.48	NiO	0.002
K_2O	1.84	Cr_2O_3	0.004
P_2O_5	0.1	BaO	0.077
Sum	96.7	La_2O_3	0.004
LOI* (%)	8.52	CeO_2	0.021
Trace Elements (%)	1.4	ThO_2	0.002

* Loss on ignition

Though obtaining total metal concentration from a contaminated area is necessary to understanding the extent of contamination, determining the phase association of each metal is an integral part in determining bioavailability and its potential for remobilization. The microbial growth and detoxification, and thus biogeochemical cycling contributions, can be linked to mineral phase [43, 44]. X-ray diffraction spectroscopy (XRD) allows the identification of crystalline mineral phases in this contaminated system. A limitation of this technique is that it cannot quantify amorphous mineral phases which may play an equally important role in biogeochemical metal cycling. Bulk sediment analysis using XRD (Figure 3) indicates quartz and siderite as major phases and this is supported in literature [6]. Muscovite [$KAl_2(Si_3Al)O_{10}(OH,F)_2$], jacobsite [$MnFe_2O_4$], and dundasite

$[Pb_2Al_4(CO_3)_4(OH)_8•3H_2O]$ are also shown as minor phases detected in CdA sediments. Due to the relatively high amounts of iron and manganese found in these sediments, jacobsite is not an unexpected mineral. Jacobsite is often associated with hematite [α-Fe_2O_3], magnetite [$Fe^{2+}Fe_2^{3+}O_4$], and coronadite [$Pb(Mn)_8O_{16}$], all of which are found in CdA sediments (Figure 7) [17, 25]. Dundasite is often associated with cerussite [$PbCO_3$], a mineral reported in the CdA mining district.

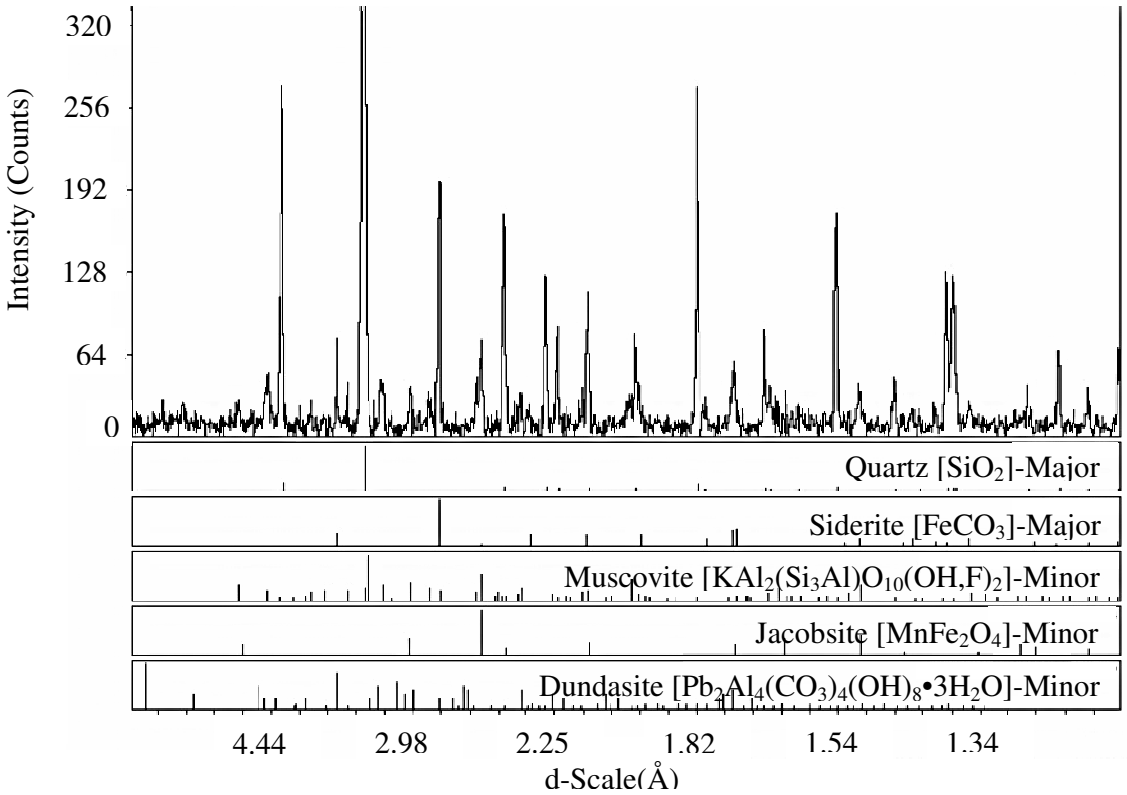

Figure 3: X-ray diffraction of bulk sediments indicating major quartz [SiO_2], siderite [$FeCO_3$]and minor phases muscovite [$KAl_2(Si_3Al)O_{10}(OH,F)_2$], jacobsite [$MnFe_2O_4$], and dundasite [$Pb_2Al_4(CO_3)_4(OH)_8•3H_2O$]

Metal characterization and phase association techniques should also focus on the micro-habitat in which these bacteria reside. A combination of synchrotron based µXRF and µXRD microscopy techniques provide the resolution needed for study on the micron scale. Synchrotron based µXRF provides the means to map the toxic metals in their

associated mineral phases followed by µXRD which allow the identification of these toxic metal bearing mineral phases. However, due to the heterogeneous nature of these sediments it is difficult to elucidate the nature of the mineral phase in all cases, even on the micron scale. Also as a cautionary note, these small scale analyses have limitations in extrapolating to the macroscopic sediments for more generalized hypotheses and should be used with care.

Figure 4 shows the elemental mapping of major heavy metals lead, iron, and zinc. Seven spots, approximately five microns square, were selected for analysis, however, only three (spots A,B,C) contributed meaningful data.

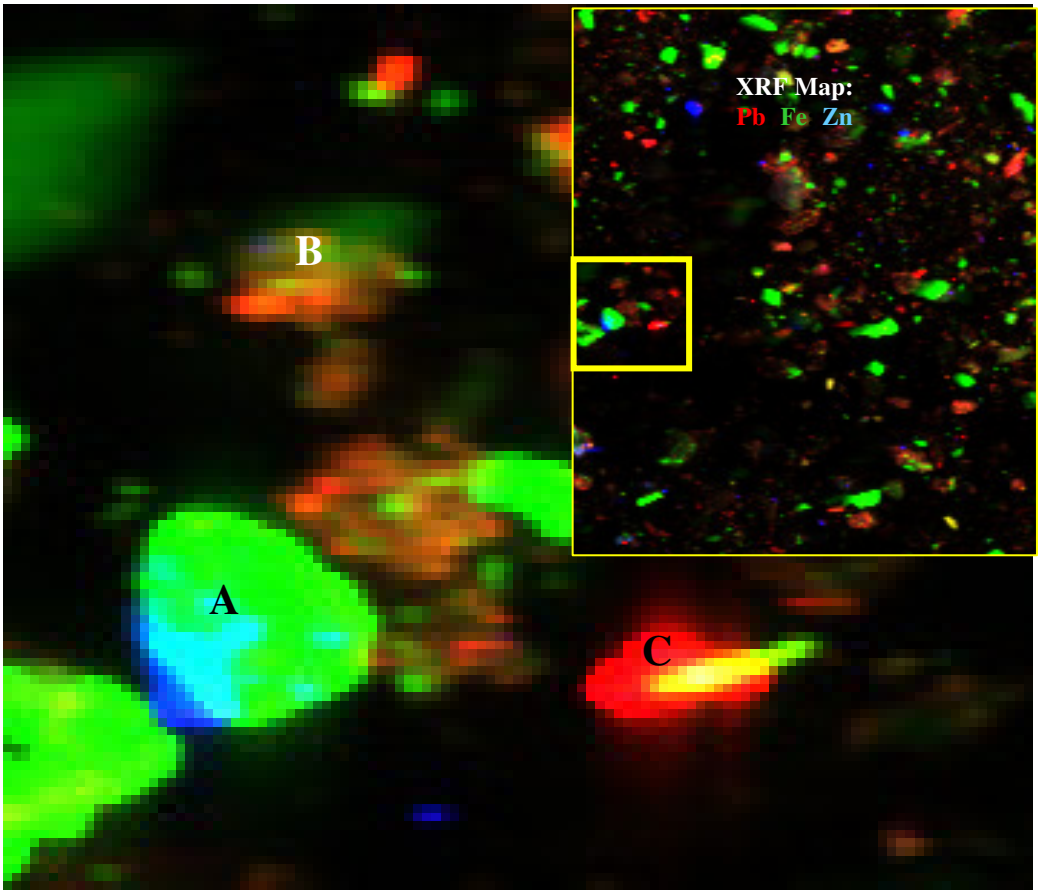

Figure 4: Synchrotron base µXRF with spot size (5X5µm) visualization overlay of elemental mapping of lead (red), iron (green) and zinc (blue)

Spot A shows smithsonite [$ZnCO_3$] and calcite [$CaCO_3$] minerals which are present in other sediments around CdA, (Figure 5) [4, 24]. Bostick et al. found that seasonal changes could effect the partitioning of zinc; sulfidic and carbonate phases predominating in flooded areas while (hydr)oxides were found in oxic, drier soils and sediments [24]. The oxic phase species were somewhat reversible to carbonate and sulfidic under submersion, however a small portion remained in the (hydr)oxide phase [24]. Under oxygenation, zinc is released and can sorb to metal (hydr)oxides, organic phases, sorb to clays and other minerals, or remain free in solution [19]. These changes in speciation and mineral phase illustrated the dynamic geochemical cycling of zinc in this system. Metal carbonates, such as smithsonite, can be formed by biotic means and this mineral type is thought to be mediated by microbes, both in formation and redox-mediated sorbtion changes [24, 37].

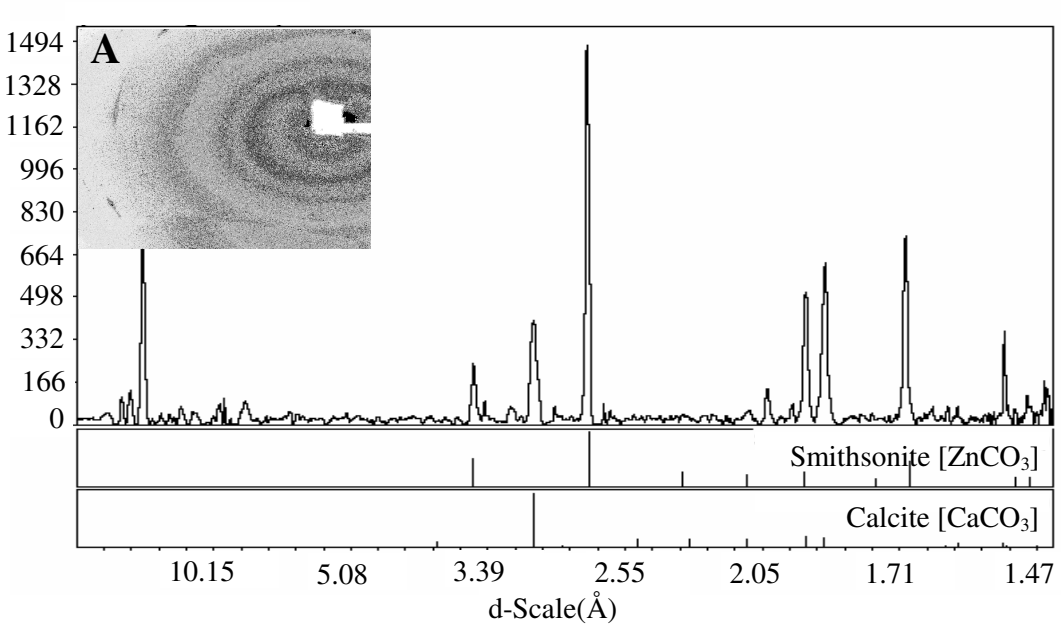

Figure 5: μXRD of spot A indicating smithsonite [$ZnCO_3$] and calcite

Analysis of spot B supports bulk XRD data as muscovite is again found as a mineral phase, (Figure 6). In addition, earlshannonite [$MnFe_2(PO_4)_2(OH)_2 \cdot 4H_2O$], stolzite [$PbWO_4$], and minor phase montmorillonite [$Na_{0.3}(Al,Mg)_2Si_4O_{10}(OH)_2 \cdot 8H_2O$] were revealed. It is unlikely that montmorillonite is a biologically active mineral, however this clay mineral type is known to exchange cations, such as magnesium, with other heavy metal groups and may aid in local metal concentration changes and sequestration and release under changing conditions [49]. Earlshannonite may provide inorganic phosphate to bacteria upon reduction of the iron/manganese hydroxide complex, a nutrient generally limiting in biological systems. Stolzite is often associated with cerussite and anglesite, both reported in the CdA mining district, and is found in tungsten-bearing lead deposits. Biological interactions with stolzite and muscovite are difficult to predict.

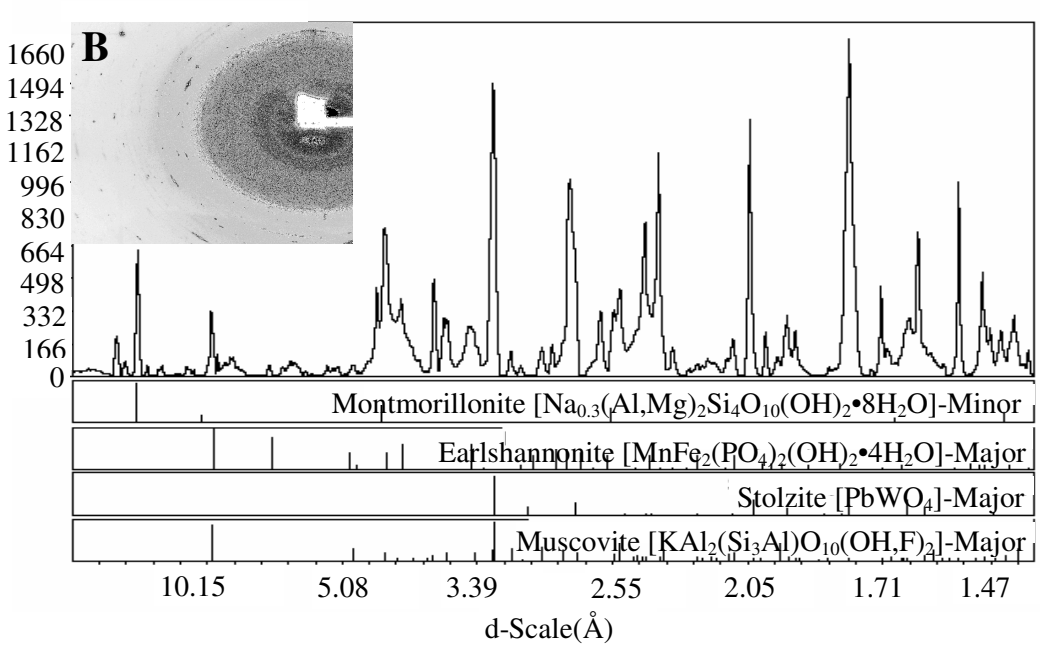

Figure 6: μXRD of spot B indicating major phases muscovite [$KAl_2(Si_3Al)O_{10}(OH,F)_2$], earlshannonite [$MnFe_2(PO_4)_2(OH)_2 \cdot 4H_2O$], stolzite [$PbWO_4$], and minor phase montmorillonite [$Na_{0.3}(Al,Mg)_2Si_4O_{10}(OH)_2 \cdot 8H_2O$]

Mineral phases reported in spot C were coronadite [$PbMn_8O_{16}$], mattheddleite [$Pb_{10}(SiO_4)_{3.5}(SO_4)_2Cl_2$], bindheimite [$Pb_2Sb_2O_7$], manganite [$Mn^{3+}O(OH)$], and diaspore [AlO(OH)], (Figure 7). Finding coronadite further supports bulk XRD analyses as it is often found associated with jacobsite, hematite, and magnetite. Manganite and diaspore show oxyhydroxide phases capable of absorbing toxic metals. The sorption of toxic metals onto these oxyhydroxide phases have been the source of several studies in the CdA area and their presence is not surprising [4, 7, 10]. Additionaly manganite and possibly coronadite may provide a source of manganese for dissimalitory metal reduction. Manganite is probably the product of biological reduction of manganese followed by oxidation to form the oxyhydroxide complex. Mattheddleite, if biologically accessible, may serve as a sulfate source, though in this system sulfate is in sufficiently excessive quantities in aqueous phase as to make this unlikely.

Sediment geochemical analyses reveal several potential mechanisms for remobilization. Remobilization can occur through physical entrainment of the small heavy metal laden particles from the upper sediment column into the river. Secondly remobilization can occur by sorbtion of toxic metals onto oxyhydroxide particles and organic compounds and these complexes are transported in the water column. Finally these oxyhydroxide and organically bound metal-complexes could sorb inside pore spaces of either contaminated or uncontaminated particles and these particles could be transported via erosion and entrainment. These pore spaces are not immune to microbial attack, however, and permanent sequestration for this system is unlikely to occur in the pore space of these sediments. Mineral phases were also identified that may provide bacterial with inorganic phosphates as well as oxidize under oxic conditions to free the

toxic metal, as in zinc. This geochemical analysis helps to better characterize the possible microbial interactions and biogeochemical cycling in CdA sediments. Further studies are warranted to monitor biogeochemical changes on select mineral phases under controlled conditions to develop a more comprehensive knowledge of this complex environment.

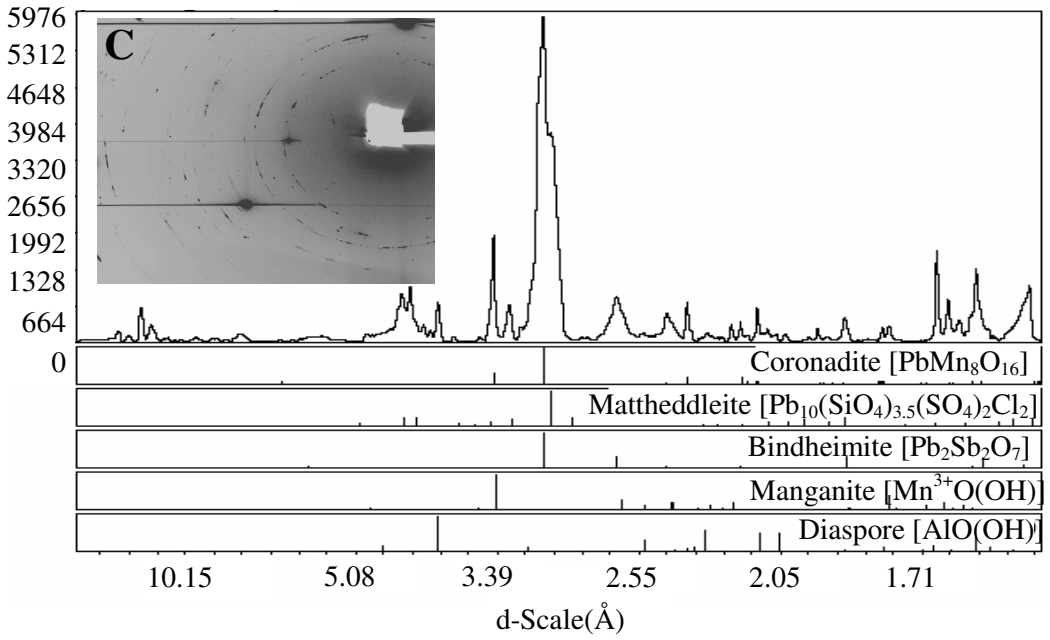

Figure 7: μXRD of spot C indicating coronadite [$PbMn_8O_{16}$], mattheddleite [$Pb_{10}(SiO_4)_{3.5}(SO_4)_2Cl_2$], bindheimite [$Pb_2Sb_2O_7$], manganite [$Mn^{3+}O(OH)$], and diaspore [AlO(OH)]

CHAPTER THREE

FLOW REACTOR STUDY AND CHARACTERIZATION OF BACTERIA

Abstract

A diverse group of organisms were identified using both culture independent and dependant techniques, including *Ralstonia, Pseudomonas, Burkholderia, Paenibacillus,* and *Bacillus* genera. Metals resistant forms of *Pseudomonas, Ralstonia, Burkholderia, Variovorax, Microbacterium,* and *Arthrobacter* species were also identified. A more diverse population of organisms was isolated from batch enrichment cultures when compared to isolates selected from the flow reactor study. Dominant members identified by culture independent techniques were somewhat absent in both batch enrichments as well as flow reactor isolations. Overall this shows a variety of diverse organisms from metal contaminated CdA previously uncharacterized.

Materials and Methods

Media Preparation

Metal toxicity media was prepared according to Sani et al. with some minor modifications [50]. Each liter of media contained 0.41 g sodium acetate (Aldrich), 0.83 g magnesium chloride hexahydrate (Fisher), 0.06 g calcium chloride dehydrate (JT Baker), 1 g ammonium chloride (Fisher), 0.05 g yeast extract (Difco), 0.5 g tryptone (Difco), and 10.93 g PIPES (Aldrich). Iron reducing media was prepared as above but included 1.911 g nitrolotriacetic acid (Acros) and 2.703 g iron chloride hexahydrate (Fisher) added after the media was autoclaved. The pH was then adjusted to 7 using PIPES buffer rather than sodium hydroxide to prevent iron hydroxide formation and filter sterilized using Corning 1 liter 0.2 μm filter system. Media for sulfate reducing bacteria replaces the magnesium chloride hexahydrate with 1.23 g magnesium sulfate heptahydrate (JT Baker) and includes in addition 0.71 g sodium sulfate (Fisher) as the primary sulfate sources.

Media developed to simulate river conditions for the novel flow reactor was prepared with filter sterilized stock solution as follows: 1032 mM magnesium chloride hexahydrate (Fisher), 195 mM ammonium chloride (Fisher), 670.7 mM potassium chloride (Fisher), 1870 mM calcium chloride dihyrate (JT Baker), 1950.4 mM sodium acetate (Aldrich), 786.35 mM sodium sulfate (Fisher), 129.1 mM trisodium nitrolotriacetic acid monohydrate (Acros), 0.583 mM nickel chloride hexahydrate (Fisher), 2.158 mM ferrous sulfate heptahydrate (Fisher), 16.17 mM manganous chloride quadhydrate (Fisher), 4.83 mM cobalt chloride hexahydrate (Fisher), 72 mM sodium molybdate dihydrate (Mallinckrodt), 129 mM boric acid (Fisher), 19.5 mM sodium phosphate dibasic (Fisher), 0.88 mM copper chloride dihydrate (Fisher), 1.151 mM lead chloride (Fisher), 5.87 mM zinc chloride (Fisher), 904.69 mM sodium bicarbonate (Fisher). Filtered stocks were added according to Table 7 and the resulting mixture autoclaved for four hours thirty minutes at 121^{o}C for a 10 L carboy (Brent Peyton, personal communication).

Table 7: Defined Reactor Media

Species	mM Stock	Add µL/L
Nickel Chloride	0.58	5
Copper Chloride	0.88	5
Manganese Chloride	16.17	10
Cobalt Chloride	4.83	10
Sodium Molybdate	72.00	10
Boric Acid	129.00	10
Lead Chloride	1.15	10
Magnesium Chloride	1032.95	1538
Ammonium Chloride	195.04	1538
Potassium Chloride	670.68	1538
Sodium Acetate	1950.40	1538
Trisodium NTA	129.10	10
Sodium Phosphate monobasic	19.50	1538
Calcium Chloride	1870.57	20
Ferrous Sulfate	2.16	50
Sodium Sulfate	786.33	537
Zinc Chloride	5.87	200
Sodium Bicarbonate	904.69	250

Bacteria isolated from the flow reactor were initially grown on a robust media containing 0.41 g sodium acetate (Aldrich) and 30 g tryptic soy broth (Difco) per liter for aerobic and facultative anaerobic bacteria. This robust media as above was amended to suit iron reducing organisms with the addition of 2.63 g iron citrate hydrate (Acros) and 10.93 g PIPES per liter and sulfate reducing bacteria with 1.42 g sodium sulfate (Fisher).

The isolates from agar plates were transferred to a minimal media prepared using trace element solution and mineral solution with basal media as follows. Each liter of basal media was composed of 0.246 g sodium acetate (Aldrich), 0.06 g sodium sulfate (Fisher), 0.02 g sodium bicarbonate (Fisher), 0.004 g sodium phosphate monobasic (Fisher), 0.016 g ammonium chloride (Fisher), and 0.02 g yeast extract (Difco). For pH values of 6-9 1.73g/L of PIPES (Aldrich) buffer was employed.

Each liter of trace metal solution was composed of 0.006 g nickel chloride hexahydrate (Fisher), 0.3 g ferric chloride hexahydrate (Fisher), 0.32 g manganous chloride quadhydrate (Fisher), 0.115 g cobalt chloride (Fisher), 1.742 g sodium molybdate dihydrate (Mallinckrodt), and 0.0004 g trisodium nitrolotriacetic acid monohydrate (Acros). To each liter of mineral solution was added 0.798 g boric acid (Fisher), 1.05 g magnesium chloride hexahydrate (Fisher), 2.75 g calcium chloride dihydrate (JT Baker), and 0.25 g potassium chloride (Fisher). To each liter of basal media 2 mL of mineral solution and 0.1 mL of trace metal solution were added and the resulting mixture autoclaved after adjusting to the pH with either 6 M hydrochloric acid or 2 M sodium hydroxide.

Novel Flow Reactor

All machining and manufacturing was completed at the Engineering Shops onsite at WSU. The flow reactor was composed of stainless steel 1/8" tubing mated to a machined stainless steel top. A polycarbonate plate was fixed to the top to allow for visual inspection of the inlet and outlet. This was sealed with hex-screws and a Viton® O-ring. The stainless steel top was attached to the polycarbonate chamber by an aluminum collar and a second Viton® O-ring. Balge tube septa were inserted and sealed with aluminum plates into the poly carbonate chamber at the sediment water interface and spaced every 1.25 inches, (Figure 8). For a more detailed schematic see appendix A**.**

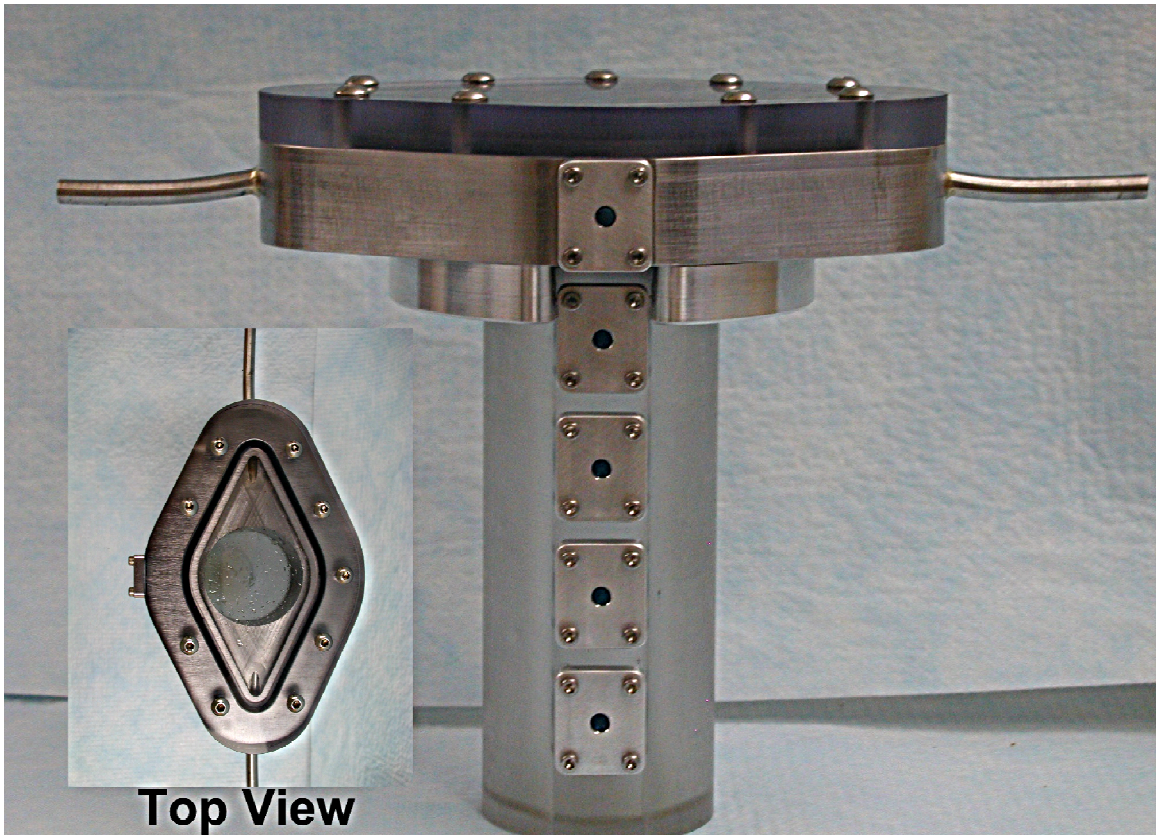

Figure 8: Novel flow reactor consisting of stainless steel top with polycarbonate viewing window and lower polycarbonate chamber with sampling ports sealed with Balge septa

The experimental design setup for the flow reactor consisted of a 10L Nalgene® carboy connected serially by a series of Tygon® tubes to a priming pump (Cole Parmer model 7553-70 6-6000 rpm with EZ load II pump head), operational pump (Cole Parmer Masterflex C/L dual channel pump), rotometer (Gilmont Instruments Inc. correlated flow meter), filter (Gelman Sciences 0.2 μm Sterile Culture Capsule), flow reactor, free-fall drip outlet, and finally to a waste trap and 55 gallon drum see appendix A**.** Glass pipettes were modified to serve as connectors between Tygon® tubing which could be flame sterilized as needed.

The flow reactor was disassembled and sterilized in an autoclave (121^{o}C for 30 minutes) then loaded and reassembled with three homogenized cores (~3 kg) under a sterile laminar flow hood. The reactor was operated at a flow rate of 0.05 mL/min for approximately 20 weeks and operated an additional 15 weeks while cultures were isolated without sampling.

Although the primary purpose of the flow reactor was to simulate fluvial conditions for bacterial enrichments, a variety of analytical procedures were performed on the reactor samples. Approximately two milliliters from each sampling port were extracted weekly and placed in 1.5 mL micro centrifuge tubes. One hundred microliters of sample was removed to measure soluble iron(II) using the ferrozine technique. Samples were then transferred to glass test tubes and sample pH was measured. Samples were re-transferred into their original 1.5 mL micro centrifuge tubes and the samples were centrifuged at 10,000Xg for 3 minutes. Nine hundred microliters were removed and was divided into 300 μL for ion chromatography (Dionex DX-500) and 600 μL was acidified in 1 mL 3% nitric acid for inductively coupled plasma-mass spectrometry

(Agilent 4500+ Quadrupole ICP-MS). Ion chromatography samples were spiked with 1.5 mM sodium acetate, 0.25 mM sodium sulfate, 0.1 mM sodium nitrate, 0.015 mM sodium nitrite, and 0.03 mM sodium phosphate with appropriate controls and this was used to determine aqueous concentrations of acetate, nitrite, sulfate, phosphate, and chloride, see appendix B for method information. Inductively coupled plasma-mass spectrometry was used to determine aqueous concentrations of manganese, lead, copper, and zinc using certified reference solution standards for each metal (Fisher).

Isolation and Sequencing of Novel Coeur d'Alene Organisms

Isolates from frozen sample cores were performed in addition to flow reactor studies, hereafter referred to as batch cultures. A single frozen core was taken, thawed, and homogenized. Aerobic, iron reducing, and sulfate reducing media types based on metal toxicity media as discussed above and were spiked with lead, zinc and copper to achieve 0, 0.01, 0.1, and 0.5 millimolar metal concentrations with a heat killed control duplicated for a total of 30 bottles. Thawed sediments were added to each bottle (5.24±0.28 g of sediment), sealed with sterile cotton plugs (aerobic media) or sealed with butyl rubber septa and sparged with 15 psig of nitrogen for 25 minutes in the case of sulfate and iron media types. Sparged bottles were then pressurized to 15 psig with nitrogen to maintain anaerobic conditions. Bottles were incubated in darkness on a Thermolyne BiggerBill shaker table at 100 rpm.

Cell concentrations from aerobic batch cultures were diluted 10,000 and 100,000 fold in a sterile 0.89% NaCl solution and 50 µL of this salt solution was plated onto agar plates consisting of metal toxicity media as above, 15 g select agar (Invitrogen), and a final concentration of 0, 0.01, 0.1, and 0.5 millimolar filter sterilized lead, copper, and

zinc solutions (added post-autoclaving) per liter. Single colonies were picked and transferred into serum bottles containing metal toxicity media and the process was repeated to ensure purity of cultures.

Due to the low concentrations of cells in the reactor, bacteria isolated from the flow reactor were first spread directly after sampling onto agar plates containing 40 g tryptic soy agar (Difco) and 0.41 g sodium acetate (Aldrich) per liter. Plates were incubated at room temperature. Single colonies were picked and transferred to serum bottles containing 30 g/L Difco tryptic soy broth (TSB). Once growth was observed in the serum bottle cultures this process was repeated and single colonies from the second plating were taken as pure and transferred into serum bottles containing TSB.

From both flow reactor and batch serum isolation bottles, 3 mL of cell culture was extracted and spun at 5000Xg for 3 minute to pellet the cells. Genomic DNA was extracted using Promega Wizard® Genomic DNA purification kit as per kit instructions. The presence of extracted DNA was confirmed using gel electrophoresis.

Each electrophoretic gel was prepared using 0.5 g of Ultrapure™ Agarose (Invitrogen) per 50 mL of 1X TAE buffer (2-Amino-2-(hydroxymethyl)-1,3-propanediol-acetate-ethylene-diamine-tetraacetic acid), heated until molten, and cooled to approximately 50^{o}C, at this time 3 μL of 10 mg/mL ethidium bromide was added before pouring into the gel apparatus (Bio-Rad mini sub cell GT electrophoresis apparatus) for gelling. Electrophoretic gels were run at a constant 80 volts for 45 minutes using an EC105 voltage controller.

Once DNA concentrations were verified, extracted DNA concentrations were amplified using polymerase chain reaction (PCR). Two microliters of DNA was added to

9.7 µL of a solution containing 1X PCR buffer (Invitrogen), 0.2 mM of each DNTPs (Fermentas), 1.5 mM $MgCl_2$ (Invitrogen) per 50 µL reaction mixture. In addition, 0.5 µL (2.5 units) of DNA Taq polymerase (Invitrogen), 2 µL (25 picomoles) of each primer, and 33.8 µL of DNA free water (Bioexpress) were added to the reaction mixture for a total of 50 µL reaction mixture. Universal bacterial primers (Invitrogen) BAC8F (5'-AGAGTTTGATCCTGGCTCAG-3') and BAC1492R (5'-GGTTACCTTGTTACGACTT-3') were used in PCR amplification targeting the 16S rDNA genes. PCR amplification was performed on a Peltier gradient thermal cycler (MJ Research PTC-200) using the following protocol; denaturing at 94°C for 4 minutes, 30 cycles of 94°C for 1 minute, 55°C for 1 minute, and 72°C for 1 minute 30 seconds, and finally a 72°C annealing step for 20 minutes. PCR products were verified using gel electrophoresis as above. Amplified PCR products were purified using gel filtration cartridges (Performa® DTR Edge Biosystems) as per BigDye™ protocol and amplified using a single forward primer BAC8F and the BigDye™ reagents as follows; 25 cycles of 96°C for 10 seconds, 50°C for 15 seconds, and 60°C for 4 minutes. Products from the fluorescent labeled BigDye™ protocol were again purified using gel filtration cartridges and analyzed using an ABI 373 automated DNA sequencer at Washington State University's DNA sequencing facility.

Bacterial sequences were analyzed using National Center for Biotechnology Information and Ribosomal Database Project databases using Basic Local Alignment Search Tool (BLAST) and Sequence Match tools for comparison. See appendix C for complete sequences. Selected organisms were imaged at the Electron Microscopy and Imaging Center user facility at WSU. Unstained whole cells were mounted on 200 mesh

carbon-formvar coated copper grids, air dried, and imaged on a transmission electron microscope (JEOL 1200EX). Repeated attempts to operate the X-ray microanalysis probes attached to the TEM met with failure so no X-ray analyses are included in this study.

Results and Discussion

Novel Flow Reactor

The flow reactor was operated continuously for 20 weeks with a variety of sampling analyses. An examination of the average normalized metals profile compares relatively well with reported trends in literature, with lead, zinc, and manganese species increasing with depth, (Figure 9) [1, 2, 21].

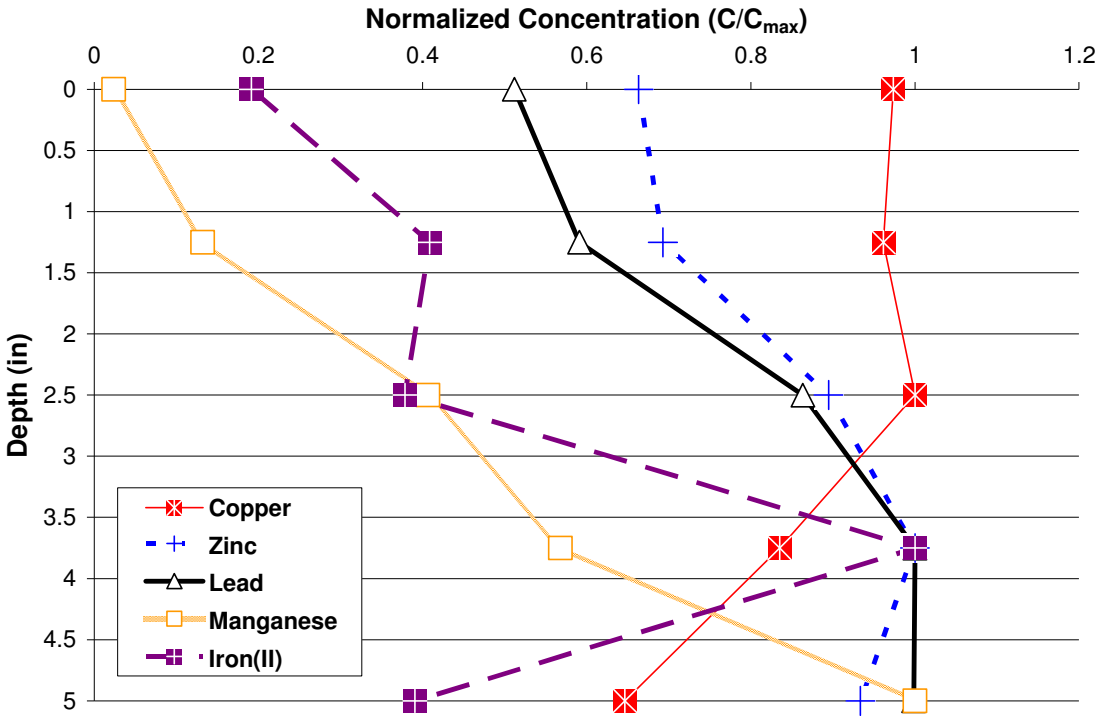

Figure 9: Average normalized concentrations from the flow reactor of copper, lead, zinc, iron, and manganese with depth. C_{max} (ppm): Cu (0.009), Pb (0.095), Zn (0.458), Mn (54.55), Fe (14.95)

Copper appears to change very little within the first 2.5 inches of depth in the reactor, then rapidly approach a minima at the bottom of the reactor. Iron appears to approach a maximum at sampling port E which corresponds to 3.75 inches in depth from the sediment-water interface. Visual inspection of this point shows the highest (darkest) concentration of what appear to be iron (hydr)oxides, (Figure 10).

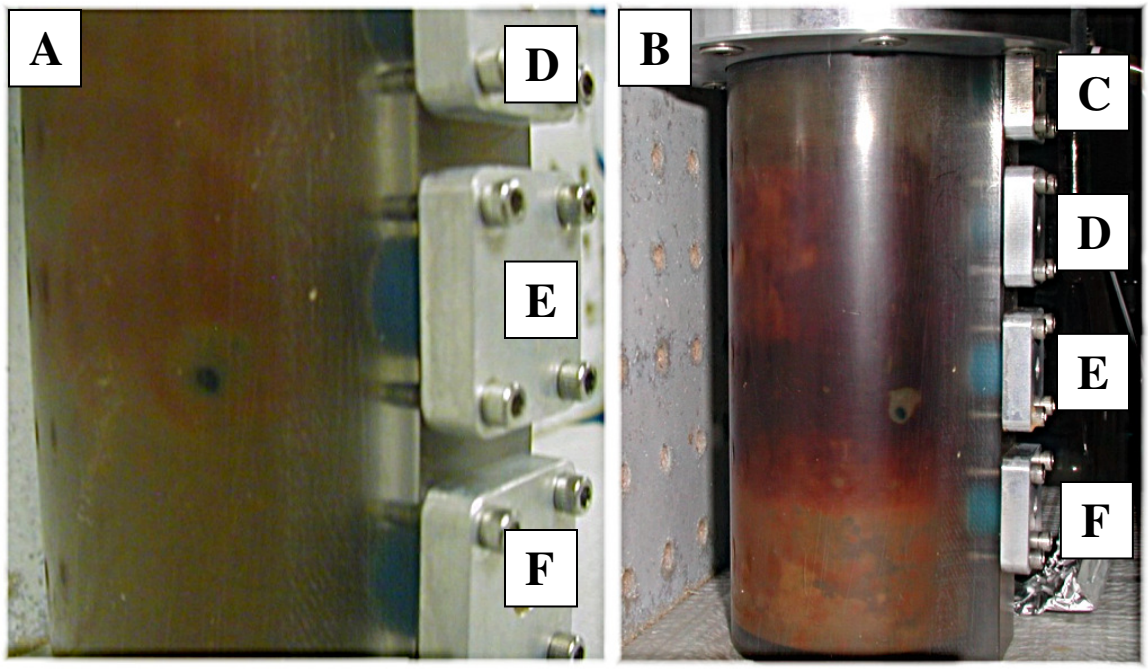

Figure 10: Novel flow reactor from a side view at 10 (A) and 32 (B) weeks operation with sampling ports C, D, E, and F corresponding to 1.25, 2.5, 3.75, and 5 inches in depth from the sediment-water interface.

At approximately 3.75 inches from the sediment-water interface (sampling port E), the pH also reached a local minimum compared to the surrounding sampling port values (Appendix B). This is of interest as iron reducing organisms should create a zone of alkalinity rather than acidity as we see here, though soluble iron concentrations at this point reach a maximum. However iron reduction may be coupled with abiotic formation

of goethite [FeO(OH)] and hematite [Fe_2O_3] which can result in a net production of hydrogen ions, as in equations 1, 2, and 3 respectively [51-53].

$$2Fe(OH)_3 + 6H^+ \rightarrow 2Fe^{2+} + 6H_2O \quad (1)$$
$$Fe^{2+} + 2H_2O \rightarrow FeO(OH) + 3H^+ \quad (2)$$
$$Fe^{2+} + 3H_2O \rightarrow Fe_2O_3 + 6H^+ \quad (3)$$

Geochemical modeling software PHREEQC 2.11 predicts the formation of both goethite and hematite mineral phases at the reactor conditions from sampling port E, supporting this theory, (Appendix E). These results should be used with caution as this is a complex system and modeling software though greatly useful cannot predict all interactions between all species.

Bacterial Isolations

The bacteria in the CdA area are capable of growth in this contaminated environment though at significantly lower numbers and less microbial diversity than from similar pristine areas [26]. Typical microbial abundance numbers in CdA sediments range between 10^5 and 10^8 cells/g wet sediment, a shift of between 10 and 100 times reduction from metal free controls [9, 22]. Novel genera and species have been identified from the CdA area [9, 18, 28]. Lead resistant forms of *Pseudomonas, Bacillus, Cotynebacterium*, and *Enterobacter* have been identified [26] and genera *Pseudomonas*, *Ralstonia, Burkholderia, Microbacterium*, and *Variovorax* tolerant to lead copper and zinc were also isolated and identified from batch cultures, (Table 8).

During the isolation process, organisms removed from the reactor showed significant lag time and diminished growth on media identical to that of the reactor, suggesting nutrient stress. To avoid nutrient stress, 20 mg/L of yeast extract was amended to the minimal reactor media to aid growth of the isolated organisms in batch

culture, as once isolated, these organisms could no longer obtain nutrients from either the sediments or other members of the microbial community inside the reactor.

Table 8: Batch Culture Microbial Diversity

Growth Condition	Taxon	Similarity Index
no metals	*Pseudomonas fluorescens strain*	0.968
no metals	*Pseudomonas fluorescens strain*	0.973
no metals	*Pseudomonas* sp. *PHLL.*	0.927
no metals	*Pseudomonas plecoglossicida; S22.*	0.897
0.01 mM Pb, Cu, Zn	*Microbacterium oxydans*	0.917
0.01 mM Pb, Cu, Zn	*Pseudomonas marginalis; JH8*	0.955
0.01 mM Pb, Cu, Zn	*Pseudomonas* sp. *WDL5*	0.931
0.1 mM Pb, Cu, Zn	*Ralstonia* sp. *C6*	0.965
0.1 mM Pb, Cu, Zn	*Burkholderia pyrrocinia*	0.964
0.1 mM Pb, Cu, Zn	*Variovorax* sp.	0.957
0.1 mM Pb, Cu, Zn	*Burkholderia pyrrocinia*	0.918

Table 9: Bacteria isolated from flow reactor with depth

Reactor Depth (in)	Taxon	Similarity Index
1.25	*Bacillus pumilus*	0.954
1.25	*Bacillus* sp *P54-2*	0.934
1.25	*Pseudomonas fluorescens*	0.954
2.5	Uncultured bacterium *(Bacillus genus)*	0.969
2.5	*Bacillus megaterium*	0.952
3.75	*Arthrobacter* sp. *Tibet-IIR23*	0.953
3.75	*Bacillus pumilus*	0.948
5	*Paenibacillus* sp. *S18-36*	0.926
5	*Bacillus* sp. *Y17*	0.964

Analysis of the *rpo*B gene from CdA soil extracted DNA show that the dominant genus in these sediments may be *Ralstonia eutropha*, a well known metal tolerant organism isolated from other metal contaminated areas, (Table 10) [54, 55]. Interestingly, Brim et al. found that although *Ralstonia eutropha* had been the dominant isolated organism from Maathedie soil in Lommel, Belgium, in his 1999 study using both culture dependant and independent techniques, *Arthrobacter* genus appeared to be dominant suggesting a displacement of the former by the latter [55]. There are a variety

of possible explanations for this occurrence including resistant plasmid gene transfer, biases in identification and culturing techniques, and an overall decrease in total zinc concentration with time. This data may indicate that *Arthrobacter* is an important member of recovering, heavy metal contaminated soils.

Genera *Pseudomonas*, *Paenibacillus*, and *Burkholderia*, were also identified and match identifications from 16S rDNA analysis from both batch cultivations and isolations from the flow reactor, (Tables 8-10). *Bacillus* species are a well characterized organisms in the CdA area and although appear to be the dominant organisms in the reactor and this may be due to media selection or temperature effects as the reactor was operated at room temperature [26, 39, 46]. The isolates selected from the reactor (Table 9) may follow the r-strategist metabolic methodology and grow very quickly when nutrients are available and thus are primarily selected when grown on agar plates as they rapidly outgrow their slower growing counterparts [40]. Indeed, it was observed that even after colonies had been selected for this study that additional colony growth of different morphology was observed on these plates after several days. These late-growing colonies were never identified and it may be of interest to explore this phenomenon in future work. It is also interesting to note that the majority of isolates identified from the reactor fall into the category of Gram-positive bacteria.

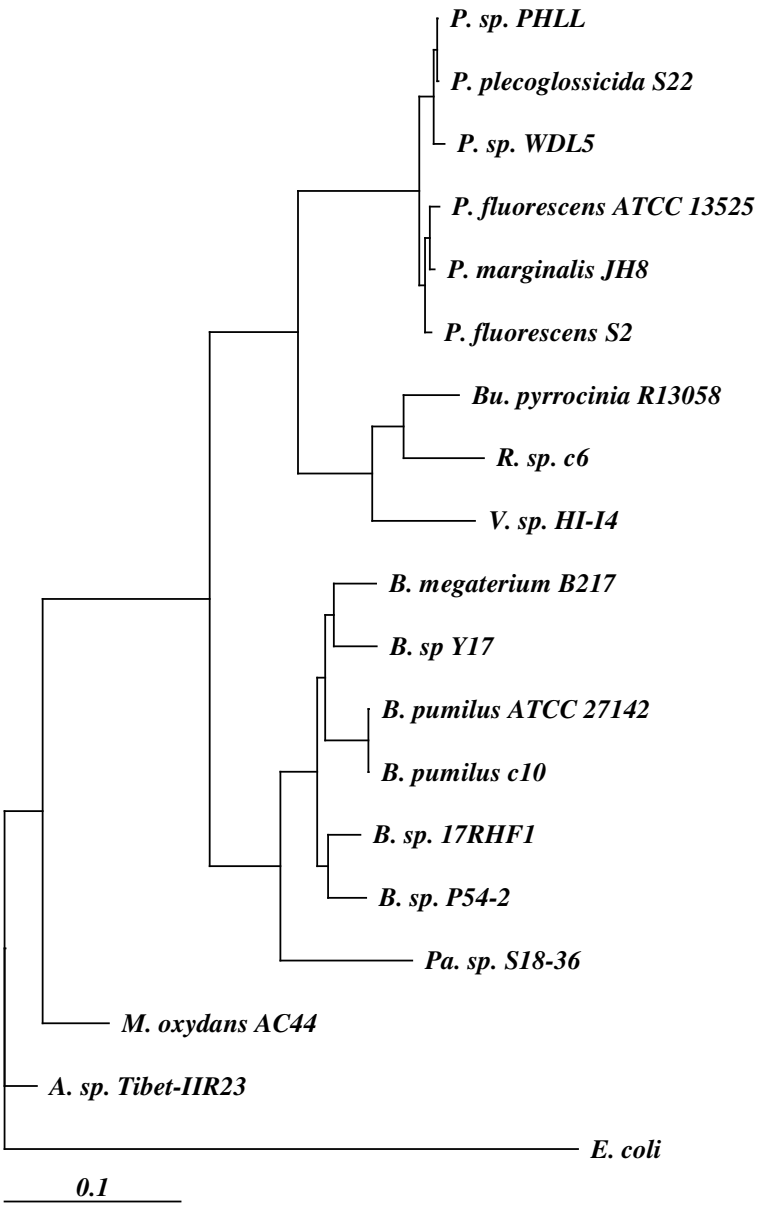

Figure 11: Phylogenetic tree of bacteria most closely related to isolates from both reactor studies and batch enrichment cultures. Abbreviated genus names: P=*Pseudomonas*, Pa=*Paenibacillus*, B=*Bacillus*, Bu=*Burkholderia*, R=*Ralstonia*, V=*Variovorax*, M=*Microbacterium*, A=*Arthrobacter*, E=*Escherichia*.

The genera *Bacillus* are Gram-positive rods and are considered low G-C organisms, typically containing about 40% G-C concentrations [29]. They are capable of surviving on a variety of substrates and are spore forming bacteria able to withstand harsh

environmental conditions while in this form [29]. Some *Bacilli* including *Bacillus megaterium* are considered mesophilic organisms and others such as *Bacillus thuringgiensis* are known to be toxic to insect larvae, and are introduced to plants to act as an insecticide [29]. *Bacilli* from CdA have been characterized and are capable of intracellular precipitation of heavy metals [26, 39].

Table 10: Bacterial diversity of soil extracted DNA using the *rpoB* gene

Taxon (% similarity)	Frequency	Physiological characteristics
Ralstonia eutropha (97%)	20/67	Chemoautotrophic metal-tolerant
Dechloromonas aromatica (92-98%)	18/67	Degrades aromatic compounds such as benzene, toluene, benzoate, and chlorobenzoate
Pseudomonas sp. (90-98%)	14/67	Opportunistic pathogen, and can degrade variety of compounds
Escherichia coli (98-99%)	6/67	Well known organism
Azoarcus sp. (95-96%)	3/67	Aromatic compounds degradation
Paenibacillus sp. (97%)	2/67	Associated with infections - septicaemia, meningitis, pneumonia
Comamonas testosteroni (93%)	3/67	Degrades aromatic compounds such as p-toluenesulfonate and toluenecarboxylate
Burkholderia pseudomallei (97%)	1/67	Saprophytic, gram-negative aerobes

Metal resistant *Pseudomonas* spp. have been isolated from the CdA area, (Tables 8,9) [39]. Possible metal sequestration (α) can be seen in Figure 12B with species which most closely relates to *Pseudomonas* sp. WDL5 while metal stress may triggers a phenotypic response in *Pseudomonas marginalis*, roughening the cell membrane. *Pseudomonas* spp. studied from other metal contaminated areas possess a variety of detoxification mechanisms [30, 34, 37, 39]. *Pseudomonas marginalis* and other *Pseudomonas* spp. are known to produce EPS as a biofilm which bind heavy metals and prevent them from entering the cell [39, 41]. *Pseudomonas* spp. use efflux mechanisms

to prevent toxic concentrations of metals from accumulating in the cell [30]. Perhaps one of the most interesting characteristics, which *Pseudomonas* shares with *Escherichia coli*, is the ability to sequester copper in the periplasmic space and outer membrane using a four-protein complex; turning the cell blue with increasing copper concentrations [30]. It is theorized that the sequestration of copper stems from an evolutionary mechanism to retain copper in times where it is scarce in the environment [30].

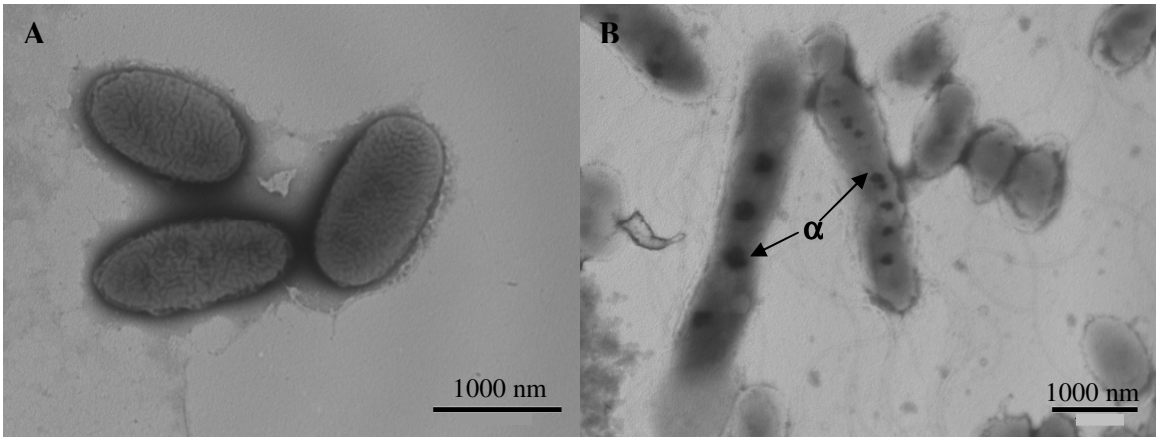

Figure 12: Transmission electron microscopy of whole cells A) *Pseudomonas marginalis* JH8 (0.955) **B)** *Pseudomonas* sp. WDL5 (0.931) with possible metal inclusions(α).

Ralstonia spp. are well known metal tolerant bacteria isolated from a variety of metal contaminated sites [30, 33-35]. This genera possess two megaplasmids upon which the majority of their metal resistance is derived [30, 33, 35]. *Ralstonia* spp. rely mainly on efflux to detoxify their environment and are also known to produce carbonate precipitates [30, 33, 35, 37]. *Ralstonia* is also known to sequester copper [56]. Figure 13A shows species most closely related to *Ralstonia* sp. C6 which shows a lack of metal inclusions suggesting that efflux is in fact the mechanism of detoxification for this organism.

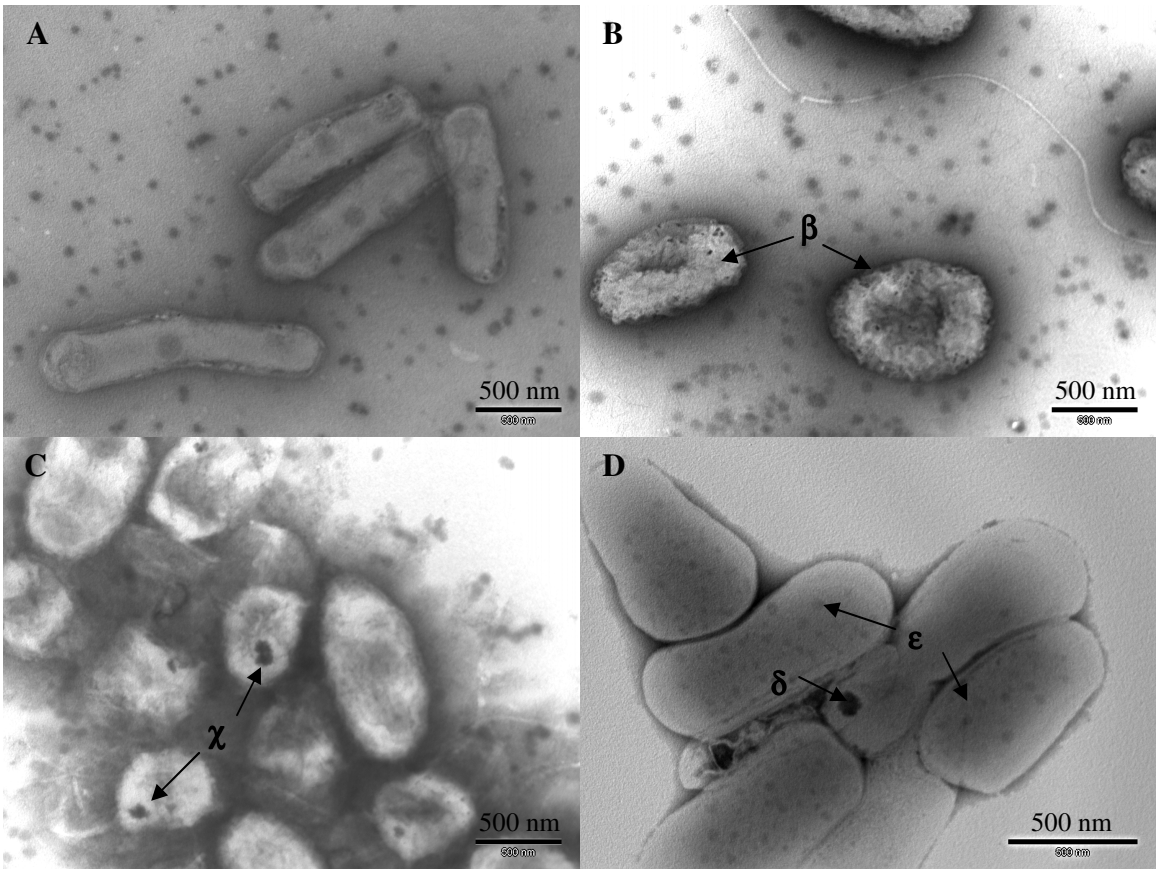

Figure 13: Transmission electron microscopy of whole cells A) *Ralstonia* sp.; C6 (0.965) **B)** *Burkholderia pyrrocinia* (0.964) with roughened membrane (β) **C)** *Variovorax sp.* (0.957) with metal possible inclusions (χ) **D)** *Microbacterium oxydans* (0.917) with possible metal inclusions (δ), (ε)

Burkholderia spp. have mainly been studied for their ability to degrade halogenated hydrocarbons with some attention to metal resistance, however little has been reported about their mechanisms for detoxifying metals [41, 57, 58]. *Burkholderia* spp. are known to produce biofilms which trap nutrients and heavy metals favoring lead over other metals [41]. Figure 13B shows *Burkholderia pyrrocinia* with a roughened cell wall and deformation of the cell wall, possibly in response to stress (Figure 13B, β) however the detoxification mechanism for this organism remains unknown.

Both *Variovorax* sp. *and Microbacterium oxydans* grow in the presence of metals but literature is scarce on metal resistance mechanisms for these genera. Both genera

(see fig. 14C, χ, 14D, δ) show what may be relatively large metal precipitates similar to *Pseudomonas* sp. WDL5 (see fig. 13B, α) and *Bacillus megaterium* [39] which suggests a similar mechanism of metal sequestration. *Microbacterium oxydans* also shows smaller inclusions which may suggest a second mechanism (see fig. 14D δ,ε), however without elemental analysis of the inclusion bodies for all specimens and proper controls these mechanisms are only speculation.

Arthrobacter genera are a ubiquitous soil organism isolated from a variety of contaminated and non-contaminated sites [36, 40, 55, 59-64]. *Arthrobacter* spp. are Gram-positive, pleomorphic bacteria which can metabolize a wide variety of substrates including herbicides, caffeine, nicotine, phenols and other unusually organic compounds [29]. This genera has a high G-C count, typically 60-70% [29]. *Arthrobacter* have been used in studies of metal biosorbtion, production of EPS which bind metals, and reduction of chromium at low temperature [32, 60, 65-67]. *Arthrobacter* species have been thought to displace more metal tolerant genera when metal concentrations begin to decrease [55]. This may indicate that *Arthrobacter* is an important transition bacterium in recovering contaminated sites.

Using culture independent techniques such as soil DNA extraction and analysis and batch and continuous flow reactor culturing techniques reveal a variety of organisms previously uncharacterized in the CdA area and these microbes possess a variety of metal detoxification mechanisms. It appears that batch culture techniques provided the most diverse populations when compared to flow reactor isolations and these differences may be due to media composition, colony time selection, and other factors. As expected, culture independent techniques show the most diverse populations illustrating the limited

knowledge which is had concerning microbe-microbe interaction, nutrient requirements, and beneficial community interactions.

CHAPTER FOUR

DUAL-MONOD KINETIC MODEL OF METAL INHIBITION

Abstract

Zinc is a toxic metal present in CdA sediments and poses a significant threat to biota and microorganisms which are the base of the food-chain. Because of its bioavailability and relatively high solubility, zinc is one of the most toxic of heavy metals under neutral pH. *Arthrobacter* species have been isolated and identified from a variety of contaminated sites including CdA and are capable of growth in the presence of zinc. Toxicity to *Arthrobacter* may stem from a variety of causations and is heavily dependant on pH and zinc speciation. *Arthrobacter* poses some capacity for sorbtion of zinc and has been used in other studies with copper, iron, and cadmium in acidic media. Kinetic expressions using a dual-Monod form can model batch kinetic data with good results.

Introduction

Zinc is used in dietary supplements, galvanizing, and many other industrial and non-industrial processes. In the body, zinc aids in immune protection and anti-aging and becomes less available with age [68]. Zinc is not stored in the body and the average amount in an adult body is between 1.4-2.3 grams [68]. Zinc is an essential trace element used for DNA-binding proteins and protecting the cell from oxidative stress in superoxide dismutase complexes [30].

The solubility of zinc makes it very bioavailable and it is hypothesized that because of its high solubility and availability under normal conditions and neutral pH, zinc may be the most toxic of heavy metals [35]. In fact zinc has exhibited the highest toxicity over lead, copper, cadmium, nickel, and manganese in studies with *Pseudomonads*, *Micrococci*, and *Bacilli* in crude oil and aromatic hydrocarbon degradation [69, 70]. Zinc is taken up by the cell via several fast and unspecific Mg^{2+}

transporters [30]. Zinc may be introduced into the cell by the Mgt E family of transporters which are present in a few gram-positive and negative bacteria and are regulated by a chemiosmotic gradient [30]. Zinc also may be favored over magnesium in the Mgt A P-type ATPase transport system, a system designed for uptake of magnesium under magnesium limited conditions however this is not a primary uptake channel for zinc [30]. Zinc efflux mediated detoxification is thought to occur through two transport systems, a P-type ATPase and RND-driven transporters, and is found in metal tolerant organisms such as *Ralstonia* [30]. Zinc was selected for this study because of its high concentration in CdA sediments and porewaters (Tables 3, 5, 18, 21) where bacteria reside and the potential for high toxicity to these organisms.

Arthrobacter genera are a ubiquitous soil organism isolated from a variety of contaminated and non-contaminated sites [36, 40, 55, 59-64]. *Arthrobacter* spp. are Gram-positive, pleomorphic bacteria which can metabolize a wide variety of substrates [29]. This genera has a high G-C count, typically 60-70% [29]. *Arthrobacter* species have been used in metal biosorbtion, production of EPS which bind metals, and metal studies of reduction of chromium at low temperature [32, 60, 65-67]. *Arthrobacter* species have been thought to displace more metal tolerant genera when metal concentrations begin to decrease [55]. This may indicate that *Arthrobacter* is an important transition bacterium in recovering contaminated sites. The *Arthrobacter* isolate from the flow reactor studies was selected for further studies due to its potential capacity for metal resistance/reduction and its presence in other contaminated environments as the dominant microbial member [32, 55, 64-67, 71].

Materials and Methods

Media Preparation

Both *Arthrobacter* species (environmental isolate and ATCC 21908) were grown on a minimal media prepared using trace element solution and mineral solution with basal media as follows. Each liter of basal media was composed of 0.246 g sodium acetate (Aldrich), 0.06 g sodium sulfate (Fisher), 0.02 g sodium bicarbonate (Fisher), 0.004 g sodium phosphate monobasic (Fisher), 0.016 g ammonium chloride (Fisher), and 0.02 g yeast extract (Difco). For pH values of 6-9 1.73g/L of PIPES (Aldrich) buffer was employed. Each liter of trace metal solution was composed of 0.006 g nickel chloride hexahydrate (Fisher), 0.3 g ferric chloride hexahydrate (Fisher), 0.32 g manganous chloride quadhydrate (Fisher), 0.115 g cobalt chloride (Fisher), 1.742 g sodium molybdate dihydrate (Mallinckrodt), and 0.0004 g trisodium nitrolotriacetic acid monohydrate (Acros). To each liter of mineral solution was added 0.798 g boric acid (Fisher), 1.05 g magnesium chloride hexahydrate (Fisher), 2.75 g calcium chloride dihydrate (JT Baker), and 0.25 g potassium chloride (Fisher). To each liter of basal media 2 mL of mineral solution and 0.1 mL of trace metal solution were added and the resulting mixture autoclaved after adjusting to the pH with either 6 M hydrochloric acid or 2 M sodium hydroxide.

Stock solutions of 5 and 40 mM zinc chloride were prepared and acidified with 6N hydrochloric acid. Zinc concentrations were added to serum bottles post-autoclaving to minimize complexation or precipitation at high temperature.

Batch Experiments

General growth trends were first observed with the *Arthrobacter* sp. reactor isolate to determine time to complete lag-phase, growth-phase, stationary-phase, and death-phase and this information was used to design further experiments. An inoculum size and age were selected as 5% of the total volume (5 mL/100 mL) and late exponential/early stationary-phase (40±8 hrs), respectively.

In all cases zinc testing was performed using the spectrophotometric ZincoVer® reagent method (Hach) and was modified to suit the needs of the experiment. The detection limit for this method is listed as 0-2 mg/L. Sample volumes were adjusted to dilute them into this range; typically 100 µL of sample was diluted in 900 µL of 18Ω deionized water. ZincoVer® 5 reagent pillows were concentrated into a stock solution consisting of 1 pillow per 10 mL. In short, 1 mL of diluted sample volume was added to 1 mL of concentrated Zincover® 5 reagent solution and vortexed for 20 seconds to mix. One hundred µL of cyclohexanone was then added to the mixture, vortexed for an additional 30 seconds, and allowed to incubate for 3 minutes. The reacted mixture was analyzed on a spectrophotometer at 620 nm. Calibration standards were prepared in the same manner as samples from stock solutions of 5 and 40 mM zinc chloride.

Preliminary screening of zinc inhibition was performed in butyl rubber septa sealed 100 mL serum bottles with metal concentrations of 0, 0.01, 0.1, 0.25, 0.5, 1, and 1.5 mM. No growth was observed with concentrations 0.25 and over so this was taken as the minimum inhibitory concentration (MIC) for further studies. This experiment was repeated twice, once by adding in 0.05 and 0.175 mM zinc concentrations and omitting all concentrations above 0.25 mM from the original screen and the second by the addition

of 0.005 mM. Additionally, the effects of metal concentration on growth phase/cell concentration were examined. One hundred milliliter serum bottles were inoculated and sacrificial bottles were spiked with 0.25 mM zinc at 10, 17, 24 hours. To examine the toxicity effects of zinc speciation on *Arthrobacter*, pH values of 6-9 were selected. The IC_{50} value (0.05 mM) was used as the test concentration as growth was expected to be observed even under the inhibition effects of pH. Comparison inhibition studies were performed with *Arthrobacter* sp. ATCC 21908, a bacterium isolated from an oil contaminated beach, using metal concentrations of 0.005, 0.01, 0.05, 0.1, 0.175, and 0.25 mM.

Results and Discussion

Zinc Inhibition of *Arthrobacter sp*

Effect of Metal Concentration on Growth

Zinc appears toxic to the *Arthrobacter* isolate even at very low concentrations and zinc toxicity at low concentration has been reported in other work [69, 70]. In fact the majority of toxicity, greater than 40%, is due to less than 2% of the MIC concentration value, (Figure 14). Comparable studies using cultures from ATCC 21908 reveal that only 27% inhibition was observed at zinc concentrations of 0.25 mM. Though the magnitudes differ between reactor isolate and ATCC culture, the general trends are the same with asymptotic inhibition at very low concentrations and liner regions for mid to high concentrations of zinc, though this is less pronounced in the ATCC cultures. The quality of high toxicity of zinc at low concentration has been reported in other works and is greatly linked to pH [69, 72]. Toxicity of zinc to *Arthrobacter* seems to be greatly linked to cell concentration and/or growth phase. During one metal inhibition run the

same volume of inoculum but slightly greater cell concentration was added which resulted in growth at the MIC value, shown as the triangle in Figure 14.

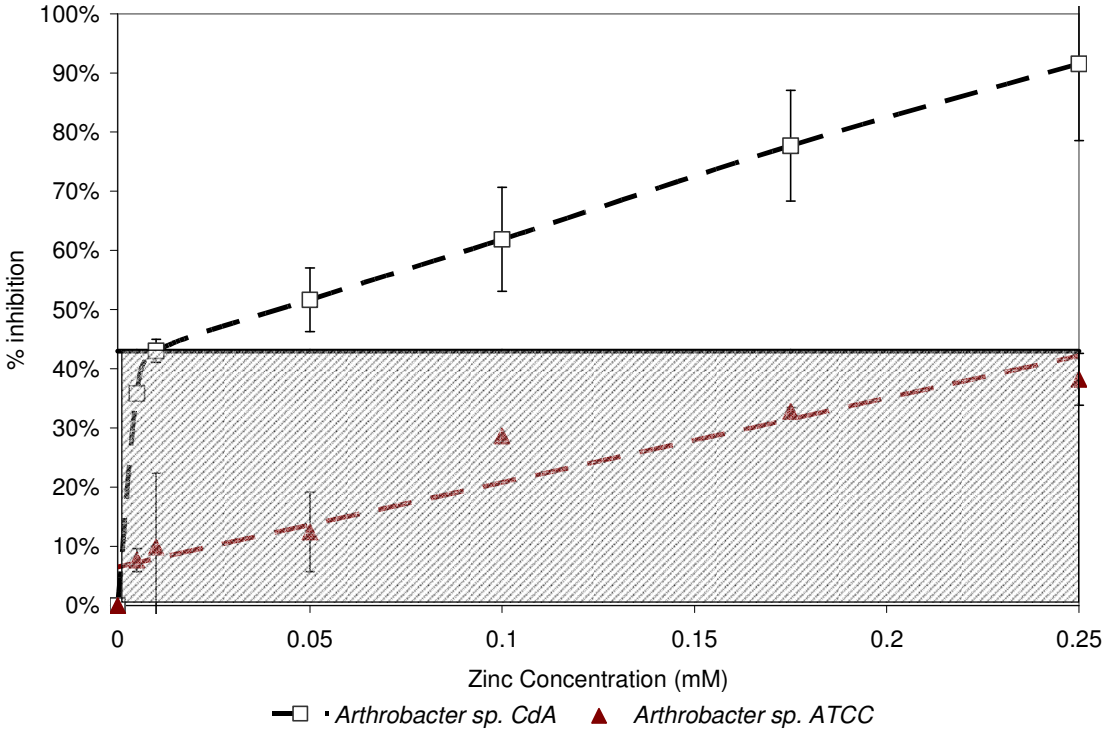

Figure 14: Inhibition of reactor isolate *Arthrobacter* sp. and a standard culture of *Arthrobacter* sp. (ATCC 21908) to zinc; note that in the reactor isolate over 40% of the toxicity is due to less than 2% of the MIC concentration (shown as grey box).

The effects of zinc concentration (MIC) on growth phase were examined. When the MIC was spiked into sacrificial bottles at 10 hours growth was almost completely halted (Figure 15). At times 17 and 24 hours substantial but not complete cessation of growth was observed and there seemed to be little difference in these times as far as maximum growth observed. Biosorbtion of zinc to the *Arthrobacter* cells at neutral pH was about 5% with live cells and less than 1% with dead cells, possibly due to total cell concentrations differences, with the standard deviation of the method at approximately

1%. Sorbtion did not appear to be growth phase dependant, though further study is recommended with additional pH trials.

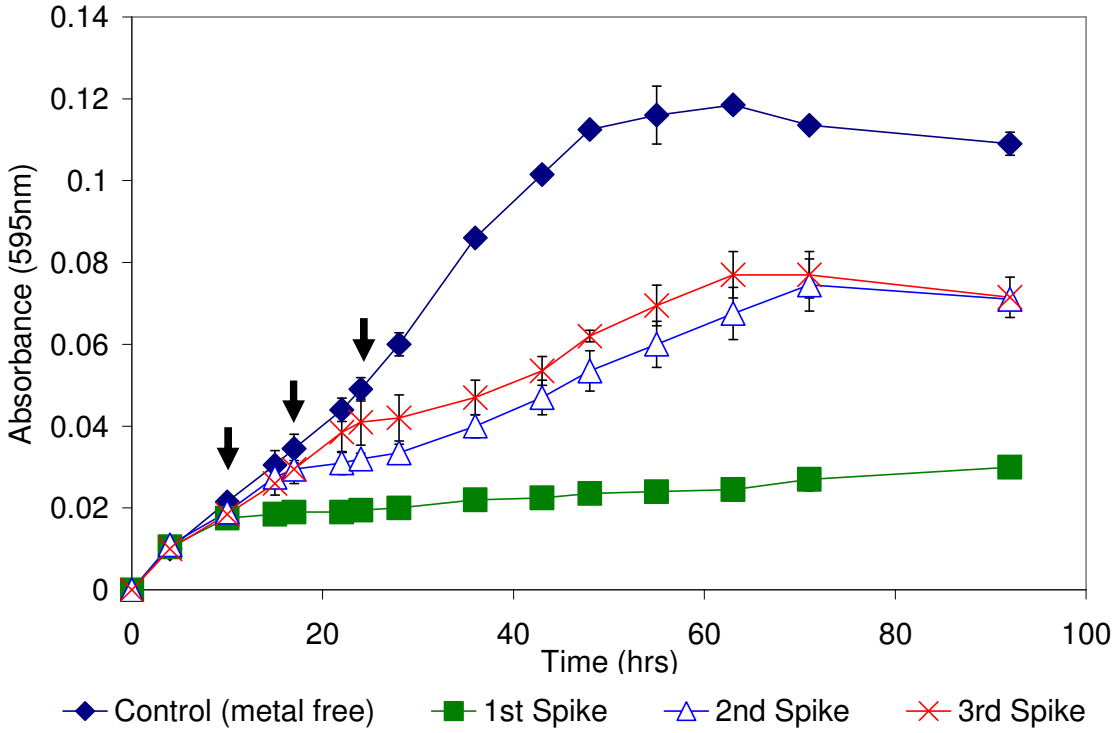

Figure 15: Effect of zinc toxicity on growth phase of *Arthrobacter* sp. Spiking of sacrificial bottles with 0.25 mM zinc at 10, 17, and 24 hours (shown with arrow).

Zinc toxicity seems to have a double effect of decreased growth and increased lag time with increasing metal concentrations. Lag phases of 14 and 32 hours were observed from bottles containing 0.1 and 0.175 mM, respectively (Figure 16A). Other works with *Pseudomonas*, *Micrococcus*, and *Bacillus* strains show zinc inhibition of maximum growth rate but do not reveal lag-time in growth [69, 70]. There could be a variety of reasons for this lack of lag-time including innoculum concentration, influence of media components, differing mechanisms between bacterial genera, and speciation dependant toxicity.

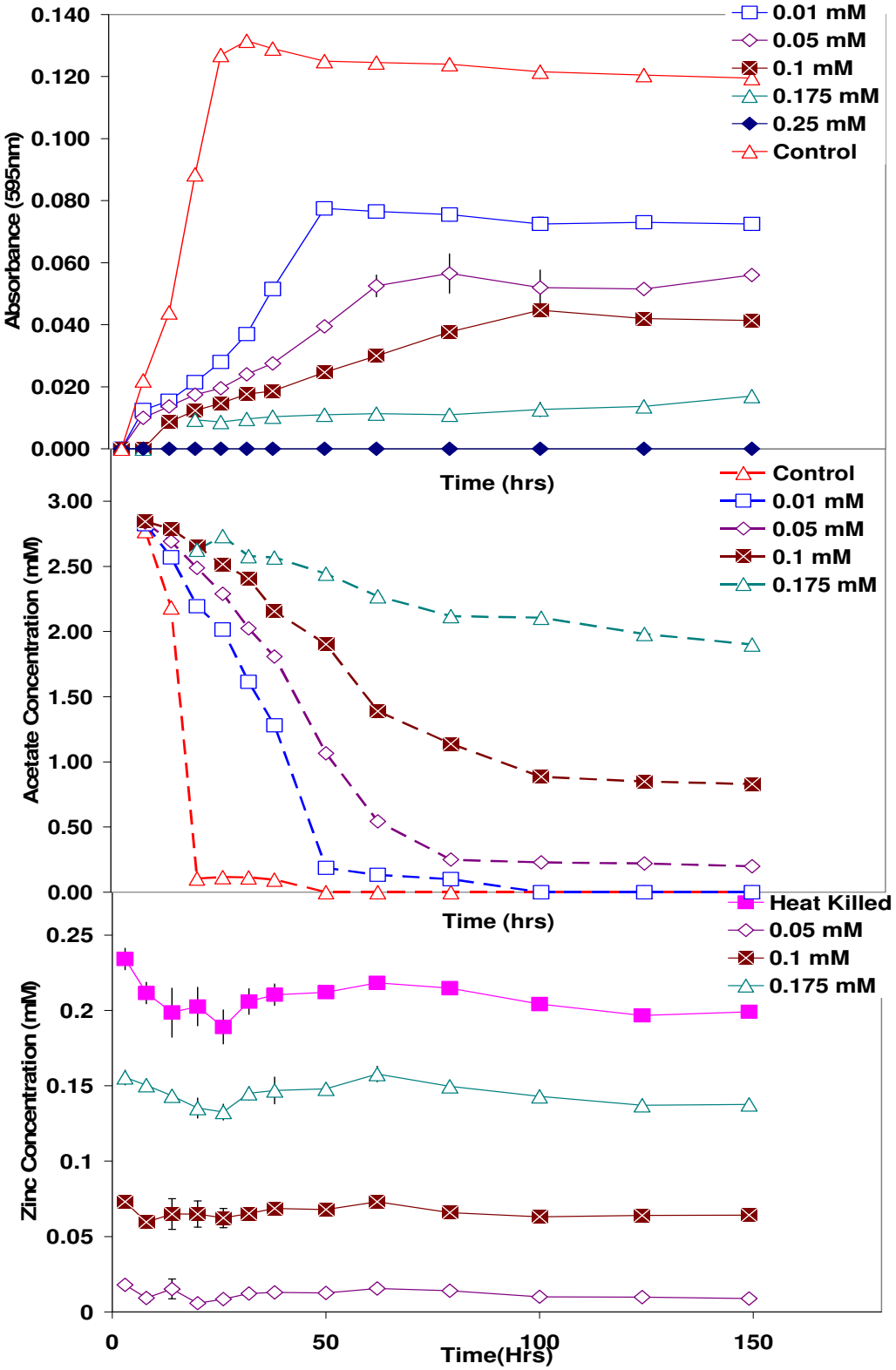

Figure 16: Inhibition of *Arthrobacter* sp. to zinc A. Growth measured as optical density, **B.** Acetate concentration, **C.** Zinc concentration with time

In *E. coli,* zinc is known to cause aggregation and precipitation of the RecA protein which regulates DNA repair, horizontal gene transfer, and homologous DNA recombination [31]. This precipitation is thought to occur via ligand binding and disruption of the RecA protein with either histidine or cysteine [31]. Without this and other DNA "policing" proteins repair of fatal mutations and advantageous adaptations via gene transfer would not take place, hindering adaptation and growth in a changing environment, possibly causing apoptosis, though it is unlikely that this RecA precipitation mechanism is the only contributor to toxicity.

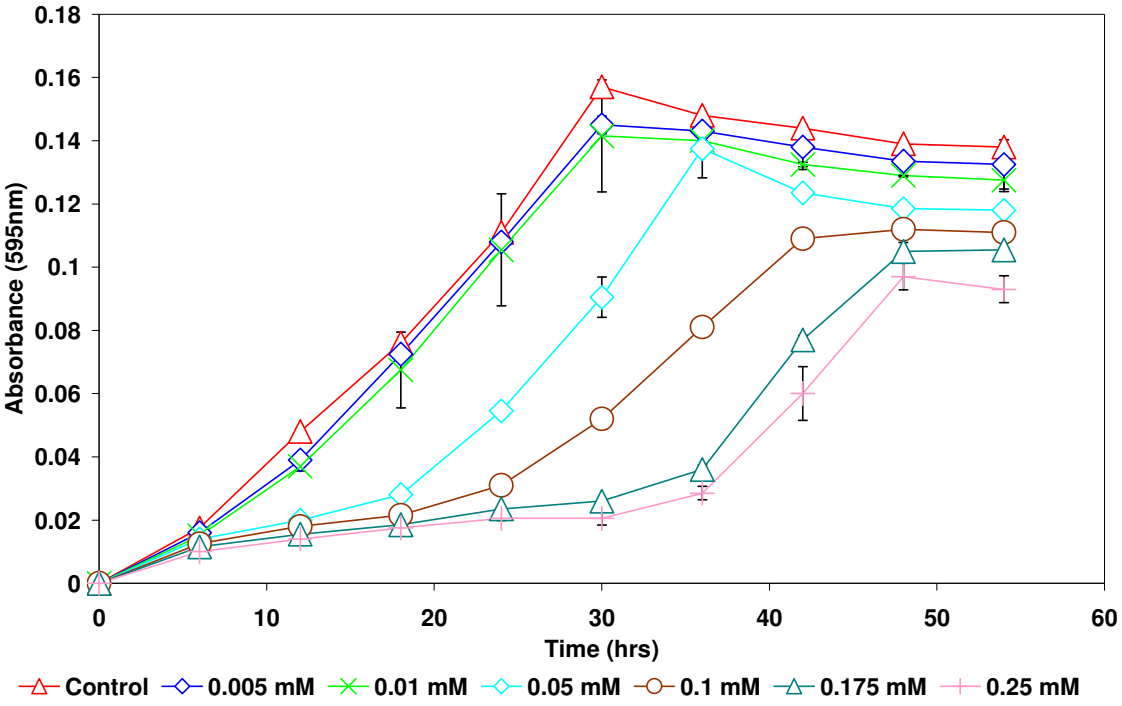

Figure 17: Inhibition of *Arthrobacter* sp. ATCC 21908 to 0, 0.005, 0.01, 0.05, 0.1, 0.175, and 0.25 mM zinc concentrations

The *Arthrobacter* sp. ATCC 21908 showed significant tolerance to equivalent concentrations of zinc (Figure 17). Growth rates for the ATCC culture were approximately 20 times greater than that of the CdA *Arthrobacter* isolate. There did not

appear to be any lag phase at all metal concentrations, as a semi-log plot of optical density versus time reveals. This extra resilience to zinc may be attributed to plasmid borne metal resistance due to the presence of heavy metal contamination in oil as these bacteria were isolated from an oil contaminated beach [73, 74]. Metal type and concentration in crude oil depends on the geographic locality of where the oils are mined however typically crude oils contain elevated levels of nickel, vanadium, lead, copper, zinc, iron, and manganese [74-76]. The presence of metals in crude oil may have contributed to *Arthrobacter* sp. ATCC 21908 significant resistance to zinc.

Effect of Metal Speciation on Growth

Significant differences in metal inhibition were observed with changes in pH as shown in Figure 18. At pH 6 little toxicity was observed at the metal concentration examined. Growth was completely inhibited at pH values of 8 and 9. It appears from optical density measurements that the pH 9 was less inhibited than pH 8 however analysis of acetate concentrations confirms that this apparent growth is actually a formation of zinc hydroxide precipitates and no real growth.

Table 11 encompasses a range of media types and pH values from 5.5-9. The most resistant organism, *Pseudomonas aeruginosa*, is able to tolerate up to 8 mM zinc concentrations in minimal salts vitamin pyruvate media (MSVP) at a pH of 6.5. The highest tolerance level at which 50% inhibition is reported is *Rhodococcus erthropolis* at a pH value of 5.5 and zinc concentration of 1.728 mM. Within a single media type increasing pH correspondingly increases zinc toxicity [72]. The divalent form of the zinc cation predominates in the majority of media types.

Increases in toxicity are probably due to the zinc species present in aqueous phase and of all the complexed zinc species only two show substantial concentrations and rapid increases in concentration at pH values of 8 and 9, $Zn(OH)_2$ and the zinc nitrolotriacetic acid ($Zn\text{-}NTA^-$) complex, (Table 12). Of these two it is likely that the $Zn\text{-}NTA^-$ complex may be more toxic due to its ability to remain inside the cell due to the nature of the chemiosmotic gradient, though without further experimentation this is conjecture. It is possible that the complexed form of zinc is unable to leave the cell by the P-type ATPase driven efflux pumps, the primary resistance mechanism of *Arthrobacter,* as this system relies on a divalent form of zinc. These toxicity effects may also stem from increasing sorbtion of zinc at the cell wall, disrupting the cell wall and causing leakage of mobile ions such as potassium, magnesium, and sodium, steric hindrance to metabolite transport by blocking uptake and efflux channels, inactivation of transport proteins, or other unknown effects.

Biosorbtion was also significantly enhanced at pH 8, though at pH 9 it was difficult to say if sorption or precipitation was the dominant effect. It appears that live cells are less efficient at zinc uptake than dead cells and from a toxicity standpoint this makes sense. At pH 8 nearly 55% of the zinc was removed from solution with dead cells compared to only about 30% with live, though visible precipitates were present at this pH for live cell and metal containing cell free bottles but not with dead cell bottles. There was little difference between pH 6 and 7 values, showing about 10% removal of zinc in both live and dead cells. With increasing pH values an increased amount of aqueous removal is though to occur and this is what is observed in both this and other studies [32, 67, 71].

Table 11: Toxic effects of zinc on pure cultures and their respective zinc speciation in different media types reported in literature

Culture Name	Media Type	pH	50% Inhibition (mM)	MIC (mM)	Primary Zn Species >10% (% aq comp)	Zinc ppt Predicted (% ppt)
Pseudomonas putida MT2[a]	Tris Buffer	5.5	0.138		Zn^{2+} (99.898)	N
Rhodococcus erthropolis[a]	Tris Buffer	5.5	1.728		Zn^{2+} (99.248)	N
Bacillus sp[b]	MSM[†]	5.9	0.4-0.43		$ZnHPO_4(aq)$ (50.545), Zn^{2+} (46.640)	Y (96.654)
Pseudomonas sp[b]	MSM[†]	5.9	0.041		$ZnHPO_4(aq)$ (50.545), Zn^{2+} (46.641)	Y (65.759)
Rhodococcus erthropolis[a]	Tris Buffer	5.9	0.811		Zn^{2+} (99.557)	N
Arthrobacter sp.[c]	Minimal Media	6		0.41[*]	Zn^{2+} (85.799)	N
Pseudomonas putida DSM 50026[a]	Tris Buffer	6	0.104		Zn^{2+} (99.849)	N
Pseudomonas putida MT2[a]	Tris Buffer	6	0.061		Zn^{2+} (99.87)	N
Pseudomonas aeruginosa[d]	MSVP‡	6.5		8	Zn^{2+} (66.279), $ZnSO_4(aq)$ (30.523)	N
Arthrobacter sp.[c]	Minimal Media	7	0.05	0.25	Zn^{2+} (82.675)	Y (37.674)
Arthrobacter sp. ATCC 21908[c]	Minimal Media	7	0.25[*]		Zn^{2+} (82.675)	Y (37.674)
Rhodococcus erthropolis[a]	Tris Buffer	7	0.321		Zn^{2+} (98.834)	N
Desulfovibrio desuluricans[e]	Sulfidogenic medium	7.2		0.21	Zn^{2+} (59.623), $ZnSO_4(aq)$ (32.107)	N
Pseudomonas putida MT2[a]	Tris Buffer	7.8	0.002		Zn^{2+} (89.973)	N
Pseudomonas putida DSM 50026[a]	Tris Buffer	7.9	0.031		Zn^{2+} (86.595)	N
Rhodococcus erthropolis[a]	Tris Buffer	7.9	0.069		Zn^{2+} (86.674)	Y (52.455)
Arthrobacter sp.[c]	Minimal Media	8		<0.05[*]	Zn^{2+} (66.926), $ZnNTA^-$ (12.556)[*]	Y (82.320)[*]
Arthrobacter sp.[c]	Minimal Media	9		<0.05[*]	$ZnNTA^-$ (44.358), $Zn(OH)_2$ (42.814)	Y (94.458)

*estimated value; ppt, precipitate
† Minimal Salts Medium
‡ Minimal Salts Vitamin Pyruvate Medium

a vanBeelen et al. [72]
b Amor et al. [69]
c this study
d Teitzel et al. [41]
e Poulson et al. [77]

Table 12: Zinc speciation change with pH

	% of total component concentration at 0.25 mM Zn			
Zinc Species	pH 6	pH 7	pH 8	pH 9
Zn-$(Acetate)_2$ (aq)	0.036	0.039	0.03	-
$Zn(OH)_2$ (aq)	-	0.082	6.051	46.972
$Zn(OH)_3^-$	-	-	-	0.161
$Zn(SO_4)_2^{2-}$	0.015	0.015	0.011	-
Zn^{+2}	87.854	86.512	63.391	4.909
Zn-$Acetate^+$	6.848	7.062	5.271	0.41
$ZnCl^+$	0.076	0.074	0.055	-
$ZnCO_3$ (aq)	0.012	0.298	1.619	1.103
$ZnHCO_3^+$	0.151	0.378	0.205	0.014
$ZnHPO_4$ (aq)	0.213	0.04	0.513	0.053
$ZnNH_3^{2+}$	-	0.022	0.157	0.084
$ZnNTA^-$	0.519	0.627	14.306	40.087
$ZnOH^+$	0.071	0.699	5.153	3.997
$ZnOHNTA^{2-}$	-	-	0.07	1.95
$ZnSO_4$ (aq)	4.202	4.152	3.164	0.247

- not listed at pH value

Biosorbtion studies of copper, cadmium, and iron have been performed on other *Arthrobacter* sp. at moderately acidic pH values of 4-6 [32, 67]. Pagnanelli et al. suggest there are two weakly acidic sites on the bacterial surface which exchange between hydrogen ions and metal ions, that these sites are probably occupied by an amide, amino, or phosphate group, and these sites are highly effected by the pH of the solution [32]. Pagnanelli et al. data for potentiometrically titrated *Arthrobacter* biomass shows a rapid increase of sorbed metal at pH values of 4-6 followed by somewhat of a leveling at pH 6 to between 7 and 8, then a rapid increase again up to pH 10 [32]. This same phenomenon is observed in this data with little change in sorbtion between pH 6 and 7 values but rapid increases in sorbtion for pH 8 and 9.

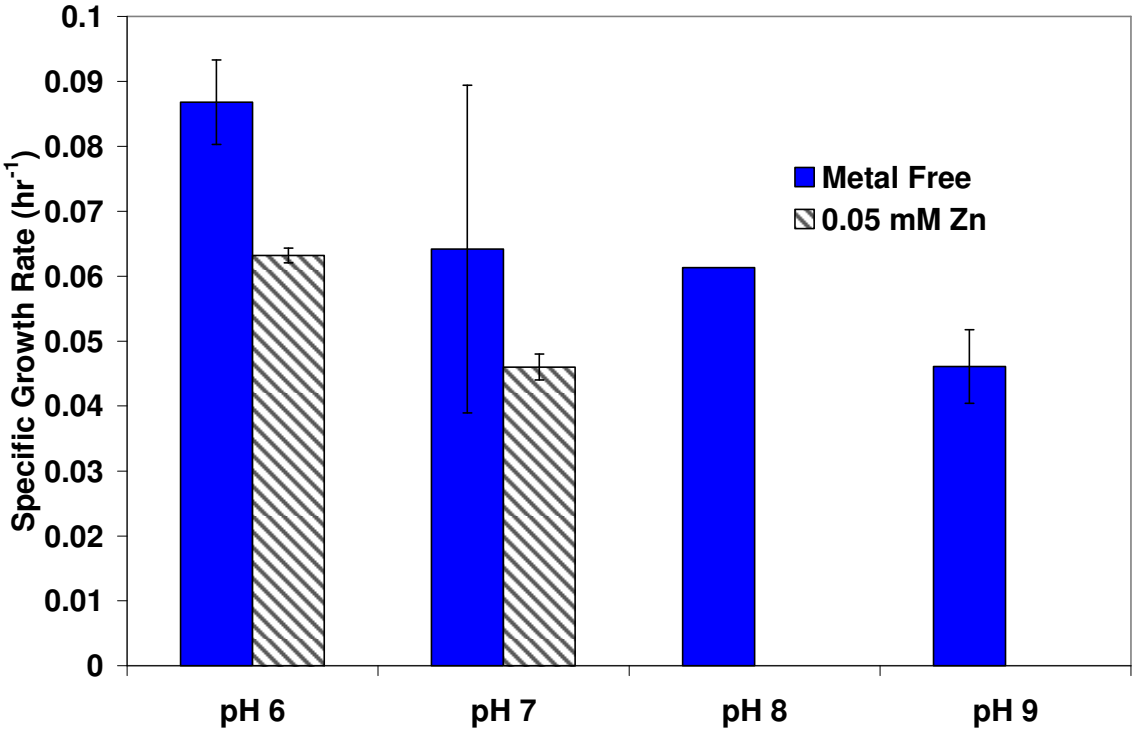

Figure 18: Inhibition effects of zinc on growth of *Arthrobacter* sp. at pH values of 6, 7, 8, and 9

Dual-Monod Kinetic Model

A dual-Monod kinetic model was adapted to the inhibition data of *Arthrobacter* species isolated from CdA and provides a quantitative estimation of the inhibition effects to this organism. A modified form of dual-Monod kinetic model was chosen for this system as it incorporates the assumption of both electron-donor and electron acceptor limited conditions and dose-dependant inhibition as in equations 1-3 below [78, 79].

$$\frac{\partial M}{\partial t} + Z\frac{\partial M}{\partial \omega} = \mu(\omega)M\left[\frac{A}{A+K_A}\right]\left[\frac{O}{O+K_O}\right] \quad (1)$$

$$\frac{dA}{dt} = -\frac{1}{Y}\mu(\omega)M\left[\frac{A}{A+K_A}\right]\left[\frac{O}{O+K_O}\right] \quad (2)$$

$$\frac{dO}{dt} = -\frac{F}{Y}\mu(\omega)M\left[\frac{A}{A+K_A}\right]\left[\frac{O}{O+K_O}\right] \quad (3)$$

$$\mu(\omega) = \mu_o e^{-v\omega} \quad (4)$$

Where $M=M(t,\omega)$ is the cell concentration measured in optical density (595nm), $Z=Z(t)$ is the zinc metal concentration in mM, $A=A(t)$ is the acetate concentration in mM, $O=O(t)$ is the oxygen concentration in mM, F is the stoichiometric utilization of acetate to oxygen, and Y is the yield of cell concentration per mM of acetate consumed. For this model it is assumed that growth rate varies exponentially and is dependant on metal dose-accumulation in the cell (ω), specific growth rate (μ_o), and an adjustable toxicity parameter (ν) fit by the data, as in equation 4. Omega (ω) is defined as the linear dose-accumulation with respect to time, equal to $\int_0^\infty Z(t')dt'$ or in the case where the metal concentration is constant, $Z \cdot t$. These equations are analogous to one dimensional, advection-reaction equations where the advection term representing spatial displacement is replaced by the dose term ($Z \cdot \partial M/\partial \omega$) representing dose accumulation.

The dual-Monod form assumes an unstructured distributed model where all cells are homogenously distributed in the solution and are treated equally. This model also assumes there are no reserves inside the cell for metabolic growth and no lag-time between inoculation and growth. When dose ω is accumulated prior to degradation, then the dose accumulation term is zero and the dose ω is set to the value achieved before degradation.

The dual-Monod kinetic model shows relatively good agreement with inhibition data, (Figure 19 A-E). The adjustable toxicity parameter is constant throughout the data collection, save for the last data point at 0.175 mM. An examination of the acetate curve for 0.175 mM reveals that acetate is still being consumed and this data set may not yet have reached its maximum growth or the fact that the model does not account for lag-

phase, which could account for the change in ν. The parameters for each modeled run are given in Table 13. Typical half saturation coefficients for acetate range greatly from 0.04 to nearly 14 mM acetate [80, 81]

Table 13: Parameters for Dual-Monod Kinetic Model

Metal Concentration (mM)	Yield (OD/mM Acetate)	K_a (mM)	K_o (mM)	μ_o (hr^{-1})	ν ($(mM*hr)^{-1}$)
0	0.046	4	0.1	0.0993	n/a
0.01	0.027	4	0.1	0.045	0.08
0.05	0.021	4	0.1	0.0296	0.08
0.1	0.021	4	0.1	0.0187	0.08
0.175	0.015	4	0.1	0.0041	0.15

It appears that the model fits very well in the exponential portion of each graph but overshoots slightly the final value. This could be due to cell death, approximations in the yield calculation, and errors in sampling and analysis which propagate in these calculations. This model does not account for lag-phase in the growth of *Arthrobacter* which may offset the model from the experimental data in the higher metal concentrations where lag-phase occurs. In fact at high metal concentrations the majority of deviation from the experimental data is observed. Overall the model does an excellent job of predicting the experimental data with only slight offset for low concentrations. Future model versions could include the dose-accumulation term which was removed by simplification and incorporate interactions between mineral phase and microbe.

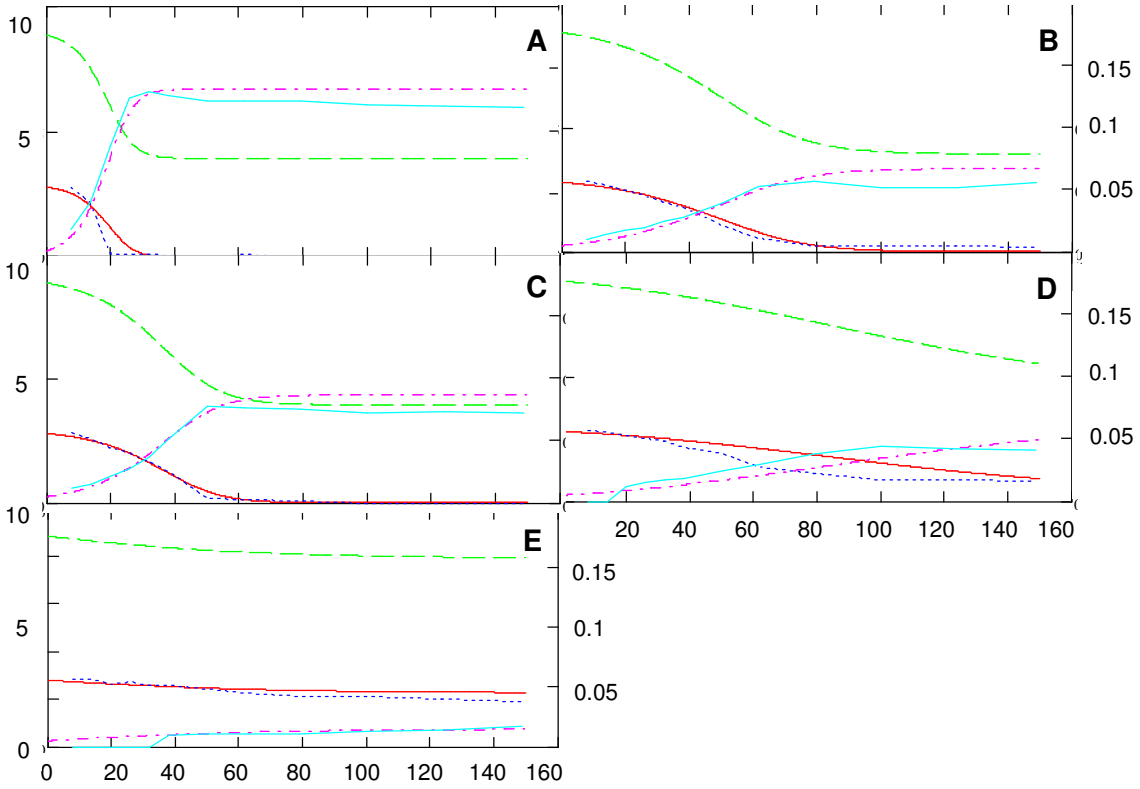

Figure 19: Dual-Monod model comparison to inhibition data: **A)** 0 mM, **B)** 0.01 mM, **C)** 0.05 mM, **D)** 0.1 mM, **E)** 0.175 mM zinc. Cell optical density (Aqua), Modeled optical density (Dashed Pink), Modeled oxygen (Dashed Green), Acetate (Dashed Blue), Modeled Acetate (Red)

CHAPTER FIVE

FUTURE WORK

The research presented in this work is only a portion of a greater design to develop a biogeochemical model to describe the complex interactions between metals and microbes in this contaminated environment. Efforts to date have focused on describing the toxic metal contaminants, mineral species, and microbial diversity in CdA sediments. Characterizing individual microbes, as in this work, or consortia of a particular metabolic segment (such as iron reducers) in other works have been described [9, 16, 26, 28, 39]. Future work in this area should not only focus on microbial consortia fixed in a particular metabolic pathway, but a holistic approach including organisms with diverse metabolic needs; combining aerobic and anaerobic cultures and interactions including both substrates and mineral phases. The design of the novel flow reactor presented in this work makes this type of analysis possible as with increasing depth redox changes occur which favor a diverse group metabolic pathways. However, to understand the complex interactions as they are within the CdA sediments contained in the reactor may be beyond our current techniques of analysis. Therefore in an effort to capture the essential details of this system, a much more simplified form must be created. A defined consortium of microorganisms combine with a defined mineral phase may simplify the system so that the essential details may be captured using current and emerging techniques. As it appears that both hematite and goethite are present in the reactor and are known to exist in CdA sediments, combining each individually or collectively with quartz substrate may yield a more tractable system. Also biogenic mineral formation and biogeochemical interactions can more closely be monitored and compared to a sterile control reactor to elucidate these changes. In the current sediment system, this would be nearly impossible.

Additionally, from this work we observed apparent growth of iron reducing organisms in the lower areas of the reactor. Future reactor designs should incorporate an increased reactor depth to facilitate increased redox changes down the reactor which may facilitate additional growth of organisms which require lower redox potentials, such as sulfate reducers and methanogens. The current reactor depth may still contain these groups, but as sulfate reducers produce hydrogen sulfide, it is expected that metal precipitation would be more pronounced (as black precipitates) and this should visually dominate in the area in the reactor where sulfate reducers are the dominant microbial member present. The reactor did show a single black "colony" at approximately 3.75 inches in depth, however apparent iron reducing organism growth or reactor fluxuations may have excluded growth for this colony as it did not increase in size.

Additional characterization of the organisms isolated from this system will need to be performed to knowledgeably select the consortium members for further study. Only single metal toxicity studies have been presented in this work, however more complex experimentation and models consisting of mixed metals will need to be performed to better understand the metal interactions with these microorganisms. Even after the biogeochemical model has been developed for the simplified system, it will need to be verified on a more complex system to see if it captures the most essential elements. The completed model will help to better understand this complex environment and better predict the results that perturbations have on this system. This model could aid in planning and development activities which may cause disturbances in this system and may be able to be extended to predict changes in other contaminated areas.

Bibliography

1. Horowitz, A.J., et al., *Effect of mining-related activities on the sediment-trace element geochemistry of Lake Coeur d'Alene, Idaho, USA. Part 1, Surface sediments*. 1992, U.S. Dept. of the Interior, U.S. Geological Survey; U.S. Geological Survey, Open-File Reports Section [distributor],: Doraville, Ga. Denver, Colo.
2. Horowitz, A.J. and Geological Survey (U.S.), *The effect of mining and related activities on the sediment-trace element geochemistry of Lake Coeur d'Alene, Idaho. Part II, Surface sediments*. 1993, U.S. Dept. of the Interior, U.S. Geological Survey ; Earth Science Information Center, Open-File Reports Section [distributor],: Atlanta, Ga. Denver, CO.
3. Horowitz, A.J., et al., *A summary of the effects of mining and related activities on the sediment-trace element geochemistry of Lake Coeur d'Alene, Idaho, USA.* Journal of Geochemical Exploration, 1995. **52**(1-2): p. 135-144.
4. Balistrieri, L.S., S.E. Box, and J.W. Tonkin, *Modeling precipitation and sorbtion of elements during mixing of river water and porewater in Coeur d'Alene River Basin.* Environ. Sci. Technol, 2003(37): p. 4694-4701.
5. Kuwabara, J.S., et al., *Importance of Sediment-Water Interactions in Coeur d'Alene Lake, Idaho, USA: Management Implications.* Environmental Management, 2003. **32**(3): p. 348-359.
6. Leach, D.L., G.P. Landis, and A.H. Hofstra, *Metamorphic origin of the Coeur d'Alene base- and precious-metal veins in the Belt basin, Idaho and Montana. .* Geology, 1985(16): p. 122-125.
7. Tonkin, J., L. Balistrieri, and J. Murray, *Modeling metal removal onto natural particles formed during mixing of acid rock drainage with ambient surface water.* Environ. Sci. Technol., 2002(36): p. 484-492.
8. Balistrieri, L., et al., *Assessing the Influence of Reacting Pyrite and Carbonate Minerals on the Geochemistry of Drainage in the Coeur d'Alene Mining District.* Environ. Sci. Technol, 1999(33): p. 3347-3353.
9. Cummings, D.E., et al., *Diversity of geobacteraceae species inhabiting metal-polluted freshwater lake sediments ascertained by 16S rDNA analyses.* Microb. Ecol., 2003(46): p. 257-269.
10. Paulson, A. and L. Balistrieri, *Modeling removal of Cd, Cu, Pb, and Zn in acidic groundwater during neutralization by ambient surface waters and groundwaters.* Environ. Sci. Technol, 1999(33): p. 3850-3856.
11. Feris, K.P., et al., *Seasonal Dynamics of Shallow-Hyporheic-Zone Microbial Community Structure along a Heavy-Metal Contamination Gradient.* Appl. Environ. Microbiol., 2004. **70**(4): p. 2323-2331.
12. EPA and IDEQ, *Proposed plan for the Bunker Hill superfund site: Bunker Hill mine water management Kellogg, Idaho. July 2001.* 2001.
13. Paulson, A.J., *The transport and fate of Fe, Mn, Cu, Zn, Cd, Pb and SO4 in a groundwater plume and in downstream surface waters in the Coeur d'Alene Mining District, Idaho, U.S.A.* Applied Geochemistry, 1997. **12**(4): p. 447-464.

14. Paulson, A.J., *Biogeochemical removal of Zn and Cd in the Coeur d'Alene River (Idaho, USA), downstream of a mining district.* The Science of The Total Environment, 2001. **278**(1-3): p. 31-44.
15. La Force, M.J., et al., *A laboratory evaluation of trace element mobility from flooding and nutrient loading of Coeur d'Alene River sediments.* Journal of Environmental Quality, 1998. **27**(2): p. 318-328.
16. Cummings, D.E., et al., *Arsenic mobilization by the dissimilatory Fe(III)-reducing bacterium Shewanella alga BrY.* Environ. Sci. Technol., 1999(33): p. 723-729.
17. Cummings, D.E., A.W. March, and B. Bostick, *Evidence for microbial Fe(III) reduction in anoxic, mining impacted lake sediments (Lake Coeur d'Alene, Idaho).* Appl. Environ. Microbiol., 2000(66): p. 154-162.
18. Niggemyer, A., et al., *Isolation and characterization of a novel As(V)-reducing bacterium: implications for arsenic mobilization and the genus Desulfitobacterium.* App. Environ. Microbiol., 2001: p. 5568-5580.
19. La Force, M.J., et al., *Redistribution of trace elements from contaminated sediments of Lake Coeur d'Alene during oxygenation.* Journal of Environmental Quality, 1999. **28**(4): p. 1195-1200.
20. Horowitz, A.J., K.A. Elrick, and R.B. Cook, *Comment on "Phase Associations and Mobilization of Iron and trace elements in Coeur d'Alene Lake, Idaho".* Environ. Sci. Technol., 1999(32): p. 201-202.
21. Harrington, J.M., M.J. LaForce, and W.C. Rember, *Phase association and mobilization of iron and trace elements in Coeur d'Alene Lake, Idaho.* . Environ. Sci. Technol., 1998(32): p. 650-656.
22. Harrington, J.M., S.E. Fendorf, and R.F. Rosenzweig, *Biotic generation of arsenic(III) in metal(oid)-contaminated freshwater lake sediments.* Environ. Sci. Technol., 1998(32): p. 2425-2430.
23. Sprenke, K.F., et al., *Toxic metal contamination in the lateral lakes of the Coeur d'Alene River valley, Idaho.* Environmental Geology, 2000. **39**(6): p. 575-586.
24. Bostick, B.C., et al., *Seasonal fluctuations in zinc speciation within a contaminated wetland.* Environmental Science & Technology, 2001. **35**(19): p. 3823-3829.
25. Farrand, W.H. and J.C. Harsanyi, *Mapping the distribution of mine tailings in the Coeur d'Alene River Valley, Idaho, through the use of a constrained energy minimization technique.* Remote Sensing of Environment, 1997. **59**(1): p. 64-76.
26. Roane, T.M. and S.T. Kellogg, *Characterization of bacterial communities in heavy metal contaminated soils.* Can. J. Microbiol., 1996(42): p. 593-603.
27. Jong, T. and D.L. Parry, *Removal of sulfate and heavy metals by sulfate reducing bacteria in short-term bench scale upflow anaerobic packed bed reactor runs.* Water Research, 2003(37): p. 3379-3389.
28. Cummings, D.E., et al., *Ferribacterium limneticum, gen. nov., sp. nov., an Fe(III)-reducing microorganism isolated from mining-impacted freshwater lake sediments.* Arch Microbiol, 1999(171): p. 183-188.
29. Madigan, M.T., J.M. Martinko, and J. Parker, *Brock Biology of Microorganisms*. 10th ed. 2003, Upper Saddle River: Prentice Hall.
30. Nies, D.H., *Microbial heavy-metal resistance.* Appl. Microbiol. Biotechnol., 1999(51): p. 730-750.

31. Lee, A.M. and S.F. Singleton, *Inhibition of the Escherichia coli RecA protein: zinc(II), copper(II) and mercury(II) trap RecA as inactive aggregates.* Journal of Inorganic Biochemistry, 2004. **98**(11): p. 1981-1986.
32. Pagnanelli, F., et al., *Biosorption of metal ions on Arthrobacter sp.: biomass characterization and biosorption modeling* Environmental Science & Technology, 2000. **34**(13): p. 2773-2778.
33. Mergeay, M., et al., *Alcaligenes eutrophus CH34 Is a Facultative Chemolithotroph with Plasmid-Bound Resistance to Heavy Metals.* Journal of Bacteriology, 1985. **162**(1): p. 328-334.
34. Dressler, C., et al., *Determinants Encoding Resistance to Several Heavy Metals in Newly Isolated Copper-Resistant Bacteria.* App. Environ. Microbiol., 1991. **57**(11): p. 3079-3085.
35. Nies, D., *Heavy metal-resistant bacteria as extremophiles: molecular physiology and biotechnological use of Ralstonia sp. CH34.* Extremophiles, 2000(4): p. 77-82.
36. Coombs, J.M. and T. Barkay, *Molecular Evidence for the Evolution of Metal Homeostasis Genes by Lateral Gene Transfer in Bacteria from the Deep Terrestrial Subsurface.* App. Environ. Microbiol., 2004. **70**(3): p. 1698-1707.
37. Lloyd, J. and D.R. Lovley, *Microbial detoxification of metals and radionuclides.* Current Opinion in Biotechnology, 2001(12): p. 248-253.
38. Lovley, D.R., *Dissimilatory metal reduction: from early life to bioremediation.* ASM News, 2002. **68**(5): p. 231-237.
39. Roane, T.M., *Lead Resistance in Two Bacterial Isolates from Heavy Metal-Contaminated Soils.* Microb. Ecol., 1999(37): p. 218-224.
40. Chapelle, F.H., *Groundwater Geobiology*. 2nd ed. 2001: John Wiley and sons. 55-56, 181-183, 343-347.
41. Teitzel, G.M. and M.R. Parsek, *Heavy Metal Resistance of Biofilm and Planktonic Pseudomonas aeruginosa.* App. Environ. Microbiol., 2003. **69**(4): p. 2313-2320.
42. Box, S.E., et al., *Stream-sediment geochemistry in mining-impacted streams : Prichard, Eagle, and Beaver Creeks, Northern Coeur d'Alene Mining District, northern Idaho*. Scientific investigations report ; 2004-5284. 2005, Reston, Va. Denver, CO: U.S. Dept. of the Interior. v, 62 p.
43. Sani, R.K., et al., *Reduction of uranium(VI) under sulfate-reducing conditions in the presence of Fe(III)-(hydr)oxides.* Geochimica Et Cosmochimica Acta, 2004. **68**(12): p. 2639-2648.
44. Sani, R.K., et al., *Reoxidation of reduced uranium with iron(III) (hydr)oxides under sulfate-reducing conditions.* Environmental Science & Technology, 2005. **39**(7): p. 2059-2066.
45. Ginder-Vogel, M., et al., *Chromate reduction and retention processes within arid subsurface environments.* Environmental Science & Technology, 2005. **39**(20): p. 7833-7839.
46. Hullar, M.A.J., L.A. Kaplan, and D.A. Stahl, *Recurring Seasonal Dynamics of Microbial Communities in Stream Habitats.* Appl. Environ. Microbiol., 2006. **72**(1): p. 713-722.

47. Mayer, L.M., et al., *Organic matter in small mesopores in sediments and soils.* Geochimica et Cosmochimica Acta, 2004. **68**(19): p. 3863-3872.
48. Feris, K., et al., *Differences in Hyporheic-Zone Microbial Community Structure along a Heavy-Metal Contamination Gradient.* Appl. Environ. Microbiol., 2003. **69**(9): p. 5563-5573.
49. Lothenbach, B., G. Furrer, and R. Schulin, *Immobilization of heavy metals by polynuclear aluminium and montmorillonite compounds.* Environmental Science & Technology, 1997. **31**(5): p. 1452-1462.
50. Sani, R.K., G. Geesey, and B.M. Peyton, *Assessment of lead toxicity to Desulfovibrio desulfuricans G20: influence of components of Lactate C medium.* Advances in Environmental Research, 2001. **5**(3): p. 269-276.
51. Benner, S.G., et al., *Reductive dissolution and biomineralization of iron hydroxide under dynamic flow conditions.* Environmental Science & Technology, 2002. **36**(8): p. 1705-1711.
52. Hansel, C.M., S.G. Benner, and S. Fendorf, *Competing Fe(II)-induced mineralization pathways of ferrihydrite.* Environmental Science & Technology, 2005. **39**(18): p. 7147-7153.
53. Hansel, C.M., et al., *Secondary mineralization pathways induced by dissimilatory iron reduction of ferrihydrite under advective flow.* Geochimica Et Cosmochimica Acta, 2003. **67**(16): p. 2977-2992.
54. Diels, L. and M. Mergeay, *DNA Probe-Mediated Detection of Resistant-Bacteria from Soils Highly Polluted by Heavy-Metals.* Applied and Environmental Microbiology, 1990. **56**(5): p. 1485-1491.
55. Brim, H., et al., *Characterization of the bacterial community of a zinc-polluted soil.* Canadian Journal of Microbiology, 1999. **45**(4): p. 326-338.
56. Konstantinidis, K.T., et al., *Microbial Diversity and Resistance to Copper in Metal-Contaminated Lake Sediment.* Microb. Ecol., 2003(45): p. 191-202.
57. Goris, J., *Characterisation of metal-resistant and chloroaromatics-degrading bacteria*, in *Biochemical, Physiology, and Microbiology*. 2003, University Gent. p. 228.
58. Stoppel, R.-D. and H.G. Schlegel, *Nickel-Resistant Bacteria from Anthropogenically Nickel-Polluted and Naturally Nickel-Percolated Ecosystems.* App. Environ. Microbiol., 1995. **61**(6): p. 2276-2285.
59. Roane, T.M. and I.L. Pepper, *Microbial Responses to Environmentally Toxic Cadmium.* Microbial Ecology, 1999. **38**(4): p. 358-364.
60. Roane, T.M., K.L. Josephson, and I.L. Pepper, *Dual-Bioaugmentation Strategy To Enhance Remediation of Cocontaminated Soil.* Appl. Environ. Microbiol., 2001. **67**(7): p. 3208-3215.
61. Trajanovska, S., M.L. Britz, and M. Bhave, *Detection of heavy metal ion resistance genes in Gram-positive and Gram-negative bacteria isolated from a lead-contaminated site.* Biodegradation, 1997. **8**(2): p. 113-124.
62. Jo, J.K., et al., *Isolation of ALU1-P gene encoding a protein with aluminum tolerance activity from Arthrobacter viscosus.* Biochemical and Biophysical Research Communications, 1997. **239**(3): p. 835-839.

63. Benyehuda, G., et al., *Metal resistance among aerobic chemoheterotrophic bacteria from the deep terrestrial subsurface.* Canadian Journal of Microbiology, 2003. **49**(2): p. 151-156.
64. Zhang, H.B., et al., *Genetic and physiological diversity of phylogenetically and geographically distinct groups of Arthrobacter isolated from lead-zinc mine tailings.* Fems Microbiology Ecology, 2004. **49**(2): p. 333-341.
65. Horton, R.N., et al., *Low temperature reduction of hexavalent chromium by a microbial enrichment consortium and a novel strain of Arthrobacter aurescens.* Bmc Microbiology, 2006. **6**: p. -.
66. Pagnanelli, F., et al., *Equilibrium biosorption studies in single and multi-metal systems.* Process Biochemistry, 2001. **37**(2): p. 115-124.
67. Pagnanelli, F., et al., *Mechanistic modeling of heavy metal blosorption in batch and membrane reactor systems.* Hydrometallurgy, 2003. **71**(1-2): p. 201-208.
68. Stefanidou, M., et al., *Zinc: a multipurpose trace element.* Archives of Toxicology, 2006. **80**(1): p. 1-9.
69. Amor, L., C. Kennes, and M.C. Veiga, *Kinetics of inhibition in the biodegradation of monoaromatic hydrocarbons in presence of heavy metals.* Bioresource Technology, 2001. **78**(2): p. 181-185.
70. Benka-Coker, M.O. and J.A. Ekundayo, *Effects of heavy metals on growth of species of Micrococcus and Pseudomonas in a crude oil/mineral salts medium.* Bioresource Technology, 1998. **66**(3): p. 241-245.
71. Esposito, A., F. Pagnanelli, and F. Veglio, *pH-related equilibria models for biosorption in single metal systems.* Chemical Engineering Science, 2002. **57**(3): p. 307-313.
72. vanBeelen, P. and A.K. FleurenKemila, *Influence of pH on the toxic effects of zinc, cadmium, and pentachlorophenol on pure cultures of soil microorganisms.* Environmental Toxicology and Chemistry, 1997. **16**(2): p. 146-153.
73. Obiajunwa, E.I., et al., *Characterisation of heavy metal pollutants of soils and sediments around a crude-oil production terminal using EDXRF.* Nuclear Instruments & Methods in Physics Research Section B-Beam Interactions with Materials and Atoms, 2002. **194**(1): p. 61-64.
74. Al-Saleh, E.S. and C. Obuekwe, *Inhibition of hydrocarbon bioremediation by lead in a crude oil-contaminated soil.* International Biodeterioration & Biodegradation, 2005. **56**(1): p. 1-7.
75. Osuji, L.C. and C.M. Onojake, *Trace heavy metals associated with crude oil: A case study of Ebocha-8 oil-spill-polluted site in Niger Delta, Nigeria.* Chemistry & Biodiversity, 2004. **1**(11): p. 1708-1715.
76. Osuji, L.C. and S.O. Adesiyan, *Extractable hydrocarbons, nickel and vanadium contents of Ogbodo-Isiokpo oil spill polluted soils in Niger Delta, Nigeria.* Environmental Monitoring and Assessment, 2005. **110**(1-3): p. 129-139.
77. Poulson, S.R., P.J.S. Colberg, and J.I. Drever, *Toxicity of heavy metals (Ni,Zn) to Desulfovibrio desulfuricans.* Geomicrobiology Journal, 1997. **14**(1): p. 41-49.
78. Ginn, T.R., *On the distribution of multicomponent mixtures over generalized exposure time in subsurface flow and reactive transport: Foundations, and formulations for groundwater age, chemical heterogeneity, and biodegradation.* Water Resources Research, 1999. **35**(5): p. 1395-1407.

79. Murphy, E.M. and T.R. Ginn, *Modeling microbial processes in porous media.* Hydrogeology Journal, 2000. **8**(1): p. 142-158.
80. Kim, H. and K.R. Pagilla, *Competitive growth of Gordonia and Acinetobacter in continuous flow aerobic and anaerobic/aerobic reactors.* Journal of Bioscience and Bioengineering, 2003. **95**(6): p. 577-582.
81. Logan, B.E., et al., *Kinetics of Perchlorate- and Chlorate-Respiring Bacteria.* Appl. Environ. Microbiol., 2001. **67**(6): p. 2499-2506.

APPENDIX A

Appendix A contains a detail schematic of the novel flow reactor as well as an outline of the experimental setup.

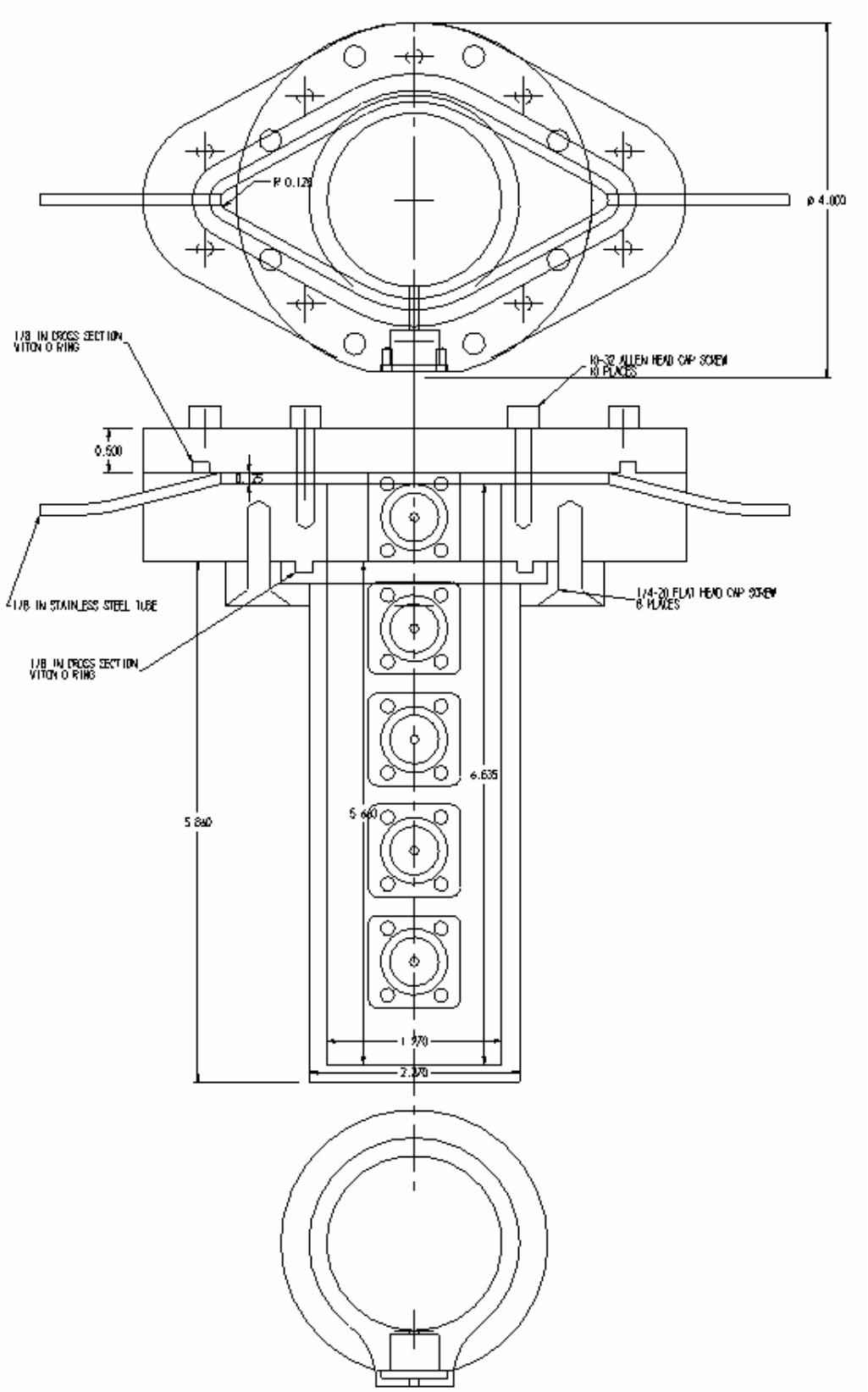
R 0.129
ø 4.000
1/8 IN CROSS SECTION VITON O RING
#8-32 ALLEN HEAD CAP SCREW 10 PLACES
0.500
0.25
1/8 IN STAINLESS STEEL TUBE
1/8 IN CROSS SECTION VITON O RING
1/4-20 FLAT HEAD CAP SCREW 6 PLACES
6.635
5.840
5.640
1.970
2.270

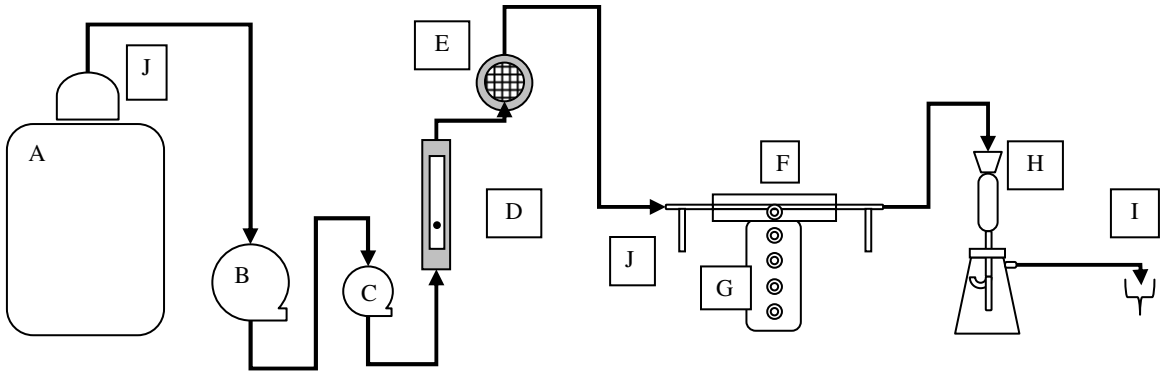

A: 10 L Media Carboy, B: Priming Pump, C: Operation Pump, D: Calibrated flow meter, E: 0.2 µm Filter Capsule, F: Flow Reactor, G: Sampling Ports, H: Free fall drip outlet, I: Drain to 55 gal drum, J: Glass pipette connecting tubing for sterilization purposes

APPENDIX B

Appendix B contains graphical representations of the spatial and temporal changes for pH, acetate, sulfate, nitrite, phosphate, chloride, iron, manganese, copper, zinc, and lead in the flow reactor operated over a 4 month period. It also includes the calibration standard for the anion species analyzed by ion chromatography (IC) and the gradient method that was used for IC analysis.

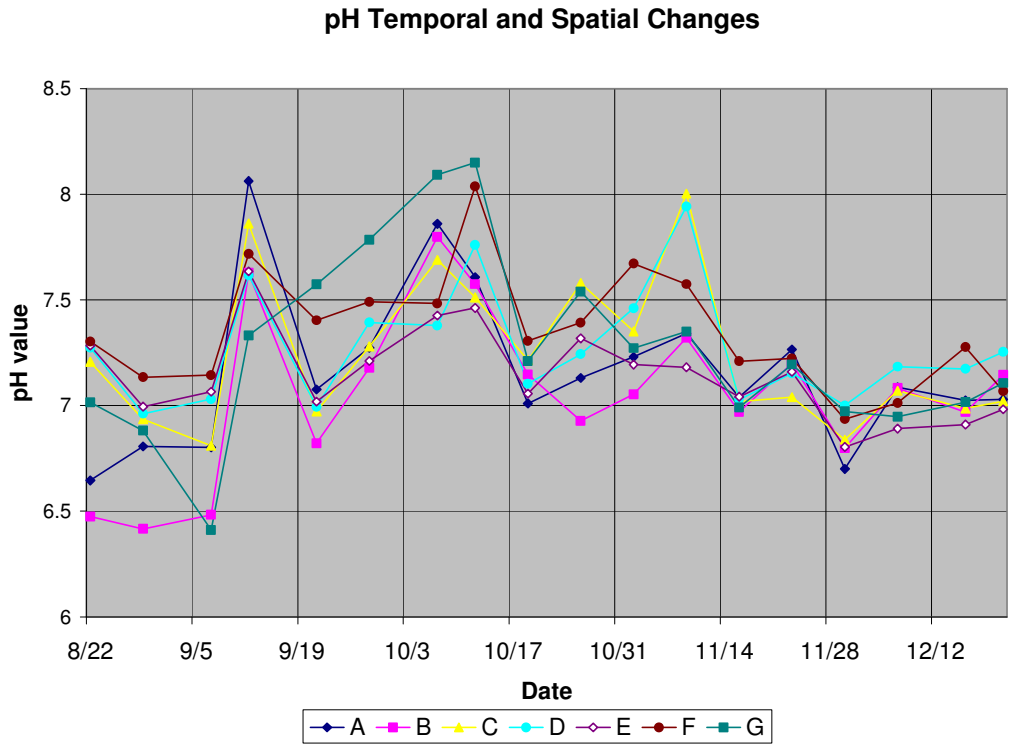
pH Temporal and Spatial Changes
pH value
8.5
8
7.5
7
6.5
6
8/22
9/5
9/19
10/3
10/17
10/31
11/14
11/28
12/12
Date
A
B
C
D
E
F
G

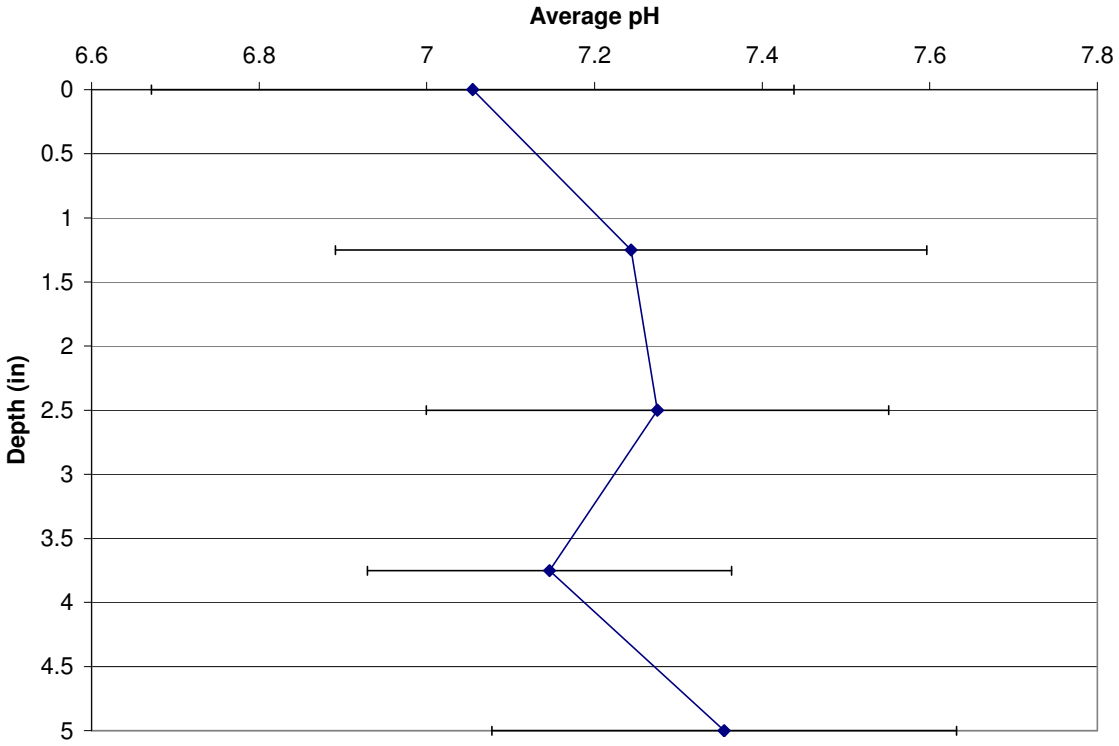
Average pH
6.6
6.8
7
7.2
7.4
7.6
7.8
Depth (in)
0
0.5
1
1.5
2
2.5
3
3.5
4
4.5
5

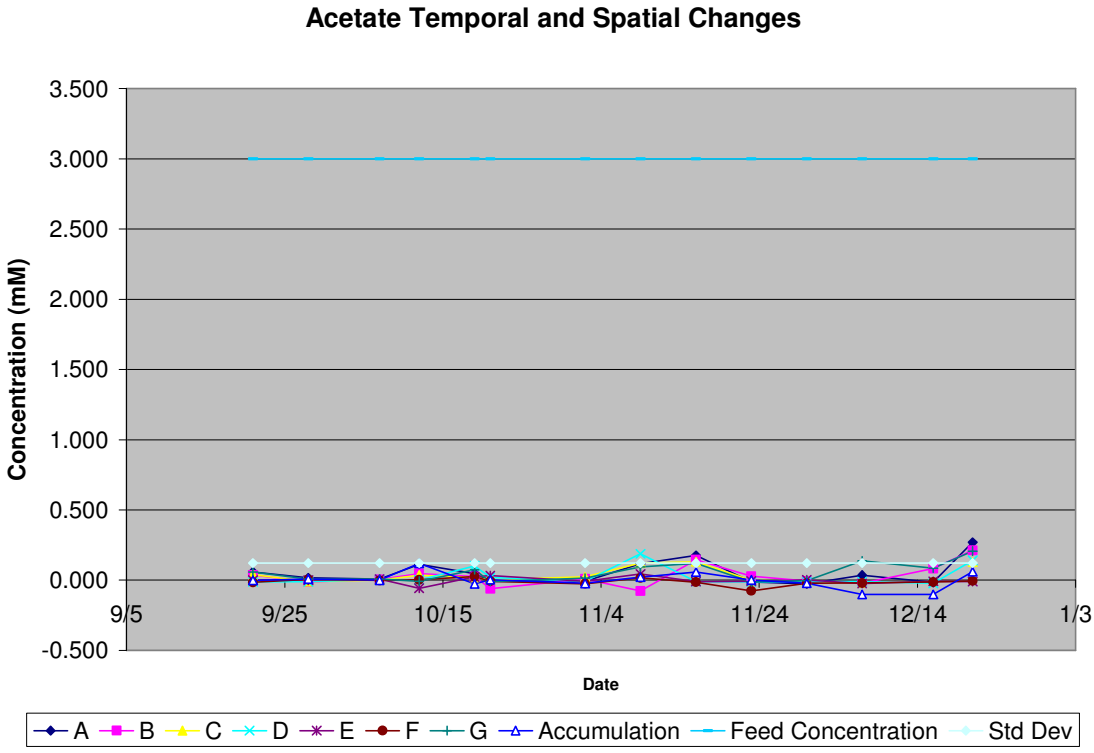
Acetate Temporal and Spatial Changes
3.500
3.000
2.500
2.000
1.500
1.000
0.500
0.000
-0.500
Concentration (mM)
9/5
9/25
10/15
11/4
11/24
12/14
1/3
Date
A
B
C
D
E
F
G
Accumulation
Feed Concentration
Std Dev

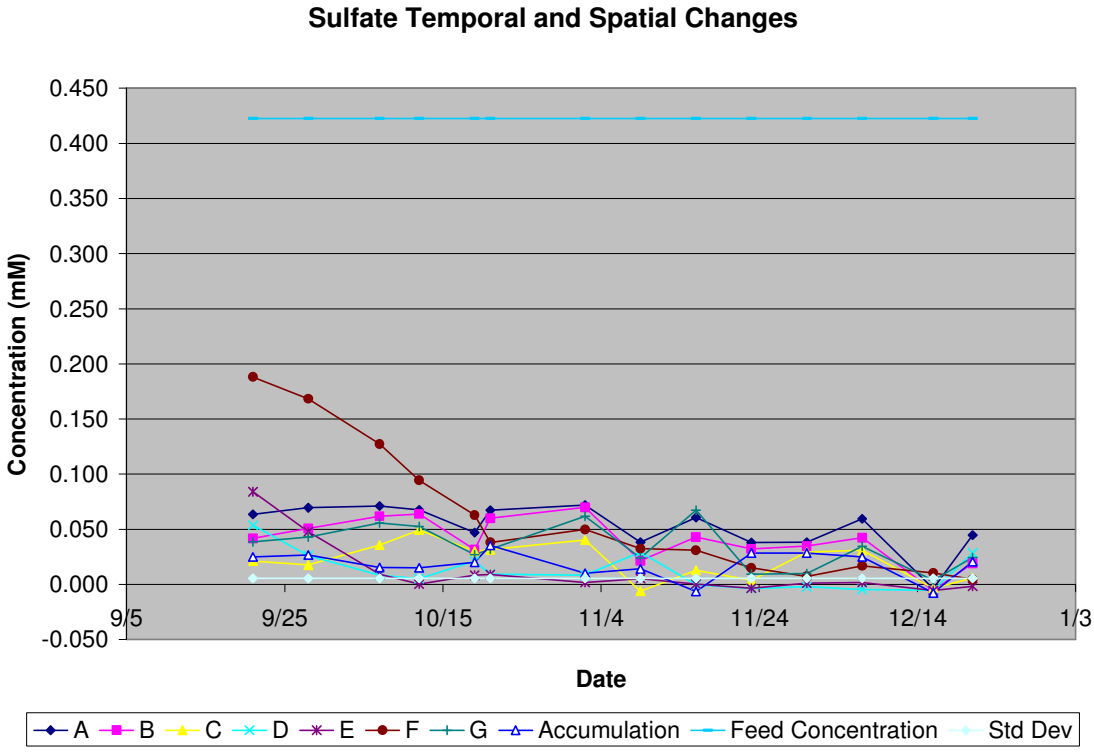
Sulfate Temporal and Spatial Changes
0.450
0.400
0.350
0.300
0.250
0.200
0.150
0.100
0.050
0.000
-0.050
Concentration (mM)
9/5
9/25
10/15
11/4
11/24
12/14
1/3
Date
A
B
C
D
E
F
G
Accumulation
Feed Concentration
Std Dev

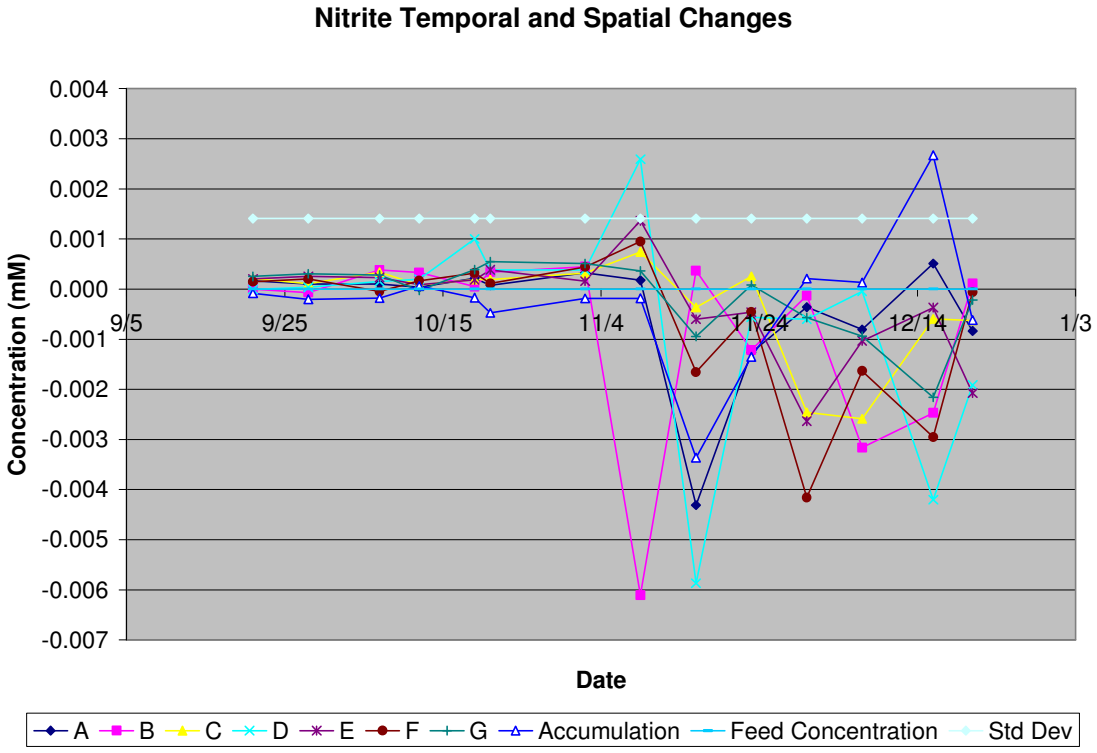
Nitrite Temporal and Spatial Changes
0.004
0.003
0.002
0.001
0.000
-0.001
-0.002
-0.003
-0.004
-0.005
-0.006
-0.007
Concentration (mM)
9/5
9/25
10/15
11/4
11/24
12/14
1/3
Date
A
B
C
D
E
F
G
Accumulation
Feed Concentration
Std Dev

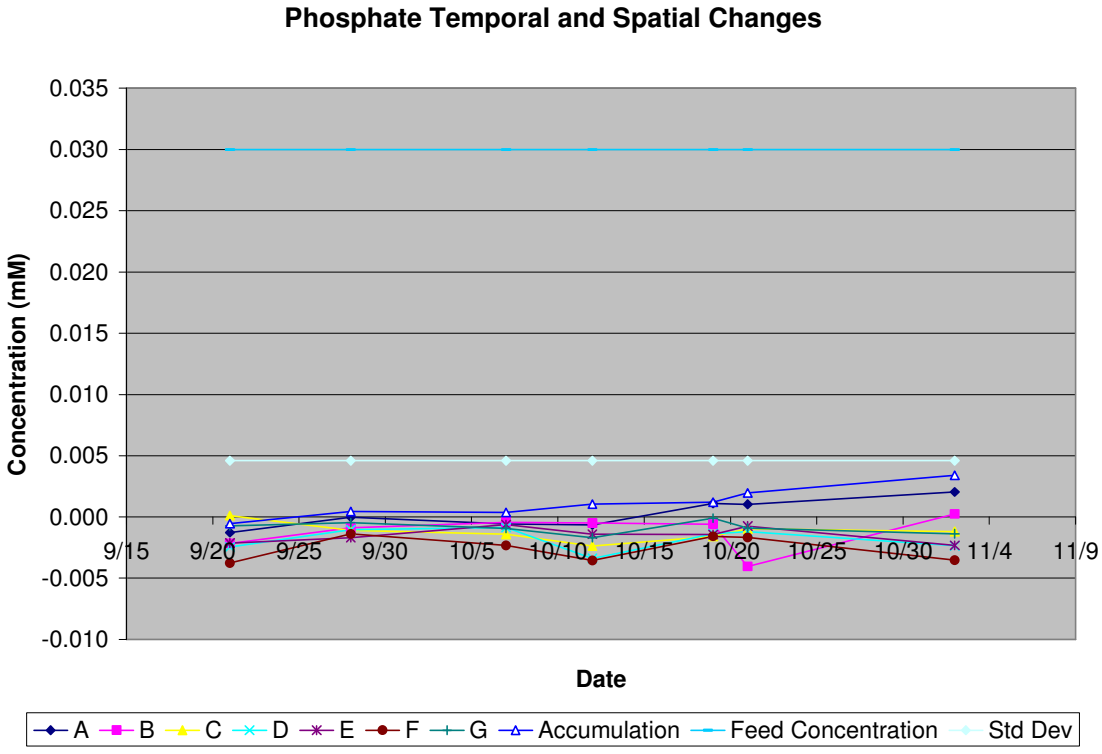
Phosphate Temporal and Spatial Changes
0.035
0.030
0.025
0.020
0.015
0.010
0.005
0.000
-0.005
-0.010
Concentration (mM)
9/15
9/20
9/25
9/30
10/5
10/10
10/15
10/20
10/25
10/30
11/4
11/9
Date
A
B
C
D
E
F
G
Accumulation
Feed Concentration
Std Dev

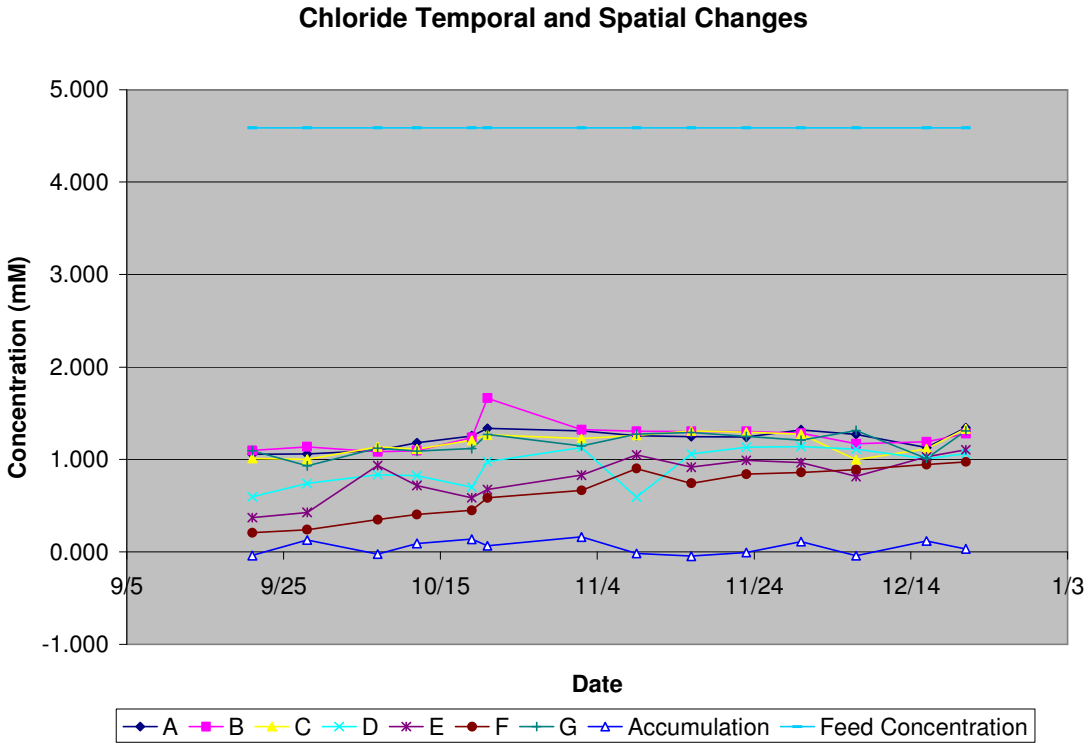
Chloride Temporal and Spatial Changes
5.000
4.000
3.000
2.000
1.000
0.000
-1.000
Concentration (mM)
9/5
9/25
10/15
11/4
11/24
12/14
1/3
Date
A
B
C
D
E
F
G
Accumulation
Feed Concentration

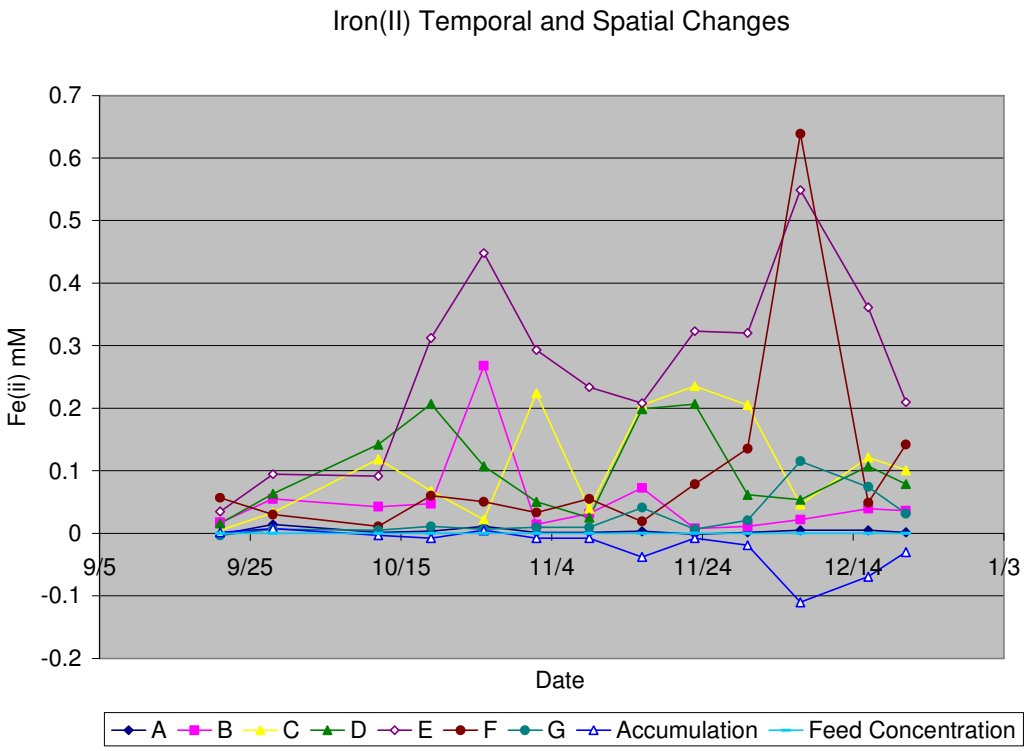
Iron(II) Temporal and Spatial Changes
0.7
0.6
0.5
0.4
0.3
0.2
0.1
0
-0.1
-0.2
Fe(ii) mM
9/5
9/25
10/15
11/4
11/24
12/14
1/3
Date
A
B
C
D
E
F
G
Accumulation
Feed Concentration

Copper Temporal and Spatial Variation

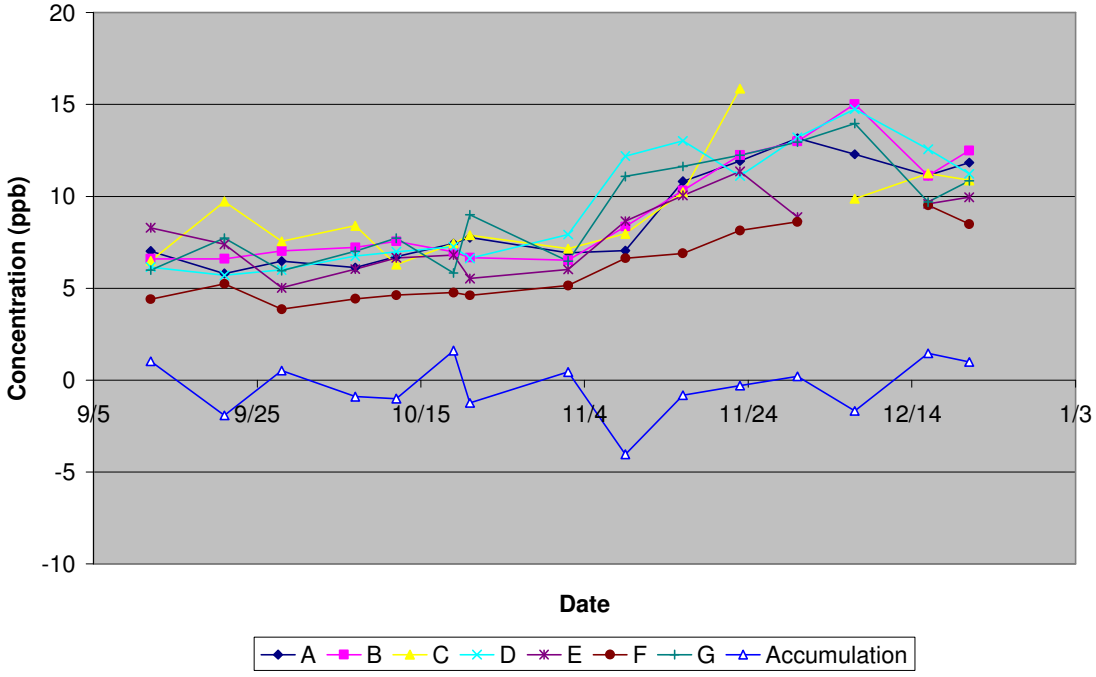

Lead Spatial and Temporal Variation

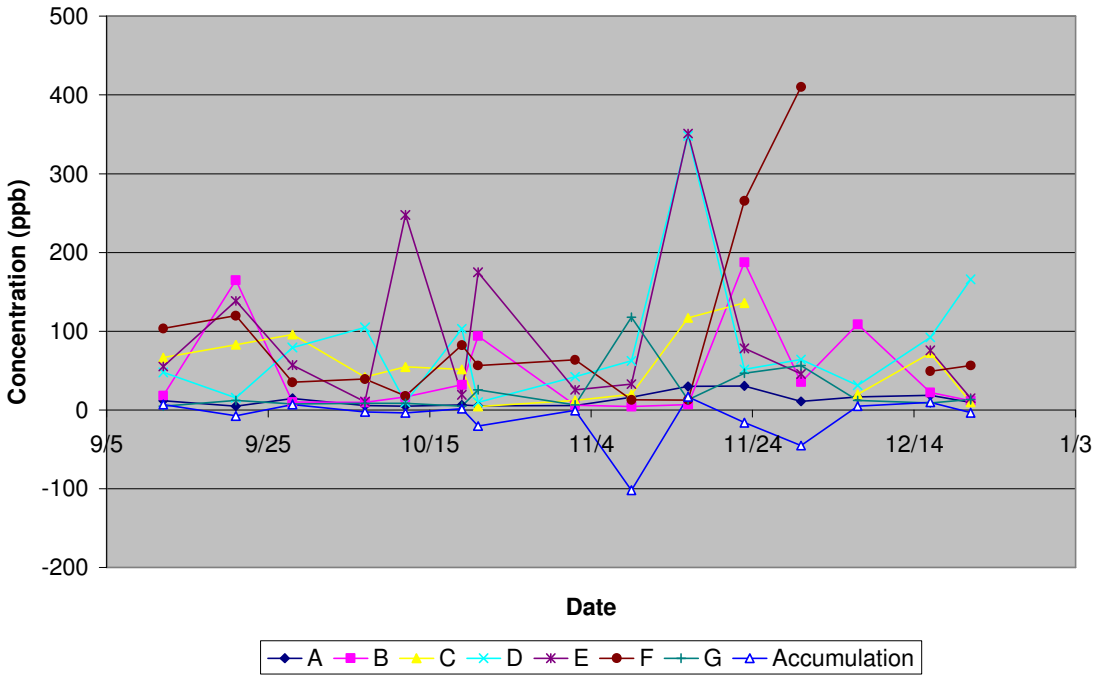

Zinc Temporal and Spatial Variation

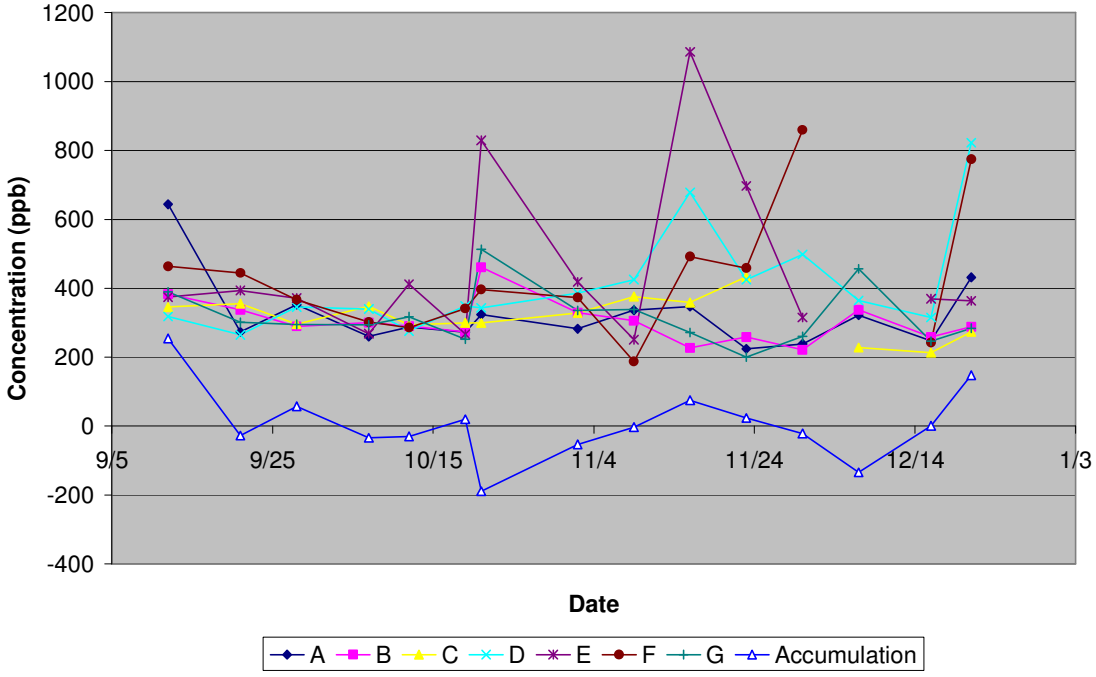

Manganese Temporal and Spatial Changes

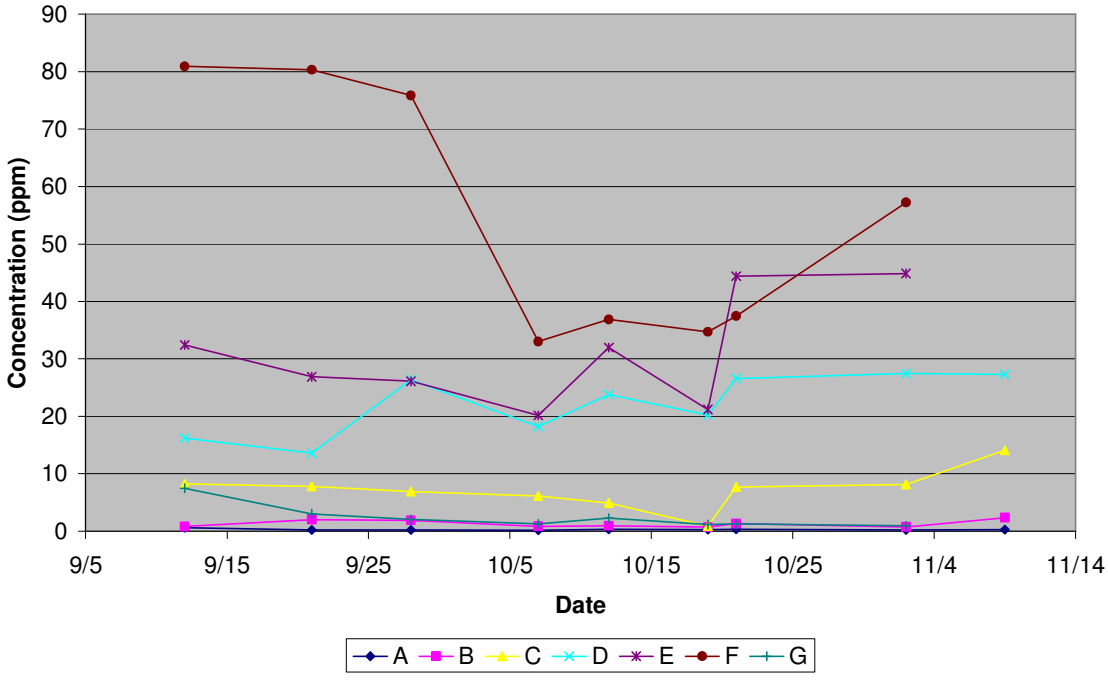

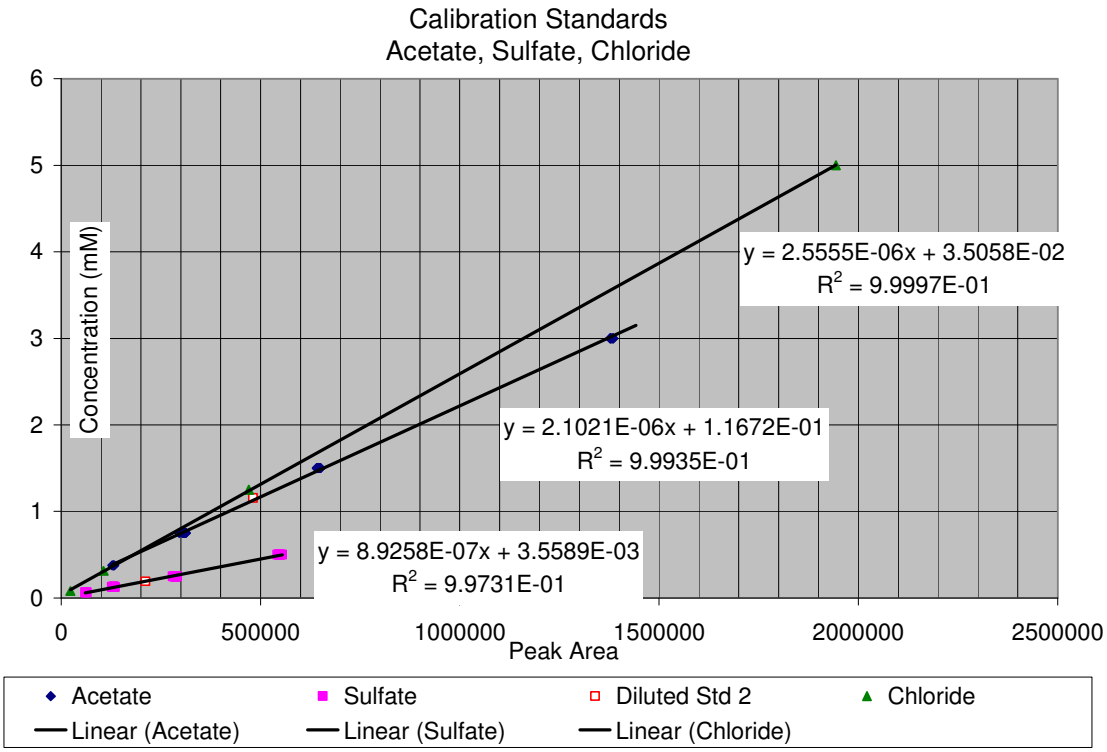
Calibration Standards
Acetate, Sulfate, Chloride
Concentration (mM)
Peak Area
y = 2.5555E-06x + 3.5058E-02
R2 = 9.9997E-01
y = 2.1021E-06x + 1.1672E-01
R2 = 9.9935E-01
y = 8.9258E-07x + 3.5589E-03
R2 = 9.9731E-01
Acetate
Sulfate
Diluted Std 2
Chloride
Linear (Acetate)
Linear (Sulfate)
Linear (Chloride)

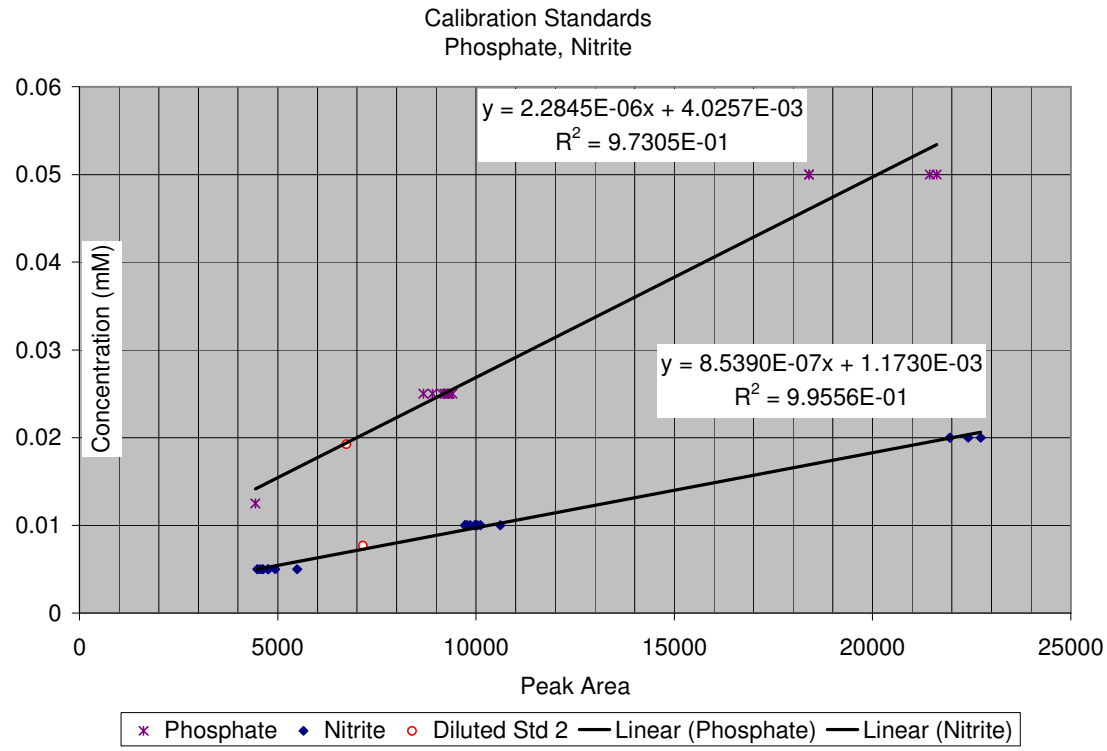
Calibration Standards
Phosphate, Nitrite
Concentration (mM)
Peak Area
y = 2.2845E-06x + 4.0257E-03
R2 = 9.7305E-01
y = 8.5390E-07x + 1.1730E-03
R2 = 9.9556E-01
Phosphate
Nitrite
Diluted Std 2
Linear (Phosphate)
Linear (Nitrite)

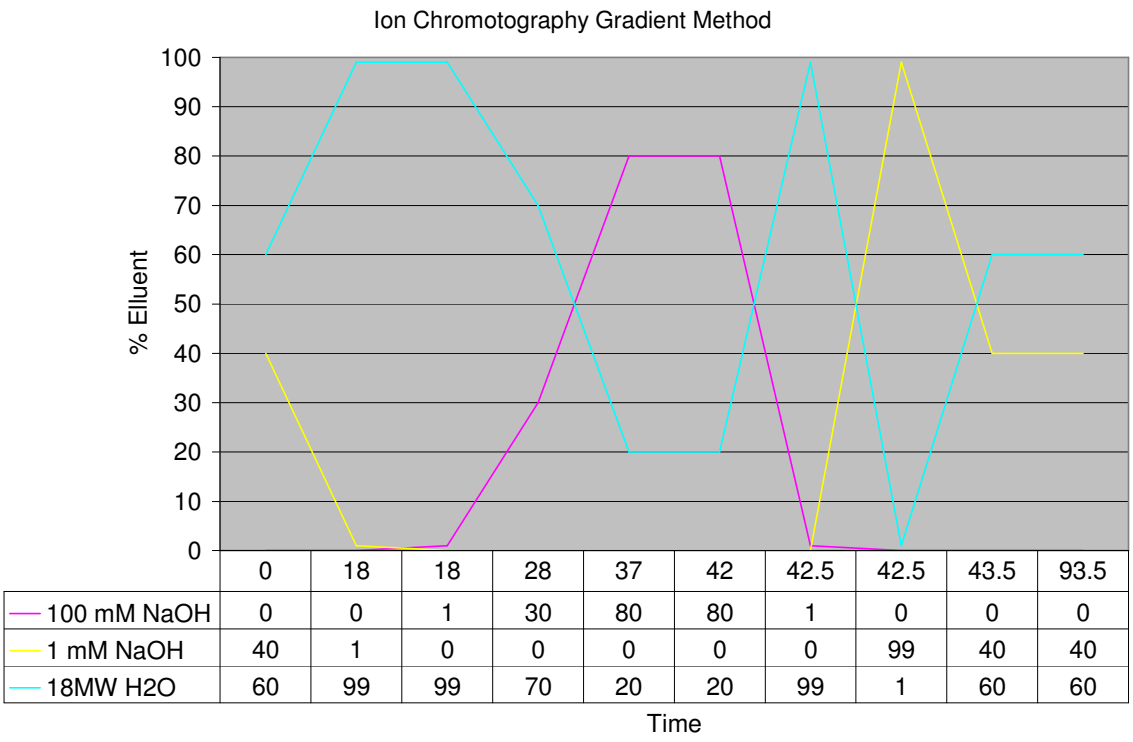

	0	18	18	28	37	42	42.5	42.5	43.5	93.5
100 mM NaOH	0	0	1	30	80	80	1	0	0	0
1 mM NaOH	40	1	0	0	0	0	0	99	40	40
18MW H2O	60	99	99	70	20	20	99	1	60	60

APPENDIX C

Appendix C contains the raw sequences obtained from 16S rDNA analysis listed with the most similar organism's name. The genus, species, and strain names are listed (where available) and an additional internal book keeping code JMXXX was added where XXX is a three digit code. On a few of the sequences you will notice a large number of N's at the beginning of the sequence. This is due to the robust nature of the BigDye® method where the detector is actually saturated.

>Bacillus_pumilus_JM013
CNNNNNNNNAGCCCGGCCNAACANTGCAGTCGAGCGAACAGAAGGGAGCTT
GCTCCCGGATGTTAGCGGCGGACGGGTGA
GTAACACGTGGGTAACCTGCCTGTAAGACTGGGATAACTCCGGGAAACCGGA
GCTAATACCGGATAGTTCCTTGAACCGC
ATGGTTCAAGGATGAAAGACGGTTTCGGCTGTCACTTACAGATGGACCCGCG
GCGCATTAGCTAGTTGGTGGGGTAATGG
CTCACCAAGGCGACGATGCGTAGCCGACCTGAGAGGGTGATCGGCCACACTG
GGACTGAGACACGGCCCAGACTCCTACG
GGAGGCAGCAGTAGGGAATCTTCCGCAATGGACGAAAGTCTGACGGAGCAA
CGCCGCGTGAGTGATGAAGGTTTTCGGAT
CGTAAAGCTCTGTTGTTAGGGAAGAACAAGTGCGAGAGTAACTGCTCGCACC
TTGACGGTACCTAACCAGAAAGCCACGG
CTAACTACGTGCCAGCAGCCGCGGTAATACGTAGGTGGCAAGCGTTGTCCGG
AATTATTGGGCGTAAAGGGCTCGCAGGC
GGTTTCTTAAGTCTGATGTGAAAGCCCCCGGCTCAACCGGGGAGGGTCATTG
GAAACTGGGAAACTTGAGTGCAGAAGAG
GAGAGTGGAATTCCACGTGTAGCGGTGAAATGCGTAGAGATGTGGAGGAAC
ACCAGTGGCGAAGGCGACTCTCTGGTCTG
TAACTGACGCTGAGGAGCGAAAGCGTGGGGAGCGAACAGGATTAGATACCC
TGGTAGTCCACGCCCGTAAACGATGAGTG
CTAAGTGTTAGGGGNTTCCGCCCTTAGTGCTGCAGCTANCGCATTAAGCACTC
CCCTGGGGAGTACGGTCNCAGACTGAA
CTCAAAGAATTGACGGGGNCCNCNCAACGGTGGAACATGT

>Bacillus_sp_Y17_JM020
CATGGGCAGCAACNNTGCAGTCGAGCGAATGGATTAAGAGCTTGCTCTTATG
AAGTTAGCGGCGGACGGGTGAGTAACAC
GTGGGTAACCTGCCCATAAGACTGGGATAACTCCGGGAAACCGGGGCTAATA
CCGGATAANATTTTGAACTGCATGGTTC
GAAATTGAAAGGCGGCTTCGGCTGTCACTTATGGATGGACCCGCGTCGCATT
AGCTAGTTGGTGAGGTAACGGCTCACCA
AGGCAACGATGCGTAGCCGACCTGAGAGGGTGATCGGCCACACTGGGACTG
AGACACGGCCCAGACTCCTACGGGAGGCA
GCAGTAGGGAATCTTCCGCAATGGACGAAAGTCTGACGGAGCAACGCCGCGT
GAGTGATGAAGGCTTTCGGGTCGTAAAA
CTCTGTTGTTAGGGAAGAACAAGTGCTAGTTGAATAAGCTGGCACCTTGACG
GTACCTAACCAGAAAGCCACGGCTAACT
ACGTGCCAGCAGCCGCGGTAATACGTAGGTGGCAAGCGTTATCCGGAATTAT
TGGGCGTAAAGCGCGCGCAGGTGGTTTC
TTAAGTCTGATGTGAAAGCCCACGGCTCAACCGTGGAGGGTCATTGGAAACT
GGGAGACTTGAGTGCAGAAGAGGAAAGT
GGAATTCCATGTGTAGCGGTGAAATGCGTAGAGATATGGAGGAACACCAGTG
GCGAAGGCGACTTTCTGGTCTGTAACTG
ACACTGAGGCGCGAAAGCGTGGGGAGCAAACAGGATTAGATACCNTGGTAG
TCCACGCCGTAAACGATGAGTGCTAAGTG
TNAGAGGNTTCCNCCCTTANTGCTGAAGTNACGCATAAGCACTCCCCTGGGG
AGTCNGCCNCAGNCTGAACTCAAGGAAT
GACNGG

>Paenibacillus_sp_S18-36_JM019
GNCCGNGNNCNATACAATGCAGTCGAGCGGAGTTATTCCTTCGGGGATAACT
TAGCGGCGGACGGGTGAGTAACACGTAG
GCAACCTGCCTGTAAGATCGGGATAACTACCGGAAACGGTAGCTAAGACCGG
ATAATCAGCTTGGTCGCATGATCGAGCT
GGGAAAAGCGGAGCAATCTGCTGCTTACAGATGGGCCTGCGGCGCATTAGCT
AGTTGGTGAGGTAACGGCTCACCAAGGC
GACGATGCGTAGCCGACCTGAGAGGGTGAACGGCCACACTGGGACTGAGAC
ACGGCCCAGACTCCTACGGGAGGCAGCAG
TAGGGAATCTTCCGCAATGGACGCAAGTCTGACGGAGCAACGCCGCGTGAGT
GATGAAGGTTTTCGGATCGTAAAGCTCT
GTTGCCAGGGAAGAACGCTTAGGAGAGTAACTGCTCTTAAGGTGACGGTACC
TGAGAAGAAAGCCCCGGCTAACTACGTG
CCAGCAGCCGCGGTAATACGTAGGGGGCAAGCGTTGTCCGGAATTATTGGGC
GTAAAGCGCGCGCAGGCGGCTTTGTAAG
TCTGGTGTTTAAACCTAGNGCTCAACNCTGGGTCGCATTGGAAACTGCAAGG
CTTGAGTGCAGAAGAGGAGAGTGGAATT
CCACGTGTAGCGGTGAAATGCGTAGAGATGTGGAGGAACACCAGTGGCGAA
GGCGACTCTCTGGGCTGTAACTGACGCTG
AGGCGCGAAAGCGTGGGGAGCAAACAGGATTAGATACCCTGGTAGTCCACG
CCGTAAACGATGAATGCTANGTGTNAGGG
GTTTCGATACCCTTGGTGCCGAANTAACACATNAGCATTCCCCTGGGGAGTA
CGGTCGCAGACTGAACTCAAGGATTGAC
GGGACC

>Bacillus_pumilus_JM019
NNAACNNNNNNNNNNCANNCAGTCGTACAGGTACCAGAGCTTGCTCCCGG
ATGTTAGCGGCggaTggGtGAGTAACACG
TGGGTAACCTGCCTGTAAGACTGGGATAACTCCGGGAAACCGGAGCTAATAC
CGGATAGTTCCTTGAACCGCATGGTTCA
AGGATGAAAGACGGTTTCGGCTGTCACTTACAGATGGACCCGCGGCGCATTA
GCTAGTTGGTGGGGTAATGGCTCACCAA
GGCGACGATGCGTAGCCGACCTGAGAGGGTGATCGGCCACACTGGGACTGA
GACACGGCCCAGACTCCTACGGGAGGCAG
CAGTAGGGAATCTTCCGCAATGGACGAAAGTCTGACGGAGCAACGCCGCGTG
AGTGATGAAGGTTTTCGGATCGTAAAGC
TCTGTTGTTAGGGAAGAACAAGTGCGAGAGTAACTGCTCGCACCTTGACGGT
ACCTAACCAGAAAGCCACGGCTAACTAC
GTGCCAGCAGCCGCGGTAATACGTAGGTGGCAAGCGTTGTCCGGAATTATTG
GGCGTAAAGGGCTCGCAGGCGGTTTCTT
AAGTCTGATGTGAAAGCCCCCGGCTCAACCGGGGAGGGTCATTGGAAACTGG
GAAACTTGAGTGCAGAAGAGGAGAGTGG
AATTCCACGTGTAGCGGTGAAATGCGTAGAGATGTGGAGGAACACCAGTGGC
GAAGGCGACTCTCTGGTCTGTAACTGAC
GCTGAGGAGCGAAAGCGTGGGGAGCGAACAGGATTAGATACCCTGGTAGTC
CACGCCGTAAACGATGAGTGCTAagTGTT
AGGGGGTTTCCGCCCCTTAGTGCTGCAGCTAACGCATAAGCACTCCCCTGGG
ANTACGNTCGCAGATGAACTCAANGAT

>Arthrobacter_sp_Tibet-IIR23_JM018
GNANCCNNNNNNNNNNCATGCAGTCGTACAGGTAACCACTTGTGGGGGGA
TTAGTGGCGAACGggNTgAGTAACACGTG
AGTAACCTGCCCTTAACTCTGGGATAAGCCTGGGAAACTGGGTCTAATACCG
GATATGACTCCTCATCGCATGGTGGGGG
GTGGAAAGCTTTATTGTGGTTTTGGATGGACTCGCGGCCTATCAGCTTGTTGG
TGAGGTAATGGCTCACCAAGGCGACGA
CGGGTAGCCGGCCTGAGAGGGTGACCGGCCACACTGGGACTGAGACACGGC
CCAGACTCCTACGGGAGGCAGCAGTGGGG
AATATTGCACAATGGGCGAAAGCCTGATGCAGCGACGCCGCGTGAGGGATG
ACGGCCTTCGGGTTGTAAACCTCTTTCAG
TAGGGAAGAAGCGAAAGTGACGGTACCTGCAGAAGAAGCGCCGGCTAACTA
CGTGCCAGCAGCCGCGGTAATACGTAGGG
CGCAAGCGTTATCCGGAATTATTGGGCGTAAAGAGCTCGTAGGCGGTTTGTC
GCGTCTGCCGTGAAAGTCCGGGGCTCAA
CTCCGGATCTGCGGTGGGTACGGGCAGACTAGAGTGATGTAGGGGAGACTGG
AATTCCTGGTGTAGCGGTGAAATGCGCA
GATATCAGGAGGAACACCGATGGCGAAGGCAGGTCTCTGGGCATTAACTGAC
GCTGAGGAGCGAAAGCATGGGGAGCGAA
CAGGATTAGATACCCTGGTAGTCCATGCCGTAAACGTTGGGCACTAGGTGTG
GGGGACATTCCACGTTTTCCGCGCCGTA
GCTANCGCATAAGTGCCCCGCCTGGGGAGTACGGCCGCAGGCTAAACTCAAG
NATTGACGGGGCCCCCCA

>Bacillus_megaterium_JM017
NCGNGGCAANNAACANTGCAGTTCGAGCGACTGATTAGAAGCTTGCTTCTAT
GACGTTAGCGGCGGACGGGTGAGTAACA
CGTGGGCAACCTGCCTGTAAGACTGGGATAACTTCGGGAAACCGAAGCTAAT
ACCGGATAGGATCTTCTCCTTCATGGGA
GATGATTGAAAGATGGTTTCGGCTATCACTTACAGATGGGCCCGCGGTGCAT
TAGCTAGTTGGTGAGGTAACGGCTCACC
AAGGCAACGATGCATAGCCGACCTGAGAGGGTGATCGGCCACACTGGGACT
GAGACACGGCCCAGACTCCTACGGGAGGC
AGCAGTAGGGAATCTTCCGCAATGGACGAAAGTCTGACGGAGCAACGCCGC
GTGAGTGATGAAGGCTTTCGGGTCGTAAA
ACTCTGTTGTTAGGGAAGAACAAGTACGAGAGTAACTGCTCGTACCTTGACG
GTACCTAACCAGAAAGCCACGGCTAACT
ACGTGCCAGCAGCCGCGGTAATACGTAGGTGGCAAGCGTTATCCGGAATTAT
TGGGCGTAAAGCGCGCGCAGGCGGTTTC
TTAAGTCTGATGTGAAAGCCCACGGCTCAACCGTGGAGGGTCATTGGAAACT
GGGGAACTTGAGTGCAGAAGAGAAAAGC
GGAATTCCACGTGTAGCGGTGAAATGCGTAGAGATGTGGAGGAACACCAGTG
GCGAAGGCGGCTTTTTGGTCTGTAACTG
ACGCTGAGGCGCGAAAGCGTGGGGAGCAACAGGATTAGATACCCTGGTAGT
CCACGCCGTAAACGATGAGTGCTAAGTGT
TAGAGGGTTTCCCCCNTTAGTGCTGCAGCTANCGCATAAGCACTCCCCTGGG
AGTACGGTCGCAGACTGAACTCAAGNAN

>Uncultured_Bacillus_sp._JM016
TGGGCANNACANTGCAGTCGAGCGATCAATAGGAGCTTGCTCCTGTTGNTTA
GCGGCGGACGGGTGAGTAACACGTGGGC
AACCTGCCTGTAAGACTGGGATAACACCGGGAAACCGGTGCTAATACCGGAT
AATCCTTTTCCTCTCATGAGGAAAAGCT
GAAAGTCGGTTTCGGCTGACACTTACAGATGGGCCCGCGGCGCATTAGCTAG
TTGGTGAGGTAACGGCTCACCAAGGCGA
CGATGCGTAGCCGACCTGAGAGGGTGATCGGCCACACTGGGACTGAGACAC
GGCCCAGACTCCTACGGGAGGCAGCAGTA
GGGAATCTTCCACAATGGACGAAAGTCTGATGGAGCAACGCCGCGTGAGCGA
TGAAGGCCTTCGGGTCGTAAAGCTCTGT
TGTTAGGGAAGAACAAGTACCGGAGTAACTGCCGGTACCTTGACGGTACCTA
ACCAGAAAGCCACGGCTAACTACGTGCC
AGCAGCCGCGGTAATACGTAGGTGGCAAGCGTTGTCCGGAATTATTGGGCGT
AAAGCGCGCGCAGGCGGTCCTTTAAGTC
TGATGTGAAAGCCCACGGCTCAACCGTGGAGGGTCATTGGAAACTGGGGGAC
TTGAGTGCAGAAGAGGAAAGCGGAATTC
CACGTGTAGCGGTGAAATGCGTAGAGATGTGGAGGAACACCAGTGGCGAAG
GCGGCTTTCTGGTCTGTAACTGACGCTGA
GGCGCGAAAGCGTGGGGAGCAAACAGGATTAGATACCCTGGTAGTCCACGC
CGTAAACGATGAGTGCTAAGTGTTAGGGG
GTTTCCGCCCTTAGTGCTGCAGCTANCGCATAANCACTCCNCCTGGGANTAC
GNCCCAAGNTNAACTCAAAGATTGACGG
GGNCC

>Pseudomonas_fluorescens_JM015
CNNNNNNNNAAGGCNNGGNCNATACAATGCAGTCGAGCGGNGTAGNCAAGC
TTGCTTCTCTTGAGAGCGGCGGACGGGTG
AGTAAAGCCTAGGAATCTGCCTGGTAGTGGGGGATAACGTTCGGAAACGGAC
GCTAATACCGCATACGTCCTACGGGAGA
AAGCAGGGGACCTTCGGGCCTTGCGCTATCAGATGAGCCTAGGTCGGATTAG
CTAGTTGGTGAGGTAATGGCTCACCAAG
GCGACGATCCGTAACTGGTCTGAGAGGATGATCAGTCACACTGGAACTGAGA
CACGGTCCAGACTCCTACGGGAGGCAGC
AGTGGGGAATATTGGACAATGGGCGAAAGCCTGATCCAGCCATGCCGCGTGT
GTGAAGAAGGTCTTCGGATTGTAAAGCA
CTTTAAGTTGGGAGGAAGGGCATTAACCTAATACGTTAGTGTTTTGACGTTAC
CGACAGAATAAGCACCGGCTAACTCTG
TGCCAGCAGCCGCGGTAATACAGAGGGTGCAAGCGTTAATCGGAATTACTGG
GCGTAAAGCGCGCGTAGGTGGTTTGTTA
AGTTGGATGTGAAATCCCCGGGCTCAACCTGGGAACTGCATTCAAAACTGAC
TGACTAGAGTATGGTAGAGGGTGGTGGA
ATTTCCTGTGTAGCGGTGAAATGCGTAGATATAGGAAGGAACACCAGTGGCG
AAGGCGACCACCTGGACTAATACTGACA
CTGAGGTGCGAAAGCGTGGGGAGCAAACAGGATTAGATACCCTGGTAGTCCA
CGCCGTAAACGATGTCAACTAGCCGTtG
GAGCTTNGAGCTCTAGTGGCGCAGCTAACGCATNANTTGACCNCTGGGGAGT
ACGGCCCNAGGTTAAACTCAATGATTGA
CGGGGCCCCCCANC

>Bacillus_sp_P54-2_JM014
AGNAGCGGCAAATACAATGCAGTTCGAGCGAATCNATGAGAGCTTGCTCCCT
GAGATTAGCGGCGGACGGGTGAGTAACA
CGTGGGCAACCTGCCTATAAGACTGGGATAACTTCGGGAAACCGGAGCTAAT
ACCGGATATGTTCTTTTCTCGCATGAGA
GAAGATGGAAAGACGGTTTCGGCTGTCACTTATAGATGGGCCCGCGGCGCAT
TAGCTAGTTGGTGAGGTAATGGCTCACC
AAGGCGACGATGCGTAGCCGACCTGAGAGGGTGATCGGCCACACTGGGACT
GAGACACGGCCCAGACTCCTACGGGAGGC
AGCAGTAGGGAATCTTCCGCAATGGACGAAAGTCTGACGGAGCAACGCCGC
GTGAACGAAGAAGGCCTTCGGGTCGTAAA
GTTCTGTTGTTAGGGAAGAACAAGTACCAGAGTAACTGCTGGTACCTTGACG
GTACCTAACCAGAAAGCCACGGCTAACT
ACGTGCCAGCAGCCGCGGTAATACGTAGGTGGCAAGCGTTGTCCGGAATTAT
TGGGCGTAAAGCGCGCGCAGGTGGTTCT
TTAAGTCTGATGTGAAAGCCCACGGCTCAACCGTGGAGGGTCATTGGAAACT
GGGGAACTTGAGTGCAGAAGAGGAAAGT
GGAATTCCAAGTGTAGCGGTGAAATGCGTAGAGATTTGGAGGAACACCAGTG
GCGAAGGCGACTTTCTGGTCTGTAACTG
ACACTGAGGCGCGAAAGCGTGGGGAGCAAACAGGATTAGATACCCTGGTAG
TCCACGCCGTAAACGATGAGTGCTAAGTG
TNAGAGGGTTCCGCCCTTAGTGCTGCAGCTAACGCATAAGCACTCNCCTGGG
GAGTACGACCCCAGGTTGAACTCAAAGA
TTGACGGGGCCCCNAAGC

>Burkholderia_pyrrocinia_JM012
TCGCTCCTTNCTGCAGTCGAACGGCAGCACGGGTGCTTGCACCTGGTGGCGA
GTGGCGAACGGGTGAGTAATACATCGGA
ACATGTCCTGTAGTGGGGGATAGCCCGGCGAAAGCCGGATTAATACCGCATA
CGATCTACGGATGAAAGCGGGGGACCTT
CGGGCCTCGCGCTATAGGGTTGGCCGATGGCTGATTAGCTAGTTGGTGGGGT
AAAGGCCTACCAAGGCGACGATCAGTAG
CTGGTCTGAGAGGACGACCAGCCACACTGGGACTGAGACACGGCCCAGACTC
CTACGGGAGGCAGCAGTGGGGAATTTTG
GACAATGGGCGAAAGCCTGATCCAGCAATGCCGCGTGTGTGAAGAAGGCCTT
CGGGTTGTAAAGCACTTTTGTCCGGAAA
GAAATCCTTGGCCCTAATACGGTCGGGGGATGACGGTACCGGAAGAATAAGC
ACCGGCTAACTACGTGCCAGCAGCCGCG
GTAATACGTAGGGTGCGAGCGTTAATCGGAATTACTGGGCGTAAAGCGTGCG
CAgGCGGTTTGTTAAGACCGATGTGAAA
TCCCCGGGCTCAACCTGGGAACTGCATTGGTGACTGGCAAGCTAGAGTATGG
CAgAAGGGGGTAGAATTCCaCGTGTAAC
AATGAAATGCGTAAANATGTGGAGGAATACCNATGGCGAANGCAGCCCCCT
GGGCCATACTGACCCTCATGCACNAAANC
GTGGGGAGCAAACANGATTAAATACCNTGGTAGTCCNCNCCCTAAACGATGT
CAACTANTTGTTGGGGATNCNTTNCTNA
TAACNTACTANCCNTGAATTNACCCCTGGGGATACGTCNCAAATAAAACTCA
AAGN

>Variovorax_sp_JM011
NCGCNCCTTNCATGCAGTTCGAACGGCAGCGCGGGAGCAATCCTGGCGGCGA
GTGGCGAACGGGTGAGTAATACATCGGA
ACGTGCCCAATCGTGGGGGATAACGCAGCGAAAGCTGTGCTAATACCGCATA
CGATCTACGGATGAAAGCAGGGGATCGC
AAGACCTTGCGCGAATGGAGCGGCCGATGGCAGATTAGGTAGTTGGTGAGGT
AAAGGCTCACCAAGCCTTCGATCTGTAG
CTGGTCTGAGAGGACGACCAGCCACACTGGGACTGAGACACGGCCCAGACTC
CTACGGGAGGCAGCAGTGGGGAATTTTG
GACAATGGGCGAAAGCCTGATCCAGCCATGCCGCGTGCAGGATGAAGGCCTT
CGGGTTGTAAACTGCTTTTGTACGGAAC
GAAACGGTCTTTTCTAATACAGAAGGCTAATGACGGTACCGTAAGAATAAGC
ACCGGCTAACTACGTGCCAGCAGCCGCG
GTAATACGTAGGGTGCAAGCGTTAATCGGAATTACTGGGCGTAAAGCGTGCG
CAGGCGGTTATGTAAGACAGTTGTGAAA
TCCCCGGGCTCAACCTGGGAACTGCATCTGTGACTGCATAGCTAGAGTACGG
TAGAgGGGGATGGAATTTCgCGTGTAgC
ANTGAAATGCGTANATATGCGGAGGAACACCGATGGCNAANGCNATCCCTG
GACCTGTACTGACGCTCATGCACNAAANC
GTGGGGAGCAAACANGGATTANATACCCTGGTAGTCCNCCCCNTAAACGATG
TCAACTGGNTGTTGGGNCTNCNCTGACT
CANTACCNAAACTAACCCGTGAANTNACCCCNTGGGGAGACGNCCCAAGGT
NNAANN

>Burkholderia_pyrrocinia_JM010
TCGCTCCTTNCATGCAGTCGAACGGCAGCACGGGTGCTTGCACCTGGTGGCG
AGTGGCGAACGGGTGAGTAATACATCGG
AACATGTCCTGTAGTGGGGGATAGCCCGGCGAAAGCCGGATTAATACCGCAT
ACGATCTACGGATGAAAGCGGGGGACCT
TCGGGCCTCGCGCTATAGGGTTGGCCGATGGCTGATTAGCTAGTTGGTGGGG
TAAAGGCCTACCAAGGCGACGATCAGTA
GCTGGTCTGAGAGGACGACCAGCCACACTGGGACTGAGACACGGCCCAGAC
TCCTACGGGAGGCAGCAGTGGGGAATTTT
GGACAATGGGCGAAAGCCTGATCCAGCAATGCCGCGTGTGTGAAGAAGGCCT
TCGGGTTGTAAAGCACTTTTGTCCGGAA
AGAAATCCTTGGCCCTAATACGGTCGGGGGATGACGGTACCGGAAGAATAAG
CACCGGCTAACTACGTGCCAGCAGCCGC
GGTAATACGTAGGGTGCGAGCGTTAATCGGAATTACTGGGCGTAAAGCGTGC
GCAGGCGGTTTGTTAAGACCGATGTGAA
ATCCCCGGGCTCAACCTGGGAACTGCATTGGTGACTGGCAAGCTAGAGTATG
GCAGAgGGGGGTAGAATTCCACGTGTAg
CAgTGAAATGCGTAgAGATGTGGAGGAATACCGATGGCGAANGCAGCCCCCT
GGGCCNATACTGACGCTCATGCACNAAA
NCGTGGGGAGCAANCANGATNAAATACCCTGGTAGTCCNCNCCNTAAACGAT
GTCAACTAGTTTTGGGGATNCATTNCTN
ANTAACNTAACTANCCNTGAANTNACCNCNTGGGN

>Ralstonia_sp._C6_JM009
NCGCTCTTNCTGCAGTCGACGGCAGCACGGGANCAATCCTGGTGGCGAGTGG
CGAACGGGTGAGTAATACATCGGAACGT
GCCCTGTCGTGGGGGATAACTAGTCGAAAGATTAGCTAATACCGCATACGAC
CTGAGGGTGAAAGCGGGGGACCGTAAGG
CCTCGCGCGATAGGAGCGGCCGATGTCTGATTAGCTAGTTGGTGGGGTAAAG
GCCCACCAAGGCGACGATCAGTAGCTGG
TCTGAGAGGACGATCAGCCACACTGGGACTGAGACACGGCCCAGACTCCTAC
GGGAGGCAGCAGTGGGGAATTTTGGACA
ATGGGGGCAACCCTGATCCAGCAATGCCGCGTGTGTGAAGAAGGCCTTCGGG
TTGTAAAGCACTTTTGTCCGGAAAGAAA
TCCCCTGCTCTAATACAGCGGGGGGATGACGGTACCGGAAGAATAAGCACCG
GCTAACTACGTGCCAGCAGCCGCGGTAA
TACGTAGGGTGCGAGCGTTAATCGGAATTACTGGGCGTAAAGCGTGCGCAGG
CGGTTTTGTAAGACAGGCGTGAAATCCC
CGAGCTCAACTTGGGAATGGCGCTTGTGACTGCAAGGCTAGAGTATGTCAGA
GGGGGGTAGAATTCCACGTGTAGCAGTG
AAATGCGTAGAGATGTGGAGGAATACCGATGGCGAANGCAGCCCCCTGGGN
ACGTCACTGACGCTCATGCACGAAAGCGT
GGGGGAGCAAACAGGATTAGATACCCTGGTAGTCCACGCCCTAAACGATGTC
ANCTAGTTGTTGGGGATCATTTCTTCAG
TAACGTANCTANCGCGTGAAGTTGACC

>Pseudomonas_sp._WDL5_JM007
NGGGNGCCTACCATGCAGTCGAGCGGATGAGAAGAGCTTGCTCTTCGATTCA
GCGGCGGACGGGTGAGTAATACCTAGGA
ATCTGCCTGGTAGTGGGGGACAACGTTTCGAAAGGAACGCTAATACCGCATA
CGTCCTACGGGAGAAAGCAGGGGACCTT
CGGGCCTTGCGCTATCAGATGAGCCTAGGTCGGATTAGCTAGTTGGTGAGGT
AATGGCTCACCAAGGCTACGATCCGTAA
CTGGTCTGAGAGGATGATCAGTCACACTGGAACTGAGACACGGTCCAGACTC
CTACGGGAGGCAGCAGTGGGGAATATTG
GACAATGGGCGAAAGCCTGATCCAGCCATGCCGCGTGTGTGAAGAAGGTCTT
CGGATTGTAAAGCACTTTAAGTTGGGAG
GAAGGGCATTAACCTAATACGTTAGTGTTTTGACGTTACCGACAGAATAAGC
ACCGGCTAACTCTGTGCCAGCAGCCGCG
GTAATACAGAGGGTGCAAGCGTTAATCGGAATTACTGGGCGTAAAGCGCGCG
TAGGTGGTTCGTTAAGTTGGATGTGAAA
TCCCCGGGCTCAACCTGGGAACTGCATCCAAAACTGGCGAGCTAGAgTAgGG
CANAAGGTGGTGGAATTTCCTGTGTAGC
GGTGAAATGCGTANATATAGGAAGGNACACCNGTGGCGAANGCGACCACCT
GGGCTCATACTGACACTGAGGTGCGAAAG
CGTGGGGAGCAAACANGANTANATACCCTGGTAGTCCNCNCCNTAAACAATG
TCAACTANCCNTTGGAATCCTNGANATT
TNTTGGGGCNCCTAACNCATTAATTNACCCCTGGGGAAACCGCCNCAGGTTA
AACTCNATG

>Pseudomonas_marginalis_JM006
NCGCGCCTACCATGCAGTCGAGCGGTAGAGAGAAGCTTGCTTCTCTTGAGAG
CGGCGGACGGGTGAGTAATGCCTAGGAA
TCTGCCTGGTAGTGGGGGATAACGCTCGGAAACGGACGCTAATACCGCATAC
GTCCTACGGGAGAAAGCAGGGGACCTTC
GGGCCTTGCGCTATCAGATGAGCCTAGGTCGGATTAGCTAGTTGGTGAGGTA
ATGGCTCACCAAGGCGACGATCCGTAAC
TGGTCTGAGAGGATGATCAGTCACACTGGAACTGAGACACGGTCCAGACTCC
TACGGGAGGCAGCAGTGGGGAATATTGG
ACAATGGGCGAAAGCCTGATCCAGCCATGCCGCGTGTGTGAAGAAGGTCTTC
GGATTGTAAAGCACTTTAAGTTGGGAGG
AAGGGCAGTTACCTAATACGTATCTGTTTTGACGTTACCGACAGAATAAGCA
CCGGCTAACTCTGTGCCAGCAGCCGCGG
TAATACAGAGGGTGCAAGCGTTAATCGGAATTACTGGGCGTAAAGCGCGCGT
AGGTGGTTTGTTAAGTTGGATGTGAAAT
CCCCGGGCTCAACCTGGGAACTGCATTCAAAACTGACAAGCTAGAGTATGGT
AGAGGGTGGTGGAATTTCCTGTGTAGCG
GTGAAATGCGTAgATATAGGAAGGAACACCNGTGGCGAANGCGACCACCTGG
ACTGATACTGACACTGANGTGCGAAAGC
GTGGGGAGCAAACANGATTANATACCCTGGTANTCCNCGCCNTAAACNATGT
CAACTANCCNTNGGAGCCTNGAGCTCTT
ANTGGCGCACTAACGCATTAATTNACCCCTGGGAGTACGNCCCCAGGTTAAA
CTCANTGATT

>Microbacterium_oxydans_JM005
TCGCGNCTACCATGCAGTCGAACGGTGACACGGAGCTTGCTCTGTGGGATCA
GTGGCGAACGGGTGAGTAACACGTGAGC
AACCTGCCCCTGACTCTGGGATAAGCGCTGGAAACGGCGTCTAATACTGGAT
ATGTGACGTGACCGCATGGTCTGCGTCT
GGAAAGAATTTCGGTTGGGGATGGGCTCGCGGCCTATCAGCTTGTTGGTGAG
GTAATGGCTCACCAAGGCGTCGACGGGT
AGCCGGCCTGAGAGGGTGACCGGCCACACTGGGACTGAGACACGGCCCAGA
CTCCTACGGGAGGCAGCAGTGGGGAATAT
TGCACAATGGGCGCAAGCCTGATGCAGCAACGCCGCGTGAGGGACGACGGC
CTTCGGGTTGTAAACCTCTTTTAGCAGGG
AAGAAGCGAAAGTGACGGTACCTGCAGAAAAAGCGCCGGCTAACTACGTGC
CAGCAGCCGCGGTAATACGTAGGGCGCAA
GCGTTATCCGGAATTATTGGGCGTAAAGAGCTCGTAGGCGGTTTGTCGCGTCT
GCTGTGAAATCCGGAGGCTCAACCTCC
GGCCTGCAGTGGGTACGGGCAGACTAGAGTGCGGTAGGGGAGATTGGAATTC
CTGGTGTAGCGGTGGAAATGCGCAGATA
TCAGGAGGAACACCGATGGCGAANGCAGATCTCTGGGCCGTAACTGACGCTG
AAGAGCGAAANGGTGGGGAGCAACAGGC
TTANATACCCTGGTAGTCCACCCGTAACGTNGGAACTAGTGTGGGGTCNNTC
CCGGATCCNTGACNCACTAACCATAANT
NCCCCCTGGGATACGNCNCAGNCTAAACTCAAGAATNACGGGACCNCNN

>Pseudomonas_plecoglossicida_JM004
NCGCNGCCTACCATGCAGTCGAGCGGATGAGAAGAGCTTGCTCTTCGATTCA
GCGGCGGACGGGTGAGTAATGCCTAGGA
ATCTGCCTGGTAGTGGGGGACAACGTTTCGAAAGGAACGCTAATACCGCATA
CGTCCTACGGGAGAAAGCAGGGGACCTT
CGGGCCTTGCGCTATCAGATGAGCCTAGGTCGGATTAGCTAGTTGGTGAGGT
AATGGCTCACCAAGGCGACGATCCGTAA
CTGGTCTGAGAGGATGATCAGTCACACTGGAACTGAGACACGGTCCAGACTC
CTACGGGAGGCAGCAGTGGGGAATATTG
GACAATGGGCGAAAGCCTGATCCAGCCATGCCGCGTGTGTGAAGAAGGTCTT
CGGATTGTAAAGCACTTTAAGTTGGGAG
GAAGGGCAGTAAGTTAATACCTTGCTGTTTTGACGTTACCGACAGAATAAGC
ACCGGCTAACTCTGTGCCAGCAGCCGCG
GTAATACAGAGGGTGCAAGCGTTAATCGGAATTACTGGGCGTAAAGCGCGCG
TAgGTGGTTCGTTAAGTTGAATGTGAAA
GCCCCGGGCTCAACCTGGGAACTGCATCCaAAACTGGCGAGCTAGAGTATGG
TAGANGGTGGTGGAATTTCCTGTGTANC
GGTGAAATGCGTANATATAGGAAGGAACACCNGTGGCGAANGCNACCNCCT
GGACTGATACTGACACTGANGTGCGAAAN
CGTGGGGAGCAAACANGATNAAATACCCNTGGTAGTCCNCNCCNTAAACNAT
GTCNACTANCCNTNGGANCCTTGAAATT
TTATGGCCCACCTAACNNTTAATTTACCCNTGGGAGACGNCNCAGGTAAACT
CAATGATTGC

>Pseudomonas_sp._PHLL_JM003
NGGCGCCTACCATGCAGTCGAGCGGATGAGAAGAGCTTGCTCTTCGATTCAG
CGGCGGACGGGTGAGTAATGCCTAGGAA
TCTGCCTGGTAGTGGGGGACAACGTTTCGAAAGGAACGCTAATACCGCATAC
GTCCTACGGGAGAAAGCAGGGGACCTTC
GGGCCTTGCGCTATCAGATGAGCCTAGGTCGGATTAGCTAGTTGGTGAGGTA
ATGGCTCACCAAGGCGACGATCCGTAAC
TGGTCTGAGAGGATGATCAGTCACACTGGAACTGAGACACGGTCCAGACTCC
TACGGGAGGCAGCAGTGGGGAATATTGG
ACAATGGGCGAAAGCCTGATCCAGCCATGCCGCGTGTGTGAAGAAGGTCTTC
GGATTGTAAAGCACTTTAAGTTGGGAGG
AAGGGCAGTAAGTTAATACCTTGCTGTTTTGACGTTACCGACAGAATAAGCA
CCGGCTAACTCTGTGCCAGCAGCCGCGG
TAATACAGAGGGTGCAAGCGTTAATCGGAATTACTGGGCGTAAAGCGCGCGT
AgGTGGTTCGTTAAGTTGAATGTGAAAG
CCCCGGGCTCAACCTGGGAACTGCATCCAAAACTGGCGAGCTAGAGTATGGT
AGAGGGTGGTGGAATTTCCTGTGTAGCG
GTGAAATGCGTAgATATAGGAAGGAACACCAGTGGCGAANGCGACCACCTGG
ACTGATACTGACACTGANGTGCGAAAGC
GTGGGGAGCAANCAGGATTANATACCCTGGTAGTCCCNCCNTAAACGATGTC
NACTANCCNTGGNATCCTTGANATTTNN
TGGCGCACCTAACNCTTAANTNACCCCTGGGGAGTACNGCCNCAGGTAAACT
CAAT

>Pseudomonas_fluorescens_JM002
NCGCNGCCTACCATGCAGTCGAGCGGATGACGNGAGCTTGCTCTCTGATTCA
GCGGCGGACGGGTGAGTAATGCCTAGGA
ATCTGCCTGGTAGTGGGGGACAACGTTTCGAAAGGAACGCTAATACCGCATA
CGTCCTACGGGAGAAAGCAGGGGACCTT
CGGGCCTTGCGCTATCAGATGAGCCTAGGTCGGATTAGCTAGTTGGTGAGGT
AATGGCTCACCAAGGCGACGATCCGTAA
CTGGTCTGAGAGGATGATCAGTCACACTGGAACTGAGACACGGTCCAGACTC
CTACGGGAGGCAGCAGTGGGGAATATTG
GACAATGGGCGAAAGCCTGATCCAGCCATGCCGCGTGTGTGAAGAAGGTCTT
CGGATTGTAAAGCACTTTAAGTTGGGAG
GAAGGGCATTAACCTAATACnTTNNTGTTTTGACGTTACCGACAGAATAAGCA
CCGGCTAACTCTGTGCCAGCAGCCGCG
GTAATACAGAGGGTGCAAGCGTTAATCGGAATTACTGGGCGTAAAGCGCGCG
TAGGTGGTTTGTTAAGTTGGATGTGAAA
GCCCCGGGCTCAACCTGGGAACTGCATTCAAAACTGACAAGCTAGAGTATGG
TAGAGGGTGGTGGAATTTCCTGTGTAGC
GGTGAAATGCGTAgATATAGGAAGGAACACCAGTGGCGAANGCGACCACCTG
GACTGATACTGACACTGANGTGCGAAAG
CGTGGGGAGCNAACAGGATNANATACCCTGGTAGTCCCCCCNTAACNATGTC
AACTANCCNTTGGAGCCTTGAGCTCTNA
NTGNCNCACCTAACCCATAANTNACNCCTGGGGAGTACG

>Pseudomonas_fluorescens_JM001
NNGCAACCTACCATGCAGTCGAGCGGATGACGGGAGCTTGCTCCCTGATTCA
GCGGCGGACGGGTGAGTAATGCCTAGGA
ATCTGCCTGGTAGTGGGGGACAACGTTTCGAAAGGAACGCTAATACCGCATA
CGTCCTACGGGAGAAAGCAGGGGACCTT
CGGGCCTTGCGCTATCAGATGAGCCTAGGTCGGATTAGCTAGTTGGTGAGGT
AATGGCTCACCAAGGCGACGATCCGTAA
CTGGTCTGAGAGGATGATCAGTCACACTGGAACTGAGACACGGTCCAGACTC
CTACGGGAGGCAGCAGTGGGGAATATTG
GACAATGGGCGAAAGCCTGATCCAGCCATGCCGCGTGTGTGAAGAAGGTCTT
CGGATTGTAAAGCACTTTAAGTTGGGAG
GAAGGGCATTAACCTAATACTTTNNTGTTTTGACGTTACCGACAGAATAAGC
ACCGGCTAACTCTGTGCCAGCAGCCGCG
GTAATACAGAGGGTGCAAGCGTTAATCGGAATTACTGGGCGTAAAGCGCGCG
TAGGTGGTTTGTTAAGTTGGATGTGAAA
GCCCCGGGCTCAACCTGGGAACTGCATTCAAAACTGACAAGCTAGAGTATGG
TAGAGGGTGGTGGAATTTCCTGTGTAGC
GGTGAAATGCGTAGATATAGGAAGGAACACCAGTGGCGAAGGCGACCACCT
GGACTGATACTGACACTGAGGTGCGAAAG
CGTGGGGAGCAAACAGGATTAGATACCCTGGTAGTCCACGCCGTAANCGATG
TCAACTAGCCGTNGGGAGCCTTGAGCTC
TTANTGGCGCAGCTAACGCATTANTTGACCGCCTG

>Bacillus_sp._JM021
CANGGGCANAACANTGCAGTCGAGCGAATCGATGGGAGCTTGCTCCCTGAGA
TTAGCGGCGGACGGGTGAGTAACACGTG
GGCAACCTGCCTATAAGACTGGGATAACTTCGGGAAACCGGAGCTAATACCG
GATACGTTCTTTTCTCGCATGAGAGAAG
ATGGAAAGACGGTTTCNGCTGTCNCTTNTNNATGGGCCCNCGGCNCATTANC
TANTTGGNGAGGTAATGGCTCNCCAAGG
NGACNATNCNTANCCNANCTGANAGGGTGATCGGCCNCNCTGGGACTGAAA
CNCGGCCCAAACTCCTNCGGGAGGNANCA
NTAGGGAATCTTCCNCAATGGACGAAAGTNTGACNGAACAACNCCCCNTGAA
CNAANAAGGCCTTCNGGTCNTAAAGTTN
TGTTGTTAGGGAANAACNAGTNCCNNANTAACTGCTGGNACCTTGACGGNAC
CTAACCNNAAAGCCNCGGCTAACTNCNT
GCCNNCAGCCNCGGTAATACNTANGTGGCAAGCGTTNTCCGGAATTNTTGGG
CGTAAAGCGNGNNCAGGNGGTTCCTTAA
GTCTGANGTGAAAGCCCNCGGCTCAACCGTGGANGGTCATTGGAAACTGGGG
AACTTGAGTGCANAANAAGAAAGTGGAA
TTCCAAGTGTAGCGGTGAAATGCGTAAAGATTTGGAGGAACACCAGTGGCGA
ANGCGACTTTCTGGTCTGTAACTGACNC
TGANGCGCGAAAGCGTGGGGAGCAAACAGGATTANATACCCTGGTAGTCCCC
CCNTAAACAATGANTGCTAATGTNANAG
GNTTCCCCCCTTTATGCTGCACTANCNNTTAANCCTCCCCTGGGGATACGGCC
CAGGNTNANCNNAAGAA

APPENDIX D

Appendix D contains graphical representations of the zinc data from the *Arthrobacter* reactor isolate experimental runs.

Zinc Inhibition of Arthrobacter: Zinc Concentrations

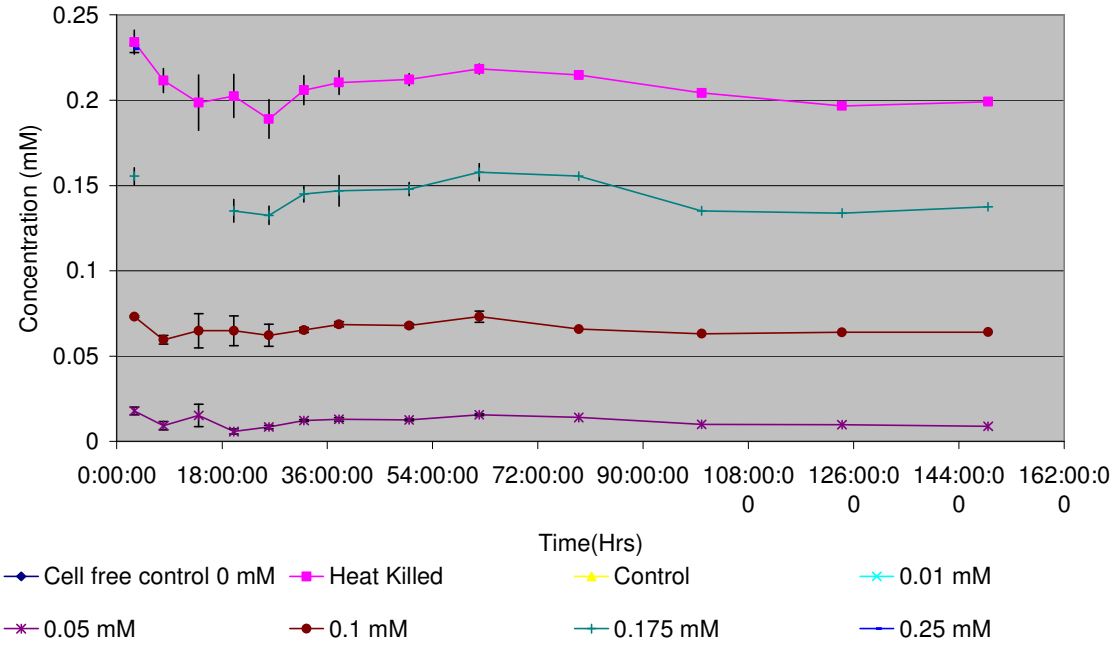

Zinc Toxicity on Growth Phase: Zinc Concentration

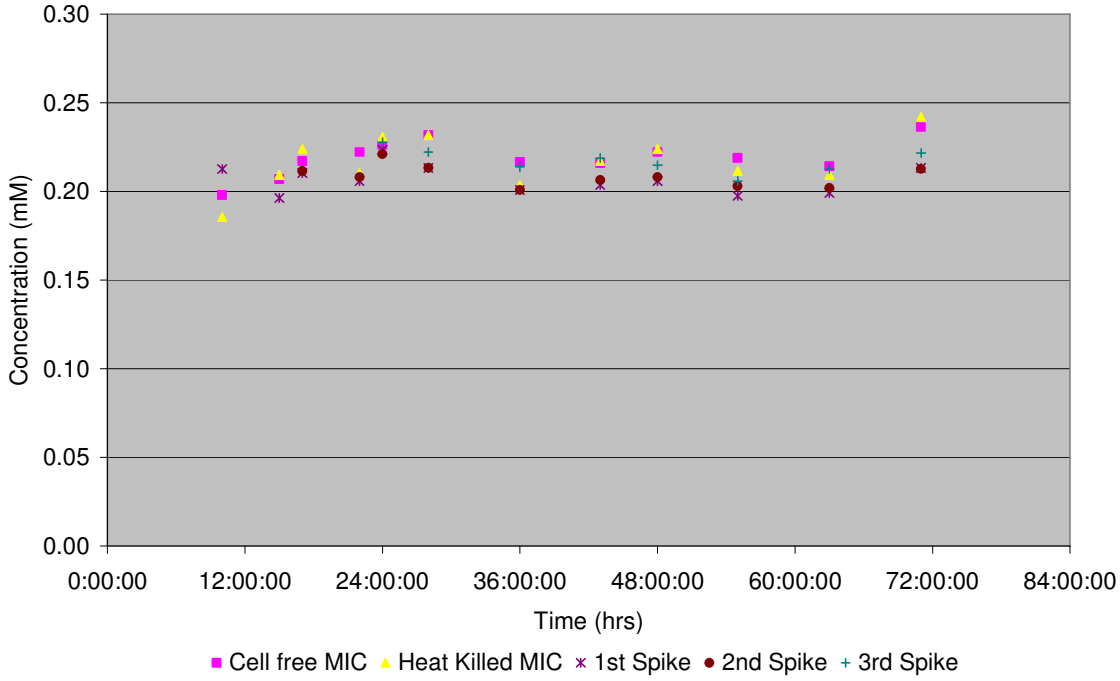

APPENDIX E

Appendix E contains the geochemical modeling done in Visual MINTEQ 2.32 and PHREEQ 2.11 to determine zinc speciation and iron bearing mineral phases, respectively.

PHREEQC 2.11 Geochemical Modeling of reactor Fe Minerals

Reading data base.

SOLUTION_MASTER_SPECIES
SOLUTION_SPECIES
PHASES
EXCHANGE_MASTER_SPECIES
EXCHANGE_SPECIES
SURFACE_MASTER_SPECIES
SURFACE_SPECIES
RATES
END

Reading input data for simulation 1.

```
DATABASE C:\Program Files\USGS\Phreeqc Interactive 2.11\phreeqc.dat
MIX 1
   1    1
SOLUTION 1
   temp      25
   pH       7.35
   pe       4
   redox     pe
   units     mmol/kgw
   density   1
   Fe(2)     0.10458
   Cu(2)     9.6e-005
   Mn(2)     0.99291
   Zn        0.0065423
   water     1 # kg
```

Beginning of initial solution calculations.

Initial solution 1.

----------Solution composition----------

Elements	Molality	Moles
Cu(2)	9.600e-008	9.600e-008
Fe(2)	1.046e-004	1.046e-004
Mn(2)	9.929e-004	9.929e-004
Zn	6.542e-006	6.542e-006

----------Description of solution----------

pH = 7.350
pe = 4.000

Activity of water = 1.000
Ionic strength = 2.206e-003
Mass of water (kg) = 1.000e+000
Total alkalinity (eq/kg) = 1.685e-006
Total carbon (mol/kg) = 0.000e+000
Total CO2 (mol/kg) = 0.000e+000
Temperature (deg C) = 25.000
Electrical balance (eq) = 2.207e-003
Percent error, 100*(Cat-|An|)/(Cat+|An|) = 99.98
Iterations = 4
Total H = 1.110124e+002
Total O = 5.550622e+001

----------Distribution of species----------

Species	Molality	Log Activity	Log Molality	Log Activity	Gamma
OH-	2.361e-007	2.241e-007	-6.627	-6.650	-0.023
H+	4.688e-008	4.467e-008	-7.329	-7.350	-0.021
H2O	5.551e+001	1.000e+000	1.744	-0.000	0.000
Cu(2)	9.600e-008				
Cu(OH)2	8.425e-008	8.430e-008	-7.074	-7.074	0.000
Cu+2	9.849e-009	8.050e-009	-8.007	-8.094	-0.088
CuOH+	1.898e-009	1.802e-009	-8.722	-8.744	-0.023
Cu(OH)3-	1.198e-013	1.137e-013	-12.922	-12.944	-0.023
Cu(OH)4-2	6.249e-019	5.079e-019	-18.204	-18.294	-0.090
Fe(2)	1.046e-004				
Fe+2	1.039e-004	8.496e-005	-3.983	-4.071	-0.088
FeOH+	6.335e-007	6.015e-007	-6.198	-6.221	-0.023
H(0)	2.824e-026				
H2	1.412e-026	1.413e-026	-25.850	-25.850	0.000
Mn(2)	9.929e-004				
Mn+2	9.924e-004	8.112e-004	-3.003	-3.091	-0.088
MnOH+	4.916e-007	4.668e-007	-6.308	-6.331	-0.023
O(0)	0.000e+000				
O2	0.000e+000	0.000e+000	-40.680	-40.680	0.000
Zn	6.542e-006				
Zn+2	6.375e-006	5.196e-006	-5.196	-5.284	-0.089
ZnOH+	1.343e-007	1.275e-007	-6.872	-6.894	-0.023
Zn(OH)2	3.277e-008	3.278e-008	-7.485	-7.484	0.000
Zn(OH)3-	2.444e-012	2.321e-012	-11.612	-11.634	-0.023
Zn(OH)4-2	1.013e-017	8.234e-018	-16.994	-17.084	-0.090

----------Saturation indices----------

Phase	SI	log IAP	log KT	
H2(g)	-22.70	-25.85	-3.15	H2
H2O(g)	-1.51	-0.00	1.51	H2O
Hausmannite	-3.50	57.53	61.03	Mn3O4
Manganite	-2.38	22.96	25.34	MnOOH
O2(g)	-37.72	-40.68	-2.96	O2
Pyrochroite	-3.59	11.61	15.20	Mn(OH)2
Pyrolusite	-7.07	34.31	41.38	MnO2

```
        Zn(OH)2(e)       -2.08    9.42   11.50  Zn(OH)2

-----------------------------------------
Beginning of batch-reaction calculations.
-----------------------------------------

Reaction step 1.

Using mix 1.

Mixture 1.

          1.000e+000 Solution 1

-----------------------------Solution composition-------------------------------

          Elements          Molality       Moles

          Cu              9.600e-008  9.600e-008
          Fe              1.046e-004  1.046e-004
          Mn              9.929e-004  9.929e-004
          Zn              6.542e-006  6.542e-006

-----------------------------Description of solution----------------------------

                                pH  =   7.327      Charge balance
                                pe  =   0.480      Adjusted to redox equilibrium
                     Activity of water  =   1.000
                        Ionic strength  =  2.206e-003
                       Mass of water (kg)  =  1.000e+000
                  Total alkalinity (eq/kg)  =  1.503e-006
                    Total carbon (mol/kg)  =  0.000e+000
                     Total CO2 (mol/kg)  =  0.000e+000
                    Temperature (deg C)  =  25.000
                  Electrical balance (eq)  =  2.207e-003
 Percent error, 100*(Cat-|An|)/(Cat+|An|)  =  99.98
                          Iterations  =  11
                            Total H  = 1.110124e+002
                            Total O  = 5.550622e+001

----------------------------Distribution of species-----------------------------

                                          Log       Log         Log
          Species          Molality    Activity  Molality  Activity    Gamma

          OH-             2.238e-007  2.124e-007    -6.650    -6.673    -0.023
          H+              4.946e-008  4.713e-008    -7.306    -7.327    -0.021
          H2O             5.551e+001  1.000e+000     1.744    -0.000     0.000
Cu(1)         9.063e-008
          Cu+             9.063e-008  8.595e-008    -7.043    -7.066    -0.023
Cu(2)         5.371e-009
          Cu(OH)2         4.654e-009  4.657e-009    -8.332    -8.332     0.000
          Cu+2            6.057e-010  4.951e-010    -9.218    -9.305    -0.088
          CuOH+           1.106e-010  1.050e-010    -9.956    -9.979    -0.023
          Cu(OH)3-        6.270e-015  5.953e-015   -14.203   -14.225    -0.023
          Cu(OH)4-2       3.101e-020  2.520e-020   -19.508   -19.599    -0.090
```

```
Fe(2)         1.045e-004
          Fe+2            1.039e-004  8.492e-005    -3.983    -4.071    -0.088
          FeOH+           6.001e-007  5.698e-007    -6.222    -6.244    -0.023
Fe(3)         9.063e-008
          Fe(OH)3         6.446e-008  6.449e-008    -7.191    -7.190     0.000
          Fe(OH)2+        2.485e-008  2.359e-008    -7.605    -7.627    -0.023
          Fe(OH)4-        1.314e-009  1.248e-009    -8.881    -8.904    -0.023
          FeOH+2          4.132e-012  3.358e-012   -11.384   -11.474    -0.090
          Fe+3            3.789e-017  2.451e-017   -16.422   -16.611    -0.189
          Fe2(OH)2+4      6.957e-022  3.035e-022   -21.158   -21.518    -0.360
          Fe3(OH)4+5      5.468e-027  1.496e-027   -26.262   -26.825    -0.563
H(0)          3.440e-019
          H2              1.720e-019  1.721e-019   -18.764   -18.764     0.000
Mn(2)         9.929e-004
          Mn+2            9.924e-004  8.112e-004    -3.003    -3.091    -0.088
          MnOH+           4.659e-007  4.424e-007    -6.332    -6.354    -0.023
Mn(3)         1.208e-028
          Mn+3            1.208e-028  7.578e-029   -27.918   -28.120    -0.203
O(0)          0.000e+000
          O2              0.000e+000  0.000e+000   -54.852   -54.851     0.000
Zn            6.542e-006
          Zn+2            6.385e-006  5.204e-006    -5.195    -5.284    -0.089
          ZnOH+           1.275e-007  1.211e-007    -6.894    -6.917    -0.023
          Zn(OH)2         2.948e-008  2.949e-008    -7.530    -7.530     0.000
          Zn(OH)3-        2.084e-012  1.979e-012   -11.681   -11.704    -0.023
          Zn(OH)4-2       8.188e-018  6.655e-018   -17.087   -17.177    -0.090

-------------------------------Saturation indices--------------------------------

          Phase               SI log IAP  log KT

          Fe(OH)3(a)        0.48    5.37    4.89  Fe(OH)3
          Goethite          6.37    5.37   -1.00  FeOOH
          H2(g)           -15.61  -18.76   -3.15  H2
          H2O(g)           -1.51   -0.00    1.51  H2O
          Hausmannite     -10.73   50.30   61.03  Mn3O4
          Hematite         14.75   10.74   -4.01  Fe2O3
          Manganite        -5.97   19.37   25.34  MnOOH
          O2(g)           -51.89  -54.85   -2.96  O2
          Pyrochroite      -3.64   11.56   15.20  Mn(OH)2
          Pyrolusite      -14.20   27.18   41.38  MnO2
          Zn(OH)2(e)       -2.13    9.37   11.50  Zn(OH)2

------------------
End of simulation.
------------------

-------------------------------------
Reading input data for simulation 2.
-------------------------------------

-----------
End of run.
```

Visual MINTEQ 2.32 Geochemical modeling of zinc speciation in reactor media

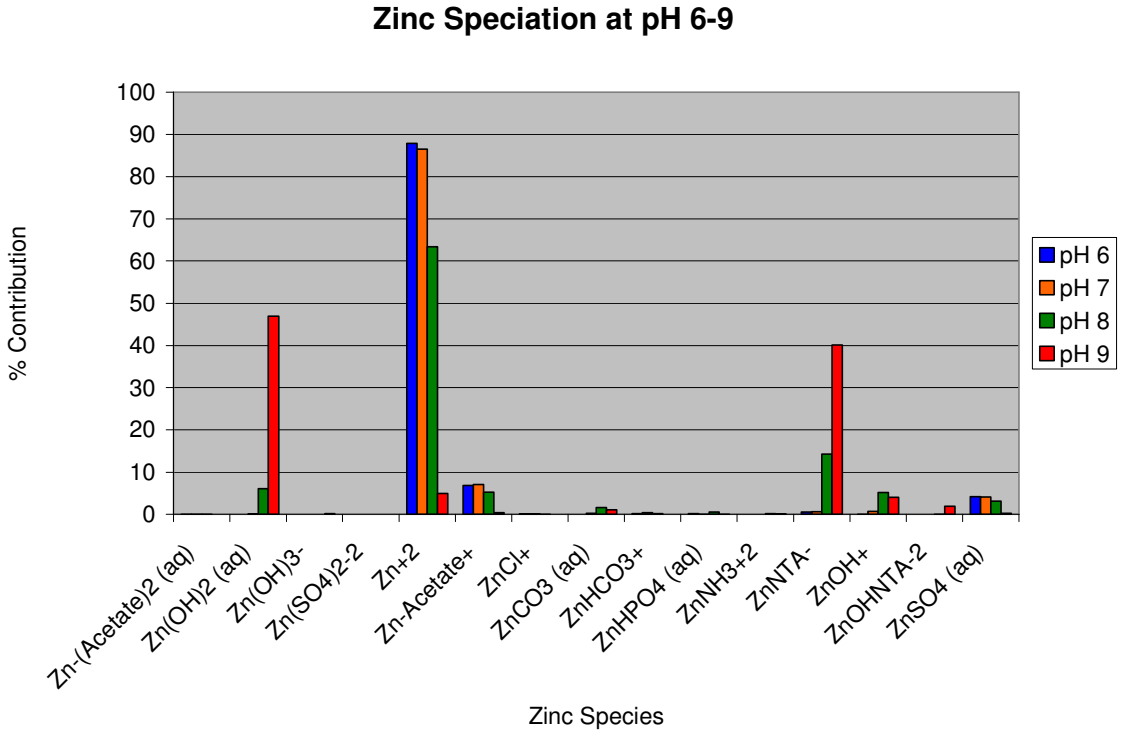

Speciation of Media Components pH 6		
Component	% of total component concentration	Species name
Zn+2	87.854	Zn+2
	6.848	Zn-Acetate+
	4.202	ZnSO4 (aq)
	0.519	ZnNTA-
	0.213	ZnHPO4 (aq)
	0.151	ZnHCO3+
	0.076	ZnCl+
	0.071	ZnOH+
	0.036	Zn-(Acetate)2 (aq)
	0.015	Zn(SO4)2-2
	0.012	ZnCO3 (aq)
Acetate-1	94.15	Acetate-1
	4.974	H-Acetate (aq)
	0.57	Zn-Acetate+
	0.012	Mg-Acetate+
	0.037	Ca-Acetate+
	0.25	Na-Acetate (aq)
Ca+2	92.203	Ca+2
	0.069	CaCl+
	4.627	CaSO4 (aq)

	0.05	CaHPO4 (aq)
	0.041	CaH2PO4+
	0.064	CaHCO3+
	0.012	CaMoO4(aq)
	2.934	Ca-Acetate+
Cl-1	99.769	Cl-1
	0.047	ZnCl+
	0.175	NaCl (aq)
PO4-3	7.17	HPO4-2
	90.013	H2PO4-
	0.012	H3PO4
	0.024	MgHPO4 (aq)
	0.062	CaHPO4 (aq)
	0.052	CaH2PO4+
	0.254	NaHPO4-
	1.78	ZnHPO4 (aq)
	0.63	NaH2PO4 (aq)
CO3-2	32.349	HCO3-
	67.398	H2CO3* (aq)
	0.013	ZnCO3 (aq)
	0.167	ZnHCO3+
	0.011	CaHCO3+
	0.057	NaHCO3 (aq)
NTA-3	0.022	HNTA-2
	99.962	ZnNTA-
	0.01	NiNTA-
H3BO3	99.832	H3BO3
	0.105	H3BO3-Acetate-
	0.063	H2BO3-
K+1	99.641	K+1
	0.129	K-Acetate (aq)
	0.017	KCl (aq)
	0.207	KSO4-
Mg+2	92.485	Mg+2
	0.11	MgCl+
	3.7	MgSO4 (aq)
	0.069	MgHPO4 (aq)
	0.052	MgHCO3+
	0.034	MgMoO4(aq)
	3.55	Mg-Acetate+
SO4-2	95.195	SO4-2
	2.486	ZnSO4 (aq)
	0.017	Zn(SO4)2-2
	0.09	MgSO4 (aq)
	0.41	CaSO4 (aq)
	1.566	NaSO4-
	0.223	NH4SO4-
Na+1	99.629	Na+1
	0.017	NaCl (aq)
	0.161	NaSO4-

	0.183	Na-Acetate (aq)
Ni+2	86.085	Ni+2
	3.71	NiSO4 (aq)
	0.014	NiH2PO4+
	0.09	NiHPO4 (aq)
	0.571	NiHCO3+
	4.474	NiNTA-
	4.914	Ni-Acetate+
	0.108	Ni-(Acetate)2 (aq)
NH4+1	99.632	NH4+1
	0.314	NH4SO4-
	0.052	NH3 (aq)
Co+2	90.698	Co+2
	0.014	CoOH+
	0.012	CoCl+
	3.909	CoSO4 (aq)
	0.119	CoHPO4 (aq)
	0.38	CoHCO3+
	0.349	CoNTA-
	4.51	Co-Acetate+
Mn+2	91.222	Mn+2
	0.027	MnCl+
	3.547	MnSO4 (aq)
	0.285	MnHPO4 (aq)
	0.099	MnHCO3+
	0.011	MnCO3 (aq)
	4.807	Mn-Acetate+
Fe+3	0.599	FeOH+2
	88.79	Fe(OH)2+
	0.046	Fe(OH)3 (aq)
	0.643	FeHPO4+
	0.325	FeNTA (aq)
	9.46	FeOHNTA-
	0.117	Fe(OH)2NTA-2
	0.013	Fe-(Acetate)2+
MoO4-2	97.418	MoO4-2
	1.342	HMoO4-
	0.012	MoO3(H2O)3(aq)
	0.546	MgMoO4(aq)
	0.681	CaMoO4(aq)

Speciation of Media Components pH 7		
Component	% of total component concentration	Species name
Zn+2	86.512	Zn+2
	7.062	Zn-Acetate+
	4.152	ZnSO4 (aq)
	0.699	ZnOH+
	0.627	ZnNTA-
	0.378	ZnHCO3+
	0.298	ZnCO3 (aq)
	0.082	Zn(OH)2 (aq)
	0.074	ZnCl+
	0.04	ZnHPO4 (aq)
	0.039	Zn-(Acetate)2 (aq)
	0.022	ZnNH3+2
	0.015	Zn(SO4)2-2
Acetate-1	98.673	Acetate-1
	0.521	H-Acetate (aq)
	0.486	Zn-Acetate+
	0.013	Mg-Acetate+
	0.038	Ca-Acetate+
	0.262	Na-Acetate (aq)
Ca+2	92.035	Ca+2
	0.069	CaCl+
	4.634	CaSO4 (aq)
	0.162	CaHCO3+
	0.013	CaMoO4(aq)
	3.067	Ca-Acetate+
Cl-1	99.778	Cl-1
	0.038	ZnCl+
	0.175	NaCl (aq)
SO4-2	95.654	SO4-2
	2.03	ZnSO4 (aq)
	0.014	Zn(SO4)2-2
	0.091	MgSO4 (aq)
	0.41	CaSO4 (aq)
	1.573	NaSO4-
	0.223	NH4SO4-
CO3-2	0.048	CO3-2
	82.06	HCO3-
	17.093	H2CO3* (aq)
	0.272	ZnCO3 (aq)
	0.345	ZnHCO3+
	0.027	CaHCO3+
	0.144	NaHCO3 (aq)
H3BO3	99.259	H3BO3
	0.109	H3BO3-Acetate-
	0.625	H2BO3-
K+1	99.639	K+1

	0.135	K-Acetate (aq)
	0.017	KCl (aq)
	0.208	KSO4-
Mg+2	92.285	Mg+2
	0.11	MgCl+
	3.704	MgSO4 (aq)
	0.013	MgHPO4 (aq)
	0.131	MgHCO3+
	0.038	MgMoO4(aq)
	3.71	Mg-Acetate+
Mn+2	90.822	Mn+2
	0.018	MnOH+
	0.027	MnCl+
	3.543	MnSO4 (aq)
	0.054	MnHPO4 (aq)
	0.25	MnHCO3+
	0.272	MnCO3 (aq)
	5.012	Mn-Acetate+
MoO4-2	98.626	MoO4-2
	0.136	HMoO4-
	0.551	MgMoO4(aq)
	0.687	CaMoO4(aq)
Na+1	99.621	Na+1
	0.017	NaCl (aq)
	0.162	NaSO4-
	0.191	Na-Acetate (aq)
Ni+2	84.075	Ni+2
	0.084	NiOH+
	3.635	NiSO4 (aq)
	0.07	NiNH3+2
	0.017	NiHPO4 (aq)
	0.185	NiCO3 (aq)
	1.414	NiHCO3+
	5.367	NiNTA-
	5.026	Ni-Acetate+
	0.116	Ni-(Acetate)2 (aq)
NH4+1	99.15	NH4+1
	0.313	NH4SO4-
	0.015	ZnNH3+2
	0.521	NH3 (aq)
NTA-3	99.935	ZnNTA-
	0.049	ZnOHNTA-2
	0.012	NiNTA-
Co+2	89.769	Co+2
	0.143	CoOH+
	0.012	CoCl+
	3.882	CoSO4 (aq)
	0.015	Co(NH3)+2
	0.023	CoHPO4 (aq)
	0.101	CoCO3 (aq)

	0.953	CoHCO3+
	0.425	CoNTA-
	4.674	Co-Acetate+
PO4-3	39.777	HPO4-2
	49.911	H2PO4-
	0.132	MgHPO4 (aq)
	0.343	CaHPO4 (aq)
	0.029	CaH2PO4+
	1.408	NaHPO4-
	8.027	ZnHPO4 (aq)
	0.349	NaH2PO4 (aq)
Fe+3	0.066	FeOH+2
	97.869	Fe(OH)2+
	0.51	Fe(OH)3 (aq)
	0.11	Fe(OH)4-
	1.282	FeOHNTA-
	0.158	Fe(OH)2NTA-2

Speciation of Media Components pH 8

Component	% of total component concentration	Species name
Zn+2	63.391	Zn+2
	14.306	ZnNTA-
	6.051	Zn(OH)2 (aq)
	5.271	Zn-Acetate+
	5.153	ZnOH+
	3.164	ZnSO4 (aq)
	1.619	ZnCO3 (aq)
	0.513	ZnHPO4 (aq)
	0.205	ZnHCO3+
	0.157	ZnNH3+2
	0.07	ZnOHNTA-2
	0.055	ZnCl+
	0.03	Zn-(Acetate)2 (aq)
	0.011	Zn(SO4)2-2
Ni+2	31.763	Ni+2
	0.321	NiOH+
	0.024	Ni(OH)2 (aq)
	1.43	NiSO4 (aq)
	0.252	NiNH3+2
	0.111	NiHPO4 (aq)
	0.518	NiCO3 (aq)
	0.396	NiHCO3+
	63.16	NiNTA-
	0.04	NiOHNTA-2
	1.936	Ni-Acetate+
	0.045	Ni-(Acetate)2 (aq)

Acetate-1	99.62	Acetate-1
	0.053	H-Acetate (aq)
	0.016	Zn-Acetate+
	0.013	Mg-Acetate+
	0.032	Ca-Acetate+
	0.266	Na-Acetate (aq)
Ca+2	91.606	Ca+2
	0.069	CaCl+
	4.797	CaSO4 (aq)
	0.164	CaHPO4 (aq)
	0.047	CaPO4-
	0.119	CaHCO3+
	0.068	CaCO3 (aq)
	0.013	CaMoO4(aq)
	3.109	Ca-Acetate+
Cl-1	99.815	Cl-1
	0.176	NaCl (aq)
SO4-2	97.644	SO4-2
	0.067	ZnSO4 (aq)
	0.094	MgSO4 (aq)
	0.351	CaSO4 (aq)
	1.621	NaSO4-
	0.219	NH4SO4-
NTA-3	99.325	ZnNTA-
	0.484	ZnOHNTA-2
	0.141	NiNTA-
	0.039	CaNTA-
H3BO3	93.95	H3BO3
	0.104	H3BO3-Acetate-
	5.904	H2BO3-
	0.033	NaH2BO3 (aq)
K+1	99.627	K+1
	0.137	K-Acetate (aq)
	0.017	KCl (aq)
	0.214	KSO4-
Mg+2	91.867	Mg+2
	0.028	MgOH+
	0.111	MgCl+
	3.834	MgSO4 (aq)
	0.228	MgHPO4 (aq)
	0.034	MgCO3 (aq)
	0.097	MgHCO3+
	0.039	MgMoO4(aq)
	3.761	Mg-Acetate+
NH4+1	94.697	NH4+1
	0.309	NH4SO4-
	4.99	NH3 (aq)
MoO4-2	98.85	MoO4-2
	0.014	HMoO4-
	0.56	MgMoO4(aq)

	0.577	CaMoO4(aq)
Na+1	99.608	Na+1
	0.017	NaCl (aq)
	0.167	NaSO4-
	0.194	Na-Acetate (aq)
Co+2	77.807	Co+2
	1.248	CoOH+
	0.092	Co(OH)2 (aq)
	0.01	CoCl+
	3.502	CoSO4 (aq)
	0.126	Co(NH3)+2
	0.342	CoHPO4 (aq)
	0.651	CoCO3 (aq)
	0.612	CoHCO3+
	11.469	CoNTA-
	4.13	Co-Acetate+
Fe+3	79.71	Fe(OH)2+
	4.161	Fe(OH)3 (aq)
	8.941	Fe(OH)4-
	3.228	FeOHNTA-
	3.951	Fe(OH)2NTA-2
CO3-2	0.567	CO3-2
	97.036	HCO3-
	2.026	H2CO3* (aq)
	0.104	ZnCO3 (aq)
	0.013	ZnHCO3+
	0.026	CaHCO3+
	0.015	CaCO3 (aq)
	0.032	NaCO3-
	0.171	NaHCO3 (aq)
Mn+2	88.176	Mn+2
	0.18	MnOH+
	0.026	MnCl+
	3.578	MnSO4 (aq)
	0.919	MnHPO4 (aq)
	0.18	MnHCO3+
	1.962	MnCO3 (aq)
	0.013	MnNTA-
	4.957	Mn-Acetate+
PO4-3	84.568	HPO4-2
	10.686	H2PO4-
	0.283	MgHPO4 (aq)
	0.61	CaHPO4 (aq)
	0.175	CaPO4-
	3.021	NaHPO4-
	0.555	ZnHPO4 (aq)
	0.075	NaH2PO4 (aq)

Speciation of Media Components pH 9		
Component	% of total component concentration	Species name
Zn+2	46.972	Zn(OH)2 (aq)
	40.087	ZnNTA-
	4.909	Zn+2
	3.997	ZnOH+
	1.95	ZnOHNTA-2
	1.103	ZnCO3 (aq)
	0.41	Zn-Acetate+
	0.247	ZnSO4 (aq)
	0.161	Zn(OH)3-
	0.084	ZnNH3+2
	0.053	ZnHPO4 (aq)
	0.014	ZnHCO3+
Acetate-1	99.71	Acetate-1
	0.013	Mg-Acetate+
	0.266	Na-Acetate (aq)
Ca+2	90.439	Ca+2
	0.015	CaOH+
	0.069	CaCl+
	4.779	CaSO4 (aq)
	0.015	CaNH3+2
	0.217	CaHPO4 (aq)
	0.622	CaPO4-
	0.103	CaHCO3+
	0.587	CaCO3 (aq)
	0.013	CaMoO4(aq)
	0.059	CaNTA-
	3.079	Ca-Acetate+
Cl-1	99.82	Cl-1
	0.176	NaCl (aq)
SO4-2	98.069	SO4-2
	0.094	MgSO4 (aq)
	0.047	CaSO4 (aq)
	1.632	NaSO4-
	0.152	NH4SO4-
NTA-3	0.03	HNTA-2
	94.885	ZnNTA-
	4.616	ZnOHNTA-2
	0.218	NiNTA-
	0.052	MgNTA-
	0.188	CaNTA-
H3BO3	61.242	H3BO3
	0.068	H3BO3-Acetate-
	38.462	H2BO3-
	0.212	NaH2BO3 (aq)
K+1	99.623	K+1
	0.137	K-Acetate (aq)
	0.017	KCl (aq)

	0.216	KSO4-
Mg+2	91.272	Mg+2
	0.283	MgOH+
	0.11	MgCl+
	3.844	MgSO4 (aq)
	0.304	MgHPO4 (aq)
	0.298	MgCO3 (aq)
	0.085	MgHCO3+
	0.039	MgMoO4(aq)
	3.748	Mg-Acetate+
NH4+1	65.336	NH4+1
	0.214	NH4SO4-
	34.449	NH3 (aq)
MoO4-2	99.36	MoO4-2
	0.561	MgMoO4(aq)
	0.077	CaMoO4(aq)
Na+1	99.596	Na+1
	0.017	NaCl (aq)
	0.168	NaSO4-
	0.195	Na-Acetate (aq)
Ni+2	1.353	Ni+2
	0.137	NiOH+
	0.102	Ni(OH)2 (aq)
	0.061	NiSO4 (aq)
	0.074	NiNH3+2
	0.194	NiCO3 (aq)
	0.015	NiHCO3+
	97.36	NiNTA-
	0.61	NiOHNTA-2
	0.083	Ni-Acetate+
Co+2	14.599	Co+2
	2.345	CoOH+
	1.739	Co(OH)2 (aq)
	0.663	CoSO4 (aq)
	0.163	Co(NH3)+2
	0.086	CoHPO4 (aq)
	1.074	CoCO3 (aq)
	0.101	CoHCO3+
	77.875	CoNTA-
	0.573	CoOHNTA-2
	0.778	Co-Acetate+
CO3-2	5.466	CO3-2
	93.778	HCO3-
	0.196	H2CO3* (aq)
	0.027	ZnCO3 (aq)
	0.024	MgCO3 (aq)
	0.019	CaCO3 (aq)
	0.311	NaCO3-
	0.166	NaHCO3 (aq)
Fe+3	6.81	Fe(OH)2+

	3.557	Fe(OH)3 (aq)
	76.389	Fe(OH)4-
	0.996	FeOHNTA-
	0.077	Fe(OH)3NTA-3
	12.17	Fe(OH)2NTA-2
PO4-3	0.058	PO4-3
	94.632	HPO4-2
	1.198	H2PO4-
	0.01	MgPO4-
	0.317	MgHPO4 (aq)
	0.091	CaHPO4 (aq)
	0.261	CaPO4-
	3.389	NaHPO4-
	0.016	ZnHPO4 (aq)
Mn+2	74.873	Mn+2
	1.529	MnOH+
	0.023	MnCl+
	3.066	MnSO4 (aq)
	0.055	MnNH3+2
	1.045	MnHPO4 (aq)
	0.134	MnHCO3+
	14.655	MnCO3 (aq)
	0.395	MnNTA-
	4.223	Mn-Acetate+

APPENDIX F

This appendix contains the code for the dual-Monod kinetic model written by Dr. Timothy Ginn at University of California, Davis. The differential equation solver was written in MathCAD version 13.

A sample calculation with the dual-Monod kinetic model

$$\frac{d}{dt}M + \frac{d}{d\omega}M := \mu(\omega)\cdot M\cdot\left(\frac{A}{A + K_A}\right)\cdot\left(\frac{O}{O + K_O}\right)$$

$$\frac{d}{dt}A := \frac{-1}{Y}\left(\mu(\omega)\cdot M\right)_T\cdot\left(\frac{A}{A + K_A}\right)\cdot\left(\frac{O}{O + K_O}\right)$$

$$\frac{d}{dt}O := \frac{-F}{Y}\left(\mu(\omega)\cdot M\right)_T\cdot\left(\frac{A}{A + K_A}\right)\cdot\left(\frac{O}{O + K_O}\right)$$

$$\mu(\omega) := \mu_o \exp(-\nu\omega) \qquad \left(\mu(\omega)\cdot M\right)_T := \int_0^\infty \mu(w)\cdot M(w,t)\,dw$$

the dose is uniquely defined and single-valued function Z*t where Z= Zn concentration, for this batch reaction but not in the case of mobile kinetically attaching microbes and/or mobile metal concentration z, so for this batch case we can write

$$\mu(\omega(t)) := \mu_o \exp(-\nu Z t) \quad \text{and} \qquad M(\omega, t) := M(t)$$

so our system reduces to

$$\frac{d}{dt}M := \mu(t)\cdot M\cdot\left(\frac{A}{A + K_A}\right)\cdot\left(\frac{O}{O + K_O}\right)$$

$$\frac{d}{dt}A := \frac{-1}{Y}\left(\mu(t)\cdot M\right)\cdot\left(\frac{A}{A + K_A}\right)\cdot\left(\frac{O}{O + K_O}\right)$$

$$\frac{d}{dt}O := \frac{-F}{Y}\left(\mu(t)\cdot M\right)\cdot\left(\frac{A}{A + K_A}\right)\cdot\left(\frac{O}{O + K_O}\right)$$

Explicit finite difference solution.

$$\text{Monod}(a,b) := \frac{a}{a+b} \qquad \mu(a,b,c) := a\cdot\exp(-b\cdot c)$$

Time discretization.

$$T := 150 \quad dt := .25 \text{ hours} \qquad NT := \frac{T}{dt} \qquad NT = 600$$

$$i := 0..NT \qquad M_i := 0 \qquad A_i := 0 \qquad O_i := 0 \qquad time_i := 0$$

Initial Conditions and Solver.

$$\begin{aligned}
&\text{Solve}(a) := \\
&\quad M_0 \leftarrow .005 \\
&\quad A_0 \leftarrow 2.8 \\
&\quad O_0 \leftarrow 8.84 \\
&\quad time_0 \leftarrow 0 \\
&\quad \text{for } k \in 1..NT \\
&\qquad time_k \leftarrow dt\cdot k \\
&\qquad turn \leftarrow \mu\left(\mu o, \nu\cdot Z, time_k\right)\cdot M_{k-1}\cdot \text{Monod}\left(A_{k-1}, Ka\right)\cdot \text{Monod}\left(O_{k-1}, Ko\right) \\
&\qquad Mtemp \leftarrow M_{k-1} + turn \\
&\qquad Atemp \leftarrow A_{k-1} - \frac{turn}{Y} \\
&\qquad Otemp \leftarrow O_{k-1} - F\cdot\frac{turn}{Y} \\
&\qquad \text{if } (Atemp < 0.) \vee (Otemp < 0.) \\
&\qquad\quad \text{if } Atemp < Otemp \\
&\qquad\qquad Atemp \leftarrow 0 \\
&\qquad\qquad Otemp \leftarrow O_{k-1} - F\cdot A_{k-1} \\
&\qquad\quad \text{otherwise} \\
&\qquad\qquad Atemp \leftarrow A_{k-1} - \frac{O_{k-1}}{F} \\
&\qquad\qquad Otemp \leftarrow 0 \\
&\qquad M_k \leftarrow Mtemp \\
&\qquad A_k \leftarrow Atemp \\
&\qquad O_k \leftarrow Otemp \\
&\quad T \leftarrow \text{augment}(\text{augment}(\text{augment}(time, M), A), O) \\
&\quad T
\end{aligned}$$

Global defined parameters:

$F \equiv \frac{3.5}{2}$ oxygen to acetate utilization ratio

$Y \equiv .04$ yield coefficient, o.d. cells per mM acetate

$Ka \equiv 4$ half-saturation constant acetate, mM

$Ko \equiv .1$ half-saturation constant oxygen, mM

$\mu o \equiv .099$ specific growth rate, per time

$\nu \equiv 0$ toxicity inhibition parameter

$Z \equiv 0$ Zinc concentration, mM

concentration (mM)	specific growth rate (hrs^{-1})
0	0.0993
0.01	0.045
0.05	0.0296
0.1	0.0187
0.175	0.0041

M optical density of microbes

A acetate concentration

O oxygen concentration

time time in hours

$X := Solve(1)$

$time := X^{\langle 0 \rangle}$ $M := X^{\langle 1 \rangle}$ $A := X^{\langle 2 \rangle}$ $O := X^{\langle 3 \rangle}$